# Investigations on the reduction of engine-nitrogen-oxide emissions at low temperatures


**Dissertation**

zur Erlangung des Doktorgrades der Naturwissenschaften (Dr. rer. nat.)

der Fakultät Chemie und Pharmazie

der Universität Regensburg

vorgelegt von

**Peter Braun**

aus Ehekirchen

2019

# Promotionsausschuss

| | |
|---|---|
| **1. Gutachter** | Prof. Dr. Frank-Michael Matysik, Fakultät Chemie und Pharmazie, Institut für Analytische Chemie, Chemo- und Biosensorik, Universität Regensburg |
| **2. Gutachter** | Prof. Dr. Hans-Peter Rabl, Fakultät Maschinenbau, Labor für Verbrennungsmotoren und Abgasnachbehandlung, OTH Regensburg |
| **3. Prüfer** | Prof. Dr. Werner Kunz, Fakultät Chemie und Pharmazie, Institut für Physikalische und Theoretische Chemie, Universität Regensburg |
| **Vorsitzender** | Prof. Dr. Alkwin Slenczka, Fakultät Chemie und Pharmazie, Institut für Physikalische und Theoretische Chemie, Universität Regensburg |

Promotionsgesuch eingereicht am: 31.07.2019

Datum der mündlichen Prüfung: 18.09.2019

Die vorgelegte Dissertation entstand in der Zeit von Februar 2016 bis Juli 2019 am Institut für Analytische Chemie, Chemo- und Biosensorik der naturwissenschaftlichen Fakultät IV -Chemie und Pharmazie- der Universität Regensburg sowie am Labor für Verbrennungsmotoren und Abgasnachbehandlung der Fakultät Maschinenbau der OTH Regensburg.

Die Arbeit wurde angeleitet von: Prof. Dr. Frank-Michael Matysik und Prof. Dr. Hans-Peter Rabl.

# ACKNOWLEDGEMENT

Die Anfertigung dieser Arbeit wäre ohne eine Großzahl an Menschen nicht möglich gewesen, bei welchen ich mich im Folgenden bedanken möchte.

Zunächst gilt mein Dank meinen beiden Betreuern, Prof. Dr. Hans-Peter Rabl und Prof. Dr. Frank-Michael Matysik, die mir die Bearbeitung dieses interessanten und hochaktuellen Themas ermöglicht haben und immer ein offenes Ohr bei Fragen hatten.

Weiter danke ich meinen Uni-Kollegen Bernhard Durner, Thomas Herl, Timo Raith, Andreas Schmidberger, Marco Peteranderl, Stefan Wert, Beate Scherer, Daniel Böhm und Nicole Heigl für ihre Hilfsbereitschaft bei Fragen aller Art sowie für die unbeschreiblich gute Stimmung am Arbeitskreis.

Ebenso danke ich meinen Kollegen Ottfried Schmidt, Johann Mieslinger, Robert Altmann, Florian Zacherl, Maximilian Schillinger, Peter Schwanzer und Christian Mühlbauer von der OTH Regensburg für ihr stets offenes Ohr bei verschiedensten Anliegen.

Ferner möchte ich mich bei meiner Oma bedanken, durch deren Hilfe daheim eine regelmäßige Anwesenheit in Regensburg überhaupt erst ermöglicht wurde.

Ebenso danke ich Markus Stegmair für die regelmäßige Hilfe daheim sowie meinen Tanten Abi und Vera.

Besonders danke ich meinem Bruder Daniel für die Hilfe und Unterstützung jeglicher Art, sowohl daheim als auch in der Forschung. Ohne dich wäre diese Arbeit nicht möglich gewesen.

Ganz besonders danken möchte ich meinen Eltern Ute und Franz, die mir überhaupt erst ermöglicht haben den “richtigen Weg“ einzuschlagen. Ich hoffe, es geht euch gut.

***Mein größter Dank gilt zum Schluss allerdings meiner Frau Lydia.***

***Danke für Alles!***

# TABLE OF CONTENTS

# LIST OF PUBLICATIONS

**Potential technical approaches for improving low-temperature $NO_x$ conversion of exhaust aftertreatment systems**

Peter Braun, Jürgen Gebhard, Frank-Michael Matysik and Hans-Peter Rabl,

*Chemie Ingenieur Technik* **2018**, 90, 762-773, DOI: 10.1002/cite.201700122.

**Abstract**

Lean-burn engines, such as diesel engines, are widely used in mobile and stationary applications. Operation of lean-burn engines leads to formation of distinct amounts of nitrogen oxides (NO and $NO_2$). Efficient aftertreatment is mandatory to meet legal requirements, especially at low exhaust temperatures, as for the future a decline of the exhaust temperature level can be predicted due to improved engine efficiencies. Within this review, potential technical solutions to enhance the DeNOx-aftertreatment efficiency at low exhaust temperatures are presented.

**Investigations on the electrochemically induced decomposition of AdBlue-urea**

Peter Braun, Hans-Peter Rabl and Frank-Michael Matysik,

*Proceedings of the 14th International Students Conference Modern Analytical Chemistry, Prague* **2018**, 55-60.

ISBN 978-80-7444-059-5

**Abstract**

Ammonia-based selective catalytic reduction (SCR) systems are the most widely used technology for reduction of nitrogen oxide emissions from lean-burn engines such as diesel engines. However, at low exhaust temperatures, the SCR process is limited by difficulties in the decomposition of the ammonia precursor urea, which is carried onboard using an aqueous solution “AdBlue”. In previous work, the nickel species NiOOH was shown to be catalytically active in decomposing urea at low temperatures, for the case of highly concentrated potassium hydroxide in AdBlue. Since this approach is difficult to apply in practice, in the present study the electrochemical behavior of a nickel surface in ammonium carbonate was compared to that in sodium hydroxide using cyclic voltammetry (CV). It was found that the electrochemical behavior changes significantly when changing the electrolyte.

**Investigations on the liquid-phase decomposition of AdBlue-urea for the selective catalytic reduction process**

Peter Braun, Hans-Peter Rabl and Frank-Michael Matysik,

*Chemie Ingenieur Technik* **2019,** 91, 961-968, DOI: 10.1002/cite.201800055.

**Abstract**

Difficulties in decomposing AdBlue to ammonia limit the applicability of selective catalytic reduction systems at low exhaust temperatures. Investigations on the decomposition of AdBlue in the liquid phase under elevated pressure at temperatures up to 165 °C were carried out. Besides effects of inorganic catalysts, the impact of pH on urea decomposition was examined. After dissolution in aqueous phase, the compounds ZnO, $WO_3$, and $MoO_3$ were found to be effective in liquid-phase AdBlue decomposition. However, the efficiency was dropping significantly over few hours. Decomposition of AdBlue-urea was also found to be favored for alkaline and acidic conditions.

**Investigations on the decomposition of AdBlue-urea in the liquid phase at low temperatures by an electrochemically induced pH shift**

Peter Braun, Bernhard Durner, Hans-Peter Rabl and Frank-Michael Matysik,

*Monatshefte für Chemie – Chemical Monthly* **2019**, in press, DOI: 10.1007/s00706-019-02406-6.

**Abstract**

Ammonia-based selective catalytic reduction (SCR) systems are the most widely used technology for reduction of nitrogen oxide emissions from lean-burn engines such as diesel engines. However, at low exhaust temperatures, the SCR process is limited by difficulties in the decomposition of the ammonia precursor urea, which is carried onboard using an aqueous solution “AdBlue”. In this study, the decomposition of AdBlue-urea induced by electrical current and the resulting associated pH shifts was investigated in a divided cell configuration in the liquid phase. The decomposition was found to be favored in both electrochemical compartments, anodic and cathodic, at temperatures of 60 – 80 °C compared to a reference without electrochemical treatment. In addition to the determination of ammonia contents using an ammonia sensor, IC/HPLC analyses were carried out for each sample. Different byproducts such as biuret, nitrate, cyanuric acid, ammelide, and others were formed. In the anodic compartment, nitrate formation could be observed due to oxidation of ammonia at the electrode surface.

# DECLARATION OF COLLABORATION

Most of the theoretical and experimental works presented in this thesis were carried out solely by the author. Some of the results, however, were obtained in cooperation with other researchers. In accordance with § 8 Abs. 1 Satz 2 Punkt 7 of the Ordnung zum Erwerb des akademischen Grades eines Doktors der Naturwissenschaften (Dr. rer. nat.) an der Universität Regensburg vom 18. Juni 2009, this section describes the nature of these collaborations. In the following, the proportion of these cooperations are specified in dependence of their appearance in the chapter sequence.

**3. Potential technical approaches for improving low-temperature $NO_x$ conversion of exhaust aftertreatment systems**

The literature study and theoretical work, on which the chapter is based, was carried out by the author in collaboration with Jürgen Gebhard. Prof. Dr. Hans-Peter Rabl was involved in discussions.

**5.1 Investigations on the liquid-phase decomposition of AdBlue-urea for the selective catalytic reduction process**

The experimental work was performed solely by the author. The work was done under supervision of Prof. Dr. Hans-Peter Rabl and Prof. Dr. Frank-Michael Matysik.

**5.2 Investigations on the electrochemically induced decomposition of AdBlue-urea**

The experimental work was performed solely by the author. The work was done under supervision of Prof. Dr. Hans-Peter Rabl and Prof. Dr. Frank-Michael Matysik.

**5.3 Investigations on the decomposition of AdBlue-urea in the liquid phase at low temperatures by an electrochemically induced pH shift**

The experimental work was done in collaboration with Bernhard Durner. Electrochemical experiments on ammonia formation were done solely by the author. HPLC analyses regarding byproduct formation were carried out by Bernhard Durner. The work was done under supervision of Prof. Dr. Hans-Peter Rabl and Prof. Dr. Frank-Michael Matysik.

**5.4 AdBlue additivation for low-temperature applicability enhancement**

The experimental work was done solely by the author. Ottfried Schmidt and Johann Mieslinger were involved in setting up the optical injection-test bench. The work was done under supervision of Prof. Dr. Hans-Peter Rabl and Prof. Dr. Frank-Michael Matysik.

# LIST OF ABBREVIATIONS AND SYMBOLS

| abbreviation | name |
|---|---|
| ASC | ammonia slip catalyst |
| ASDS | ammonia storage and delivery system |
| CO | carbon monoxide |
| CRT | continuously regenerating trap |
| CV | cyclic voltammetry |
| DEF | diesel exhaust fluid |
| DOC | diesel oxidation catalyst |
| DPF | diesel particulate filter |
| DSC | differential scanning calorimetry |
| EGR | exhaust gas recirculation |
| HC | hydrocarbons |
| LNT | lean-$NO_x$ trap |
| NEDC | new European driving cycle |
| NO | nitrogen monoxide |
| $NO_2$ | nitrogen dioxide |
| $NO_x$ | nitrogen oxides (NO + $NO_2$) |
| NSC | $NO_x$ storage catalyst |
| RDE | real driving emissions |
| SCR | selective catalytic reduction |
| SDPF | SCR coated diesel particulate filter |
| WLTP | worldwide harmonized light vehicles test procedure |

| symbol | name | unit |
|---|---|---|
| $H^{cp}$ | henry constant | [mol/(L bar)] |
| $c(NH_3)$ | concentration of ammonia | [mol/L] |
| $\kappa$ | specific conductivity | [mS/cm] |
| $p(Reactor)$ | pressure inside autoclave reactor | [bar] |
| $\gamma$ | surface tension | [mN/m] |
| $P$ | laplace pressure | [bar] |
| $R_1$, $R_2$ | radii of pendant-drop curvature | [m] |

# 1 INTRODUCTION AND MOTIVATION

The invention of the combustion engine in the 19th century represented a pertinent revolution in human mobility. In ancient times, people were dependent on the use of horses and other livestock for transporting people, goods, and agriculture. The development of the steam machine improved the way of transport [1]. However, it was the introduction of the so-called Model T in 1909 by Henry Ford, powered by an internal combustion engine, which made the automobile widely available and by that enormously improved efficiency as well as flexibility and reliability of any transportation process [2].

While fuel consumption and exhaust gas emissions of internal combustion engines during Henry Ford's time played a rather subordinate role compared to the general functionality and power, its emissions have become a decisive engine feature today [3]. In addition to increasing environmental awareness among the population, the main reason for the importance of engine emissions are the increasingly more stringent becoming emission regulations, compliance with which is a precondition for type approval of any vehicle run by an internal combustion engine. Precisely for this reason, the emission regulations lead to constantly ongoing research in the field of internal combustion engines [4].

While most passenger cars were equipped with gasoline engines until the mid-1990s, the diesel engine has become increasingly important over the past two decades [5, 6]. Thus, the share of diesel engines on German roads increased by about 160 % between 1991 and 2018 [7]. This is due to the advantages that have made it irreplaceable since its invention by Rudolf Diesel in 1893 in the field of commercial vehicles and agriculture: high torque combined with low fuel consumption [5, 8].

In the context of compliance with emission regulations, the diesel engine has received involuntary attention since autumn 2015 [9]. During an investigation, a research team in the USA recognized a large discrepancy between the measured nitrogen-oxide ($NO_x$) emissions, meaning the sum of nitrogen monoxide (NO) and nitrogen dioxide ($NO_2$), on the test bench and in real road traffic [10]. As, after subsequent investigations, a software was discovered in the engine control, which was able to detect a test bench cycle and activate a shutdown device to reduce the emission control in real road operation, the so-called “dieselgate” developed [11]. Its consequences are today, even 4 years after the first allegations were known, still widely discussed. This manipulation shocked the

economy even far beyond the borders of Germany and underscored the need for action regarding engine emissions.

Of course, since these scandalous events, the diesel engine and the combustion engine in general, are questioned. Discussions about alternative drives such as electric or hydrogen vehicles even increase these doubts [12]. However, taking the high energy density of diesel or gasoline into account, the combustion engine brings benefits.

Therefore, efficient pollutant reduction is an essential condition for developing new combustion engines. Exhaust aftertreatment has become an irreplaceable complement to any internal combustion engine [13].

In the last years, especially the limit value for nitrogen-oxide emissions has been and will be cut significantly. This fact presents a problem especially for lean-burn engines, such as the diesel engine, operating with a combustion mixture that is characterized by excess quantities of oxygen. While in the case of stoichiometrically operated engines, e.g. gasoline engines, pollutants can efficiently be reduced by a so-called three-way catalyst, the exhaust aftertreatment setup of lean-burn engines is more complex. Here, suitable individual measures have to be applied for the reduction of the pollutant components [5, 14, 15].

Moreover, exhaust gas temperatures below 200 °C, which can be observed for example during cold start and low-engine-load phases, lead to additional challenges since the aftertreatment components cannot reach the required operating temperature. This fact will be even more problematic for future aftertreatment systems, due to enhanced thermal and overall engine efficiency leading to a decline of the exhaust gas-temperature level. Insufficient conversion rates can result, and the allowed limits cannot be met. Taking these facts into account, measures for emission control have to be applied, which enable complying with current and especially future emission limits [16].

During the last years, the selective catalytic reduction (SCR) technology has evolved as the standard method for the elimination of $NO_x$ from diesel engines [17]. However, the system with its additional operating material AdBlue is also facing problems as exhaust temperatures become lower. Targeting particularly the described low-temperature issue with respect to nitrogen-oxide emissions from diesel engines, this dissertation focusses on the reduction of engine $NO_x$ emissions at low temperatures. In chapter 3, a theoretical evaluation of different attempts based on detailed

literature and patent research is presented. Potential strategies are tested in chapter 5. In the first part 5.1, the liquid-phase decomposition of AdBlue using different catalysts is investigated. The second and third part, chapter 5.2 and 5.3 describe experiments regarding the decomposition of AdBlue using electrochemical methods. A nickel species is checked for its catalytic capacity regarding the decomposition of AdBlue and an in-situ generated pH shift is studied as a method to enhance ammonia generation at low temperatures. Additives for the AdBlue solution are the focus of the fourth part 5.4. At the end of this work, a general summary is given.

## 1.1 References


[1] E. Gregersen, *The Complete History of Wheeled Transportation: From Cars and Trucks to Buses and Bikes*, Britannica Educational Publishing, **2011**.

[2] R. H. Casey, *The Model T: A Centennial History*, Johns Hopkins University Press, **2016**.

[3] J. Merkisz, J. Pielecha and S. Radzimirski, *New Trends in Emission Control in the European Union*, Springer Science & Business Media, **2013**.

[4] R. K. Maurya, A. K. Agarwal, *Applied Energy* **2011**, 88, 1169-1180.

[5] K. Mollenhauer, H. Tschöke, *Handbuch Dieselmotoren*, 3, Springer, Berlin, **2007**.

[6] A. Faiz, C. S. Weaver, M. P. Walsh, *Air Pollution from Motor Vehicles: Standards and Technologies for Controlling Emissions*, World Bank Publications, **1996**.

[7] Umweltbundesamt, Verkehrsinfrastruktur und Fahrzeugbestand, **2019**.

[8] P. Geng, E. Cao, Q. Tan, L. Wei, *Renewable and Sustainable Energy Reviews* **2017**, 71, 523-534.

[9] J. Ewing, *Wachstum über alles: Der VW-Skandal*, Droemer eBook, **2017**.

[10] C. Baunach, *Der Abgasmanipulationsskandal bei Volkswagen. Zusammenfassung der Fakten, technischen Hintergründe, Folgen und Auswirkungen*, GRIN Verlag, **2015**.

[11] M. Frigessi di Rattalma, *The Dieselgate*, Springer, **2017**.

[12] A. Boretti, *SAE Technical Paper* **2017,** 0148-7191.

[13] İ. A. Reşitoğlu, K. Altinişik, A. Keskin, *Clean Technologies and Environmental Policy* **2015**, 17, 15-27.

[14] R. van Basshuysen, F. Schäfer, *Handbuch Verbrennungsmotoren*, 7, Springer, Wiesbaden, **2015**.

[15] G. P. Merker, C. Schwarz, R. Teichmann, *Grundlagen Verbrennungsmotoren*, 5, Springer, Wiesbaden, **2011**.

[16] P. Braun, J. Gebhard, H.-P. Rabl, *Low-Temperature DeNOx*, Final Report FVV Project 1115, Frankfurt am Main, **2017**.

[17] I. Nova, E. Tronconi, *Urea-SCR Technology for deNOx After Treatment of Diesel Exhausts*, Springer Science & Business Media, **2014**.

# 2 FUNDAMENTALS AND BACKGROUND

## 2.1 Working principle of combustion engines, the diesel engine

Combustion engines, such as gasoline and diesel engines, can, in general, be described as energy converters. The energy which is chemically bound in the fuel molecules is converted into mechanical energy [1]. The principle is schematically visualized in Figure 1. The energy-conversion process takes place within two steps: in the first step, via combustion, the chemically bound energy is transferred into heat and in the second step, the heat from step one is transferred into the required mechanical energy [2].

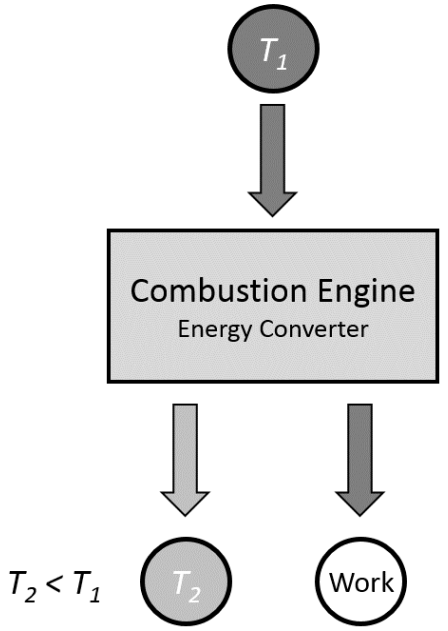


Figure 1: Schematic working principle of engine's energy-conversion characteristic [2].

Combustion engines can be described as piston engines. Depending on the constructive implementation, piston engines can be divided into two classes: the reciprocating piston engine and the rotary piston engine. Today, almost exclusively the former class is used. A cross-section of a cylinder of a reciprocating piston engine is shown in Figure 2 [3]. The working process of a 4-stroke gasoline engine can be described by the following operational steps: in the first step, a homogeneous air-fuel mixture is sucked into the cylinder. In the second step the mixture is compressed by the cylinder, subsequently followed by an external ignition. In the last step, the combustion mixture is pushed out again.

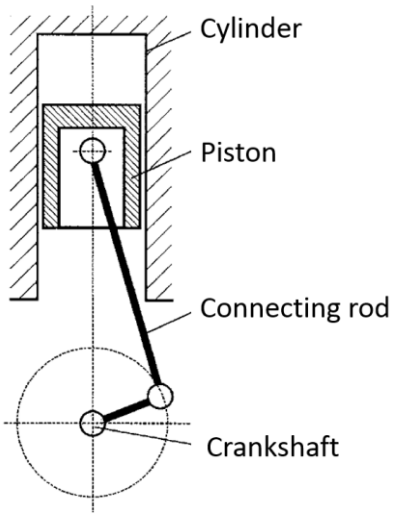


Figure 2: Schematic view of a reciprocating piston engine cylinder [3].

In contrast to the described principle, the diesel combustion process differs. Here, firstly air without any fuel is sucked into the cylinder. In the next step, the air is compressed by the piston and subsequently, diesel fuel is injected via a high-pressure injection system (e.g. a Common-Rail-System at pressures of up to 2000 bar) into the hot, compressed air [4]. After injecting the fuel, spontaneous inflammation of the diesel fuel in the environment of the hot air occurs [1]. Caused by the heat and the resulting pressure increase inside the cylinder, the piston is pressed down and this kinetic energy is transmitted via the connecting rod to the crankshaft, see Figure 2. In the last step, the mixture is again emitted to the exhaust tract. Table 1 summarizes the most important technical differences between gasoline and diesel engines [1].

Table 1: Technical differences between gasoline and diesel engine [1].

| Feature | diesel engine | gasoline engine |
|---|---|---|
| **cylinder charge** | heterogeneous | homogeneous |
| **ignition** | self-ignition | spark-ignition |
| **air ratio** | $\lambda_{min} > 1$ | $\lambda = 1$ |
| **combustion** | diffusion flame | premixed flame |

The gasoline engine is operated at a stoichiometric air ratio ($\lambda = 1$). In contrast, a diesel engine is operated at a lean air ratio ($\lambda > 1$), meaning inside the cylinder an excess of air is present compared

to the amount of fuel. In general, diesel engines are characterized by a higher level of efficiency and thereby also lower exhaust gas temperatures compared to gasoline engines. The consequence of it can be found in low fuel consumption and correspondingly low $CO_2$ emissions. This important feature makes the diesel engine a suitable choice to comply with steadily tightened $CO_2$-emission regulations [3].

## 2.2 Emissions of a diesel engine and formation of pollutants

In case of an ideal, stoichiometric combustion, the oxidation process of the fuel can be described by equation 1.

$$C_nH_{2n+2} + (1.5\,n + 0.5)\,O_2 \rightarrow n\,CO_2 + (n+1)\,H_2O + \text{Heat} \quad \text{(equation 1)}$$

As can be seen, the hydrocarbons of the diesel fuel are oxidized to water and carbon dioxide, the latter is contributing to the greenhouse effect. However, equation 1 considers an ideal case. In reality, other products are also formed as byproducts. Due to their toxic characteristics towards nature and humans, these byproducts are called pollutants [1]. Figure 3 shows exemplarily the composition of raw exhaust gas and pollutant components of a diesel engine in partial-load range [4].

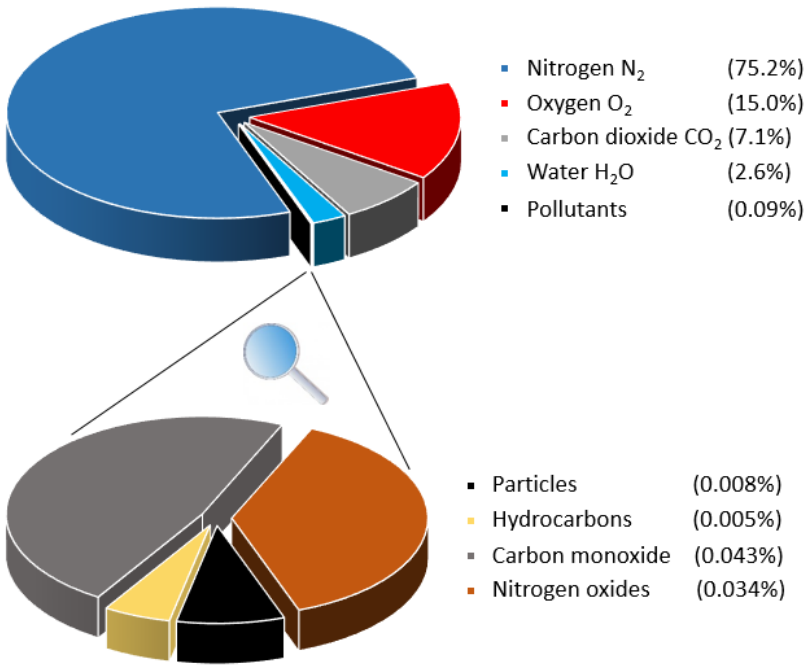


Figure 3: Composition of raw exhaust gas and pollutant components of a diesel engine in partial-load range, numbers in mass percent [4].

As can be seen, the exhaust gas of a diesel engine consists of 99.9 wt% of harmless and non-toxic components. Only about 0.1 wt% contribute to the legally limited pollutants. Although the pollutants represent only a very small part of the diesel's exhaust gas, these substances significantly contribute to various detrimental effects for nature and human health [5]. The pollutants consist basically of 4 different classes: unburned or partially oxidized hydrocarbons, carbon monoxide, particles and nitrogen oxides.

### 2.2.1 Hydrocarbons

The main reason for hydrocarbons (HC) in the exhaust gas is due to a (partially) incomplete combustion of the fuel. The reason is mostly insufficiently prepared fuel in areas of the combustion chamber, in which the temperature for combustion is not high enough [1]. More detailed, various mechanisms for the emission of unburned hydrocarbons in diesel engines are mentioned in the literature, for example: [6]

- the mixture composition in the outer range of the spray is outside of the ignition range (too lean)
- the mixture composition in the inner spray area is too rich
- the extinguishing of the diffusion flame by rapid pressure- and temperature drop during the expansion phase
- fuel attached to the walls evaporates only slowly due to too low temperatures and is thereby not completely oxidized

A condition for a (partially) incomplete combustion and thus oxidation of the fuel is thus a lack of oxygen, which is caused by the heterogeneous air-fuel mixture in the diesel engine. Depending on the composition of the hydrocarbon emissions, various hazards can arise for humans [6].

Due to the light-off temperature of the diesel oxidation catalyst, high emissions of unburned hydrocarbons mainly occur after a cold start [7].

### 2.2.2 Carbon monoxide

As product of an incomplete combustion, besides hydrocarbons, also carbon monoxide is observed. During the combustion process, carbon monoxide can occur as an intermediate product of oxidation. At local oxygen deficiency ($\lambda < 1$) due to the heterogeneity of the combustion mixture, CO remains as a product of incomplete combustion [3].

In addition to a lack of oxygen, an abrupt drop in temperature due to cool surfaces in the cylinder also can hinder the oxidation of CO to $CO_2$. Moreover, in extremely lean combustion mixtures the lower temperature level can hinder CO oxidation [6].

As in case of hydrocarbons, since the diesel engine is basically operated with an excess of oxygen, the amounts of carbon monoxide present in the raw exhaust gas are substantially lower than in the stoichiometrically operated gasoline engine [1].

Carbon monoxide is dangerous for humans since it is a colorless, odorless and tasteless respiratory poison [8].

### 2.2.3 Particles

The formation of particles can typically be found for an inhomogeneous, non-premixed combustion [8]. “Particle” emissions mean the overall amount of solids and attached substances emitted by the combustion engine. The by far largest contribution is soot, meaning elementary carbon, but also organic compounds are contained.

Regarding the formation mechanism, two genesis hypotheses are existing: the elemental carbon hypothesis and the polycycles hypothesis. According to both hypotheses, firstly, so-called primary particles with diameters of below 10 nm are formed. From these primary structures, the actual particles are formed by agglomeration, whereby the individual particles stick to each other [1].

Particles are produced in general in areas of the combustion chamber, in which lack of air is present, meaning in rich areas and above a minimum-temperature level.

The particles can be classified according to their size. $PM_{10}$ means particles with maximum 10 µm diameter, whereas $PM_{2.5}$ means particles smaller than 2.5 µm. Especially the very small particles can cause serious problems for human health as causing of cardiopulmonary adverse health effects can be observed [9].

Particles of modern diesel engines with direct injection are usually relatively small and thus not visible in the exhaust gas [1].

### 2.2.4 Nitrogen oxides

Nitrogen-oxide emissions mean the sum of all oxides of nitrogen, however, in the exhaust gas only nitrogen monoxide (NO) and nitrogen dioxide ($NO_2$) are present in significant amounts. Therefore, $NO_x$ is used to describe the sum of NO and $NO_2$ [1].

Formation of nitrogen oxides can occur in principle by four mechanisms, the prompt-NO, the fuel-NO, the NO formed by the $N_2O$-mechanism and the thermic-NO [6]. $NO_x$ formation in the cylinder of combustion engines is mainly thermic NO, described by the so-called Zeldovich-mechanism. The mechanism is based on radical reactions and can be described by the following equations 2 - 5 [1, 10]:

$$O_2 \leftrightarrow 2\,O\cdot \qquad \text{(equation 2)}$$

$$N_2 + O\cdot \leftrightarrow NO + N\cdot \qquad \text{(equation 3)}$$

$$O_2 + N\cdot \leftrightarrow NO + O\cdot \qquad \text{(equation 4)}$$

$$OH + N\cdot \leftrightarrow NO + H\cdot \qquad \text{(equation 5)}$$

Elementary oxygen leads to the formation of a first equivalent of NO and a nitrogen radical, which can react subsequently with molecular oxygen to form a second NO equivalent and again an oxygen radical. The presence of atomic oxygen is needed for the chain reaction. As this occurs at temperatures of about 2200 K, the mechanism is favored by locally high peaks in combustion temperatures which can partially be significantly higher than the average combustion temperature.

The largest part of engine-out $NO_x$ consists of NO with 85 - 95 %, meaning $NO_2$ is contained only to 5 - 15 % [1].

Nitrogen oxides have several adverse impacts on human health and environment. NO can spread to several parts of the respiratory system. $NO_x$ diffuses through the Alveolar-cells and adjacent capillary vessels of the lung and thereby disturb the Alveolar structures and their functions [11]. Moreover, nitrogen oxides promote the formation of ground-level ozone and photochemical smog [6].

## 2.3 Emission legislation

Regarding environmental protection, the emissions of pollutants need to be kept low. In order to reduce the amount of pollutants emitted to the environment, legislation worldwide limits the amount of allowed emission [1, 3]. For this purpose, laws are enacted which exactly limit the maximum permitted emissions of a certain pollutant. To get approval of the respective vehicle type, the legal conditions have to be met.

In the European Union, the statutory framework conditions for passenger cars, light-duty vehicles and heavy-duty vehicles are specified by the so-called Euro standards [12]. The development of the Euro standards from Euro 1 – Euro 6 for diesel passenger cars is shown in Figure 4. The pollutants CO, HC, $NO_x$ and Particulates described above are limited. In the case of hydrocarbons and particulates, legislation limits the amount of total emitted amount, without differentiation between the components. A limit value for nitrogen oxide emissions itself was introduced with the Euro 3 standard in the year 2001. In the years before, a limit value together with the number of hydrocarbons was set.

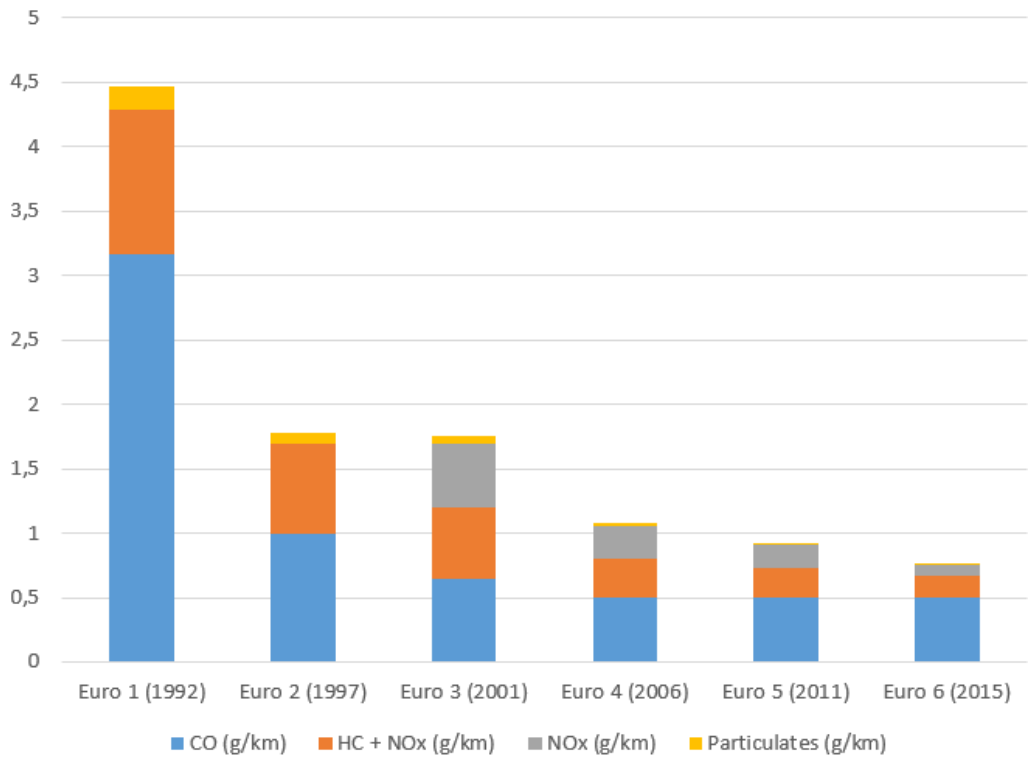


Figure 4: Development of the Euro standards from Euro 1 (1992) - Euro 6 (2015) [12].

As shown, from 1992 until today the limit values for the different pollutants have become significantly lower. The trend was observed not only in Europe but also in other parts of the world such as in the USA or in Japan [3, 13]. To comply with the more stringent becoming emission legislations, manufacturers need to apply measures to limit the pollutant emissions [14].

## 2.4 Pollutant limitation and exhaust aftertreatment

To comply with the limits that are legally prescribed, far-reaching measures regarding pollutant control have to be applied [14]. These measures can, in general, be divided into two groups. First, approaches are possible to lower the amount of pollutants formed in the combustion chamber. These measures are therefore called inner-engine measures [14].

Regarding the formation of $NO_x$, the most important strategy to reduce the amount formed is the so-called exhaust gas recirculation (EGR) [15]. The approach focusses on a reduction of the local-peak temperature during combustion, thereby lowering the extent of the Zeldovich-mechanism described in 2.2. By lowering the oxygen concentration, the flame temperature is reduced. However, as a negative effect of EGR, particulate formation increases as a result of lower oxygen amount present [15].

For complying with the latest emission standards, such as the Euro 6 standard in the European Union, an exhaust aftertreatment is necessary in addition to inner-engine measures [14]. As indicated by their name, these methods are not directly coupled to the engine operation but are integrated into the exhaust tract. While in case of stoichiometrically operated engines, the so-called three-way catalyst is able to reduce the amount of HC, CO and $NO_x$ within “one step” [16], the setup for modern diesel engines comprises different catalytic converters [14].

For lowering the amount of HC and CO, the so-called diesel oxidation catalyst (DOC) is applied. Downstream of the DOC, a diesel particulate filter (DPF) is used to reduce the mass and number of solid particles in the exhaust gas. Especially in light-duty applications, one component, comprising the SCR and DPF functionality, is used. For $NO_x$ abatement, mostly a selective catalytic reduction system is used [14]. An exemplary schematic illustration of a Euro 6 exhaust aftertreatment setup is shown in Figure 5.

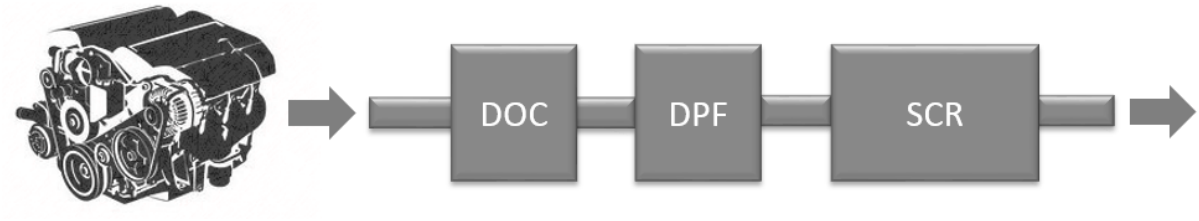


Figure 5: Schematic layout of Euro 6 exhaust aftertreatment setup. The SCR and the DPF can also be applied in a combined, single compartment, called SDPF [14].

## 2.5 References

[1] K. Mollenhauer, H. Tschöke, *Handbuch Dieselmotoren*, 3, Springer, Berlin, **2007**.

[2] H.-P. Rabl, *script for lecture combustion engines,* OTH Regensburg, **2008**.

[3] R. van Basshuysen, F. Schäfer, *Handbuch Verbrennungsmotoren*, 7, Springer, Wiesbaden, **2015**.

[4] K. Reif, *Dieselmotor-Management. Systeme Komponenten Steuerung und Regelung,* 5, Springer, Wiesbaden, **2012**.

[5] U. Förstner, *Umweltschutztechnik*, 8, Springer, Berlin, **2012**.

[6] G. P. Merker, C. Schwarz, R. Teichmann, *Grundlagen Verbrennungsmotoren*, 5, Springer, Wiesbaden, **2011**.

[7] S. Ye, Y. H. Yap, S. T. Kolaczkowski, K. Robinson, D. Lukyanov, *Chemical Engineering Research and Design* **2012**, 90, 834-845.

[8] R. Pischinger, M. Kell, T. Sams, *Thermodynamik der Verbrennungskraftmaschine*, 3, Springer, Wien, **2009**.

[9] M. M. Maricq, *Aerosol Science* **2007**, 38, 1079-1118.

[10] A. M. Mellor, J. P. Mello, K. P. Duffy, W. L. Easley, J. C. Faulkner, *SAE Journal of Fuels and Lubricants* **1998**, 107, 786-801.

[11] T. Boningari, P. Smirniotis, *Current Opinion in Chemical Engineering* **2016**, 13, 133-141.

[12] Umweltbundesamt, *regulation 715/2007/EG,* **2007**.

[13] K. Mori, *SAE Technical Paper* 970753, **1997**.

[14] P. Braun, J. Gebhard, F.-M. Matysik, H.-P. Rabl, *Chemie Ingenieur Technik* **2018**, 90, 762-773.

[15] M. Zheng, G. T. Reader, J. G. Hawley, *Energy Conversion and Management* **2004**, 45, 883-900.

[16] D. Chatterjee, O. Deutschmann, J. Warnatz, *Faraday Discussions* **2001**, 119, 371-384.

# 3 POTENTIAL TECHNICAL APPROACHES FOR IMPROVING LOW-TEMPERATURE $NO_x$ CONVERSION OF EXHAUST AFTERTREATMENT SYSTEMS

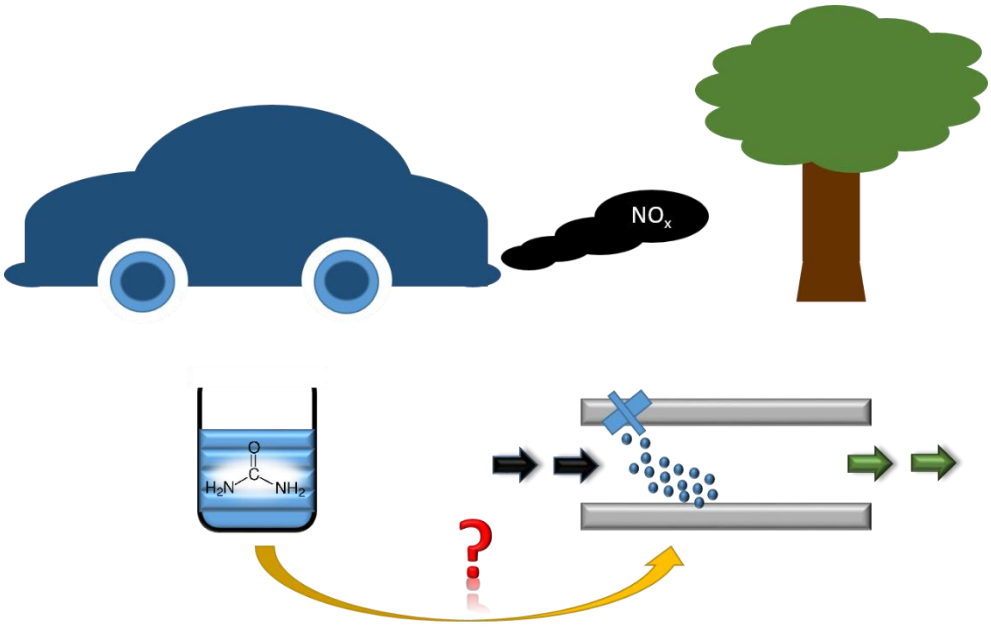


---

This chapter has been published and adopted from:

Peter Braun, Jürgen Gebhard, Frank-Michael Matysik and Hans-Peter Rabl,

*Chemie Ingenieur Technik* **2018**, 90, 762-773, DOI: 10.1002/cite.201700122.

**Abstract**

Lean-burn engines, such as diesel engines, are widely used in mobile and stationary applications. Operation of lean-burn engines leads to the formation of distinct amounts of nitrogen oxides (NO and $NO_2$). Efficient aftertreatment is mandatory to meet legal requirements, especially at low exhaust temperatures, as for the future a decline of the exhaust temperature level can be predicted due to improved engine efficiencies. Within this review, potential technical solutions to enhance the DeNOx-aftertreatment efficiency at low exhaust temperatures are presented.

## 3.1 Introduction and background

In terms of reducing hazardous substances in exhaust gases, environmental protection agencies gradually pass progressively more stringent regulations for machines driven by combustion engines, which limit the permitted amount of emissions. Specifically, the threshold for nitrogen oxide ($NO_x$) emissions, meaning the sum of nitrogen monoxide (NO) and nitrogen dioxide ($NO_2$), has been and will be cut drastically, thus posing a considerable challenge for exhaust gas aftertreatment systems. This fact is especially problematic for so-called lean-burn engines, which operate with a combustion mixture that in general exhibits excess quantities of oxygen. Lean-burn engines, such as diesel engines, are commonly used in mobile and stationary applications. Their comparatively high efficiency entails low fuel consumption, presenting the main benefit compared to engines working with a stoichiometric air ratio. While in case of stoichiometrically operated engines, such as gasoline engines, pollutants can efficiently be eliminated via the so-called three-way catalyst, the setup for exhaust aftertreatment of lean-burn engines is more complex.

Additionally, under conditions of adverse exhaust gas temperatures below 200 °C, as for example during cold start and low-engine-load phases, the situation turns even worse since the aftertreatment components do not reach their required operating temperatures. This issue will be even more challenging for future engine systems due to enhanced thermal and overall efficiency leading to reduced exhaust temperatures. Consequently, insufficient conversion rates result, hence, the regulatory limits cannot be met. Due to these facts, far-reaching measures regarding emission control have to be applied to meet current and particularly future emission limits. Especially

regarding air pollution control, emission regulation and more extensive test procedures as well as the reduction of fuel consumption, high need for action exists in this area.

Targeting particularly the described low-temperature issue with respect to nitrogen oxides, several approaches trying to solve this problem are presented. A defined list of different technical solution approaches has been investigated in order to identify measures that are able to effectively eliminate nitrogen oxides at lower exhaust temperatures. Either these solutions have to exhibit the potential to increase the conversion rates affected by denitrification systems (DeNOx systems) at low exhaust gas temperatures or, as a secondary goal, accelerate the heat-up of aftertreatment components, respectively catalysts, in a way to faster reach the temperature level necessary for the underlying physicochemical processes [1].

## 3.2 State of the art and reference systems

For comparative analysis of technical solutions for low-temperature DeNOx, reference systems according to state-of-the-art setups have been established. These references serve as a basis to which the different approaches can be referred to. For diesel passenger cars, the setup consists of a diesel oxidation catalyst (DOC), followed by a SDPF ("SCR catalyst on diesel particulate filter" technology) and a second small oxidation catalyst, mainly to prevent ammonia emission, called ammonia slip catalyst (ASC), see Figure 6.

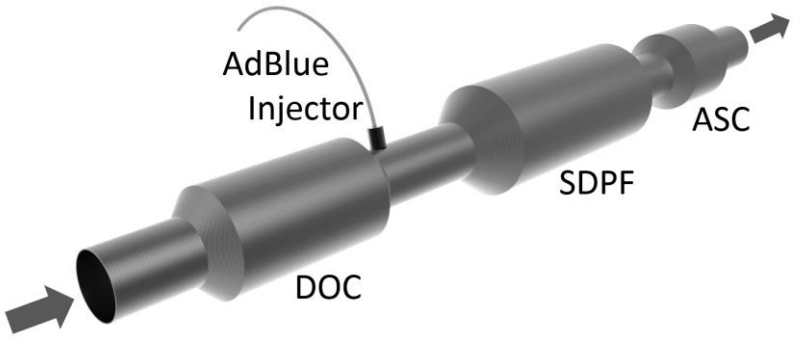


Figure 6: State-of-the-art aftertreatment system for diesel passenger cars.

For heavy-duty vehicles and so-called non-road applications such as tractors and construction machines, the state-of-the-art aftertreatment system consists of a DOC, a particulate filter (DPF) followed by a separate SCR catalyst and ASC, see Figure 7.

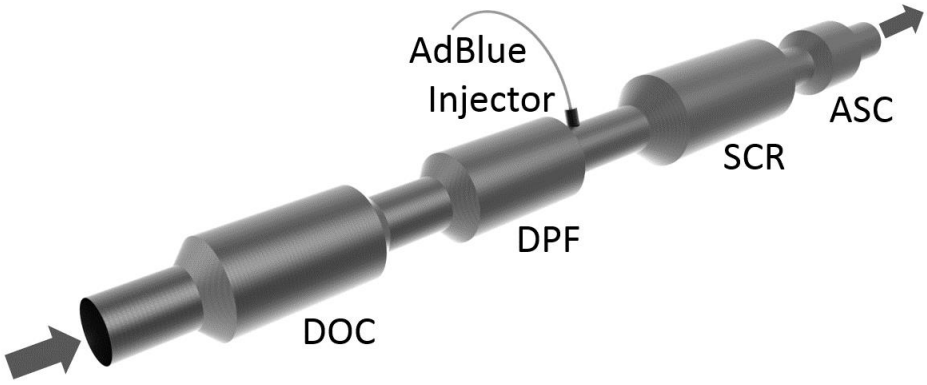


Figure 7: State-of-the-art aftertreatment system for heavy-duty vehicles and non-road applications.

As can be derived from the reference systems, today the most commonly used approach to reduce $NO_x$ emissions of lean-burn engines is the so-called SCR system (selective catalytic reduction). It ensures lowest $NO_x$ tailpipe emissions at best fuel consumption, and thus, lowest $CO_2$ emissions [2]. Because of that, the operating principle will be shortly explained.

The SCR process needs ammonia as selective reducing agent. Since carrying gaseous ammonia onboard is too dangerous, mobile applications make use of an ammonia precursor, namely urea. An eutectic solution of 32.5 wt% urea in water (AdBlue® or DEF®) is injected into the exhaust tract, upstream of the SCR catalyst. Thermal activation leads to decomposition of urea to 2 equivalents of ammonia and 1 equivalent of carbon dioxide. The generated ammonia is subsequently stored on the surface of the SCR catalyst.

Inside the SCR catalyst, ammonia selectively reacts with the nitrogen oxides to harmless nitrogen and water. Depending on the prevailing ratio of $NO_2/NO_x$ different reactions occur. The most important ones are the fast-SCR, the standard-SCR and the $NO_2$-SCR reaction, see equations 6, 7 and 8 [3].

| | | |
|---|---|---|
| *Fast-SCR reaction:* | $2\ NH_3 + NO + NO_2 \rightarrow 2\ N_2 + 3\ H_2O$ | (equation 6) |
| *Standard-SCR reaction:* | $4\ NH_3 + 4\ NO + O_2 \rightarrow 4\ N_2 + 6\ H_2O$ | (equation 7) |
| *$NO_2$-SCR reaction:* | $8\ NH_3 + 6\ NO_2 \rightarrow 7\ N_2 + 12\ H_2O$ | (equation 8) |

As the name indicates, the most advantageous type of possible reactions is the fast-SCR reaction as it proceeds with higher conversions especially in the low-temperature range compared to the other pathways. As shown in equation 6, the desired $NO_2/NO_x$ ratio is 50 %. In contrast, if the share of $NO_2$ gets higher than 50 %, the $NO_2$-SCR reaction is prevalent, for which the required amount of ammonia is 30 % higher than for the other reactions, thereby leading to increased AdBlue consumption. As the $NO_x$ raw emissions mainly consist of NO (85-95 %), the $NO_2$ required for the fast-SCR reaction has to be generated upstream of the SCR catalyst [3].

## 3.3 Overview of technical solutions for elimination of nitrogen oxides

### 3.3.1 Catalysis

#### *3.3.1.1 Improved catalyst for low-temperature SCR coating*

Besides providing the reducing agent ammonia out of urea, another essential condition for reduction of $NO_x$ at low temperatures is a catalytic coating which is highly active in the low-temperature range. Well established copper-zeolite coatings are effective in the low-temperature range and ensure fast light-off. In Figure 8 the $NO_x$ conversion of a commercial Cu-SAPO-34 catalyst is shown:

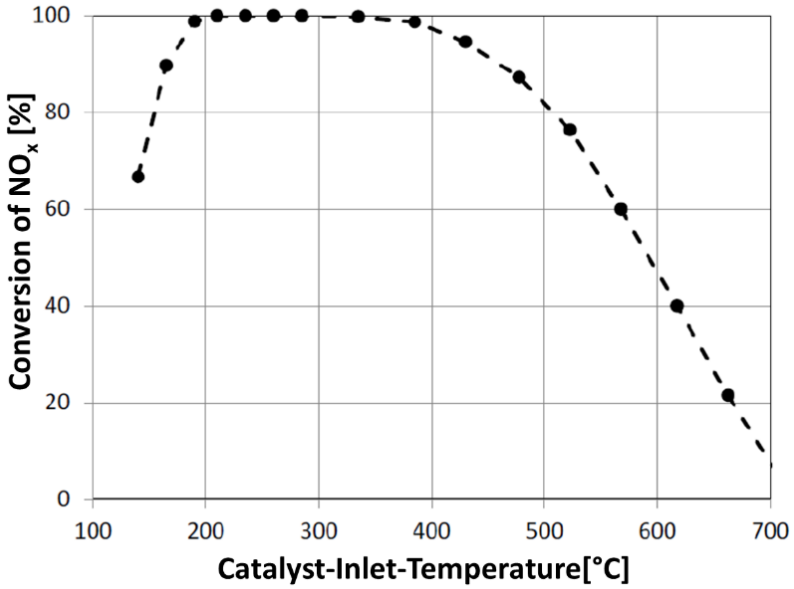


Figure 8: Conversion efficiencies of a modern Cu-SAPO-34 SCR catalyst for $[NO_2]/[NO_x]$ = 50 %. [4]

As shown, the SCR catalyst exhibits a high $NO_x$ reduction efficiency of 65 % at 140 °C or 90 % at 165 °C. A prerequisite for the high activity is a ratio of $NO_2/NO_x$ of 0.5, enabling the fast-SCR reaction [4]. Nevertheless, an even better light off and low-temperature activity is desired, considering the high efficiency of modern engines resulting in low exhaust temperatures. The engine-out $NO_x$ emissions consist of about 60-90 % NO. $NO_2$ is required for the fast-SCR reaction and can be produced by the DOC. Since the $NO_2/NO_x$ ratio practically cannot be tuned exactly to 0.5, catalytic materials having a greater activity, independent of this ratio would be desirable, thereby enabling SCR at low temperatures with varying amounts of $NO_x$.

A distinction of the different catalytic materials described in the literature can be made, depending on the composition of the catalyst.

***Zeolite-based SCR catalysts***

It has been verified that zeolite-based catalytic materials are very promising for $NH_3$-SCR, especially in the low-temperature range [5, 6].

Particularly iron and copper zeolites seem to be beneficial. They have been studied extensively and have a large market share today [6]. An important advantage of Cu zeolite compared to Fe zeolite is the lower sensitivity of the SCR reaction to the $NO_2/NO_x$ ratio [7, 8]. Cu zeolite shows higher

activity in the low-temperature range compared to Fe zeolite [6, 7]. However, at the ideal ratio of $NO_2/NO_x$ of 0.5, the low-temperature efficiency of Fe zeolite outperforms Cu zeolite [7]. In contrast to Fe zeolites, Cu zeolites also show no $NH_3$-inhibition effects [8].

Starting from the mechanism of SCR by ammonia on Cu zeolite catalysts, Zha et al. [9] identified intermediately formed ammonium nitrate behavior as the key to develop new low-temperature active catalysts. The decomposition of ammonium nitrate is a decisive contributor to SCR activity. In summary, a SCR catalyst formulation enabling conversion of 90 % at 150 °C and optimal $NO_2/NO_x$ ratio in the lab was developed.

Seo et al. [10] found an improved low-temperature activity of Cu-ZSM-5 by adding $ZrO_2$. The $NO_x$ conversion of the Cu-ZSM-5-$ZrO_2$ (2 wt%) catalyst was improved by 10 – 20 % compared to that of Cu-ZSM-5 or Fe zeolite. Hydrothermal aging at temperatures above 700 °C decreased the DeNOx performance of the catalysts significantly, making real application problematic.

Sultana et al. [11] found a Cu-Fe/ZSM-5 catalyst to show higher $NO_x$ conversion compared to Fe-ZSM-5 or Cu-ZSM-5. The presence of small amounts of Cu in xCu-yFe/ZSM-5 catalysts was sufficient to improve the low-temperature $NO_x$ conversion without affecting high-temperature performance significantly. Co-presence of Cu increased the reducibility of Fe and increased strong acid sites in Cu-Fe/ZSM-5. By varying the amount of copper and iron in the catalyst, the $NO_x$ conversion temperature window could be controlled.

Stanciulescu et al. [12] investigated Mn-ion exchanged zeolites (CBV-2314, a MFI zeolite). The catalyst activity increased with the Mn concentration. They found that by promoting the Mn exchanged zeolite with Cu or Ce, the $NO_x$ conversion could be shifted to lower temperatures, with 50 % conversion at about 130 °C in the case of 2.8Cu/2.8MnCBV.

Kim et al. [13] developed a Mn-Fe/ZSM5 catalyst showing promising low-temperature activity. The efficiency of the catalyst decreased upon hydrothermal aging due to the partial transformation of $MnO_2$ to $Mn_2O_3$ and partial sintering of $MnO_x$ on the catalyst surface. However, the remarkably improved hydrothermal stability of the catalyst was reported by the increase of Mn content and/or the addition of Erbium (Er) onto the catalyst.

***Vanadia-based SCR catalysts***

$TiO_2$-supported $V_2O_5$, promoted with $WO_3$ as SCR catalyst was widespread introduced into the market for power plants and diesel engines. However, the $V_2O_5$-$WO_3/TiO_2$ catalyst is associated with

some crucial disadvantages: rapid decrease in activity and selectivity above 550 °C, high toxicity of the vanadium species towards the environment and a high activity for oxidation of $SO_2$ to $SO_3$ [6].
Studies on long-term hydrothermal stability showed that Fe and Cu zeolite catalysts surpass commercially used vanadia-based SCR systems in real diesel application after hydrothermal aging [6, 7, 14].
Another problem is the narrow operating temperature window of 300 – 400 °C, making such a catalyst not suitable for low-temperature applications [5]. A positive point is, compared to other catalytic materials, $V_2O_5$-based SCR leads to less formation of $N_2O$ and is superior resistant to sulfur poisoning [15]. It may, therefore, be suitable for emerging market countries where ultra-low sulfur diesel is not yet available [7].
Moreover, studies on many other types of SCR catalysts are known, such as single- and multi-metal oxide-based SCR catalysts [6, 16-23], active carbon fiber-supported SCR catalysts [5, 24], $Al_2O_3$-supported SCR catalysts [25, 26] or $TiO_2$-supported SCR catalysts [27]. Especially $MnO_x$-based catalysts showed promising activity in the low-temperature range [28]. However, the obstacle of application of many Mn-based catalysts is the poor resistance towards $H_2O$ and $SO_2$. If their composition can be changed to improve $H_2O$ and $SO_2$ resistance, catalysts based on $MnO_x$ could possibly be used in the future [6].
Combinations of improved SCR materials with methods enhancing the decomposition of urea would present an efficient way to enable the overall SCR process at lower temperatures. Nevertheless, in case of $NH_3$-SCR, especially in the low-temperature range, the formation of ammonium nitrate inside the exhaust tract is a critical issue, as it might lead to deposit formation and thereby increased back pressure.

#### *3.3.1.2 Passive-$NO_x$ adsorber*

The working principle of a passive-$NO_x$ adsorber (PNA) is the storage of nitrogen oxides selectively at operating points with incomplete $NO_x$ conversion, meaning at exhaust gas temperatures lower than the light-off temperature of the DeNOx system with the subsequent release of $NO_x$ at higher exhaust temperatures. By applying an appropriate storage material, $NO_x$ is stored at low temperatures and gets desorbed at higher temperatures without active regeneration, meaning no rich phases have to be initiated [29, 30]. Potential materials are typically voluminous structures with large surfaces. Studies on PNAs based on activated carbon [31], $Al_2O_3$ [32], Ba [33], $CeO_2$ [34], Ag [35] or Pt/Pd [30] are available.

As the adsorbents cannot convert the stored $NO_x$ into harmless substances, an additional aftertreatment component is needed. A useful addition might be a downstream SCR system, which can transform the desorbed $NO_x$ by the injected reducing agent after reaching the catalyst's light-off temperature [36].

#### *3.3.1.3 Lean-$NO_x$ trap (LNT)*

Especially in diesel passenger cars, lean-$NO_x$ traps (LNTs) present the most frequently applied system for DeNOx applications besides the SCR technology [37-39]. LNT enables selective storage of $NO_2$ on an appropriate surface. $NO_2$ undergoes a chemical reaction with a storage component (mostly barium compounds) to form (barium) nitrates which get stored. Release of $NO_x$ is introduced by a rich engine operation mode and subsequent reduction by hereby generated hydrocarbons, carbon monoxide and hydrogen, see Figure 9 [3].

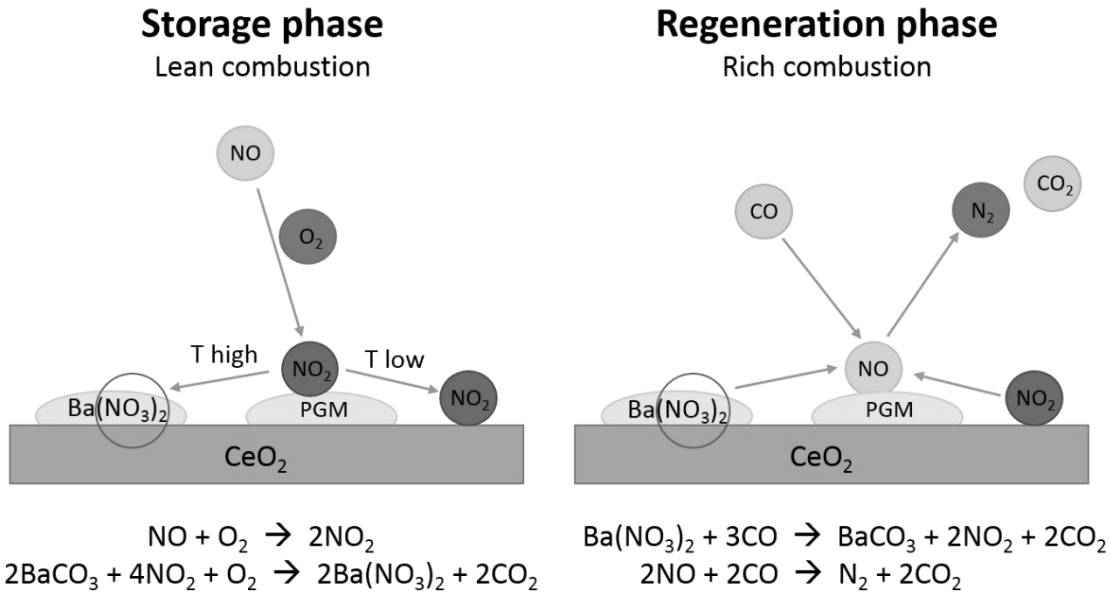


Figure 9: Adsorption and desorption mechanism of a Ba-based lean-$NO_x$ trap. PGM stands for platinum group metal [3].

The typical temperature range of an LNT is 150 – 500 °C. Optimal storage temperature is usually between 200 – 300 °C. At temperatures below 200 °C $NO_x$ storage is limited by the low oxidation rate of NO to $NO_2$ [37].

The storage capacity decreases with increasing $NO_x$ load until complete saturation. Different catalytic materials can be applied and show slightly different performances. Ce compounds show advantages regarding the activity at low temperatures [40].

As regeneration is introduced by a rich engine phase, the application of an LNT leads to higher fuel consumption, thereby negatively influencing the low $CO_2$ emissions of diesel engines. The engine operation strategy is directly coupled to the LNT. Therefore, it cannot be continuously run at optimal operating conditions.

Moreover, combinations of a LNT with a SCR system can be applied. They can generally be divided into so-called active SCR and passive SCR applications. While in case of an active SCR combination an external AdBlue injection is required, in a passive SCR combination, the LNT generates ammonia (by NO and $H_2$) during an excessive engine rich phase (discontinuously), which can be absorbed and used by a downstream SCR catalyst [37, 41]. However, the ammonia formation by the LNT during the regeneration depends on various factors. The emitted ammonia amount increases with the regeneration duration and decreases with increasing LNT temperature. High $NO_x$ load at the start of the regeneration leads to a strong ammonia production [42].

A combination of a $NO_x$ storage catalyst (NSC) and a SCR coated diesel particulate filter (SDPF) was shown to outperform DOC/SDPF configurations [43]. Replacing the DOC by an NSC in a SDPF system is an effective way to ensure the $NO_x$ abatement at lower temperatures and to enlarge the temperature window of the aftertreatment system [42, 44].

As LNT and SCR present the most sophisticated approaches in $NO_x$ aftertreatment, one aim for future emission control systems may be the synergetic combination of both technologies [37].

#### *3.3.1.4 $H_2$-Selective catalytic reduction*

Because of the superior efficiency of $NH_3$, application of $H_2$ did not attract much attention in the selective catalytic reduction of $NO_x$. However, diverse investigations have shown that hydrogen can also act as a selective reductant towards nitrogen oxides, meaning it can preferentially react with $NO_x$ in presence of excess oxygen by means of suitable catalysts [45]. However, ammonia is still the only reductant to reduce $NO_x$ in a stoichiometric ratio of 1:1 [46]. Due to side reactions with oxygen, the SCR selectivity of $H_2$ is lower and hydrogen has to be applied in excess. Therefore, the term *selective* catalytic reduction has to be applied carefully regarding the use of $H_2$. According to literature, platinum (Pt) and palladium (Pd) combined with different supporting materials (e.g. $V_2O_5$, $TiO_2$, $Al_2O_3$) are the most promising catalytic materials for $H_2$-SCR of $NO_x$ [45]. Maximum NO-

conversion efficiencies and product selectivities of 100 % have been described in the literature [47-55]. However, catalytic materials having both high conversion efficiency and high conversion selectivity are still rare, since many of the tested materials tend to form higher amounts of $N_2O$. For Pt-based catalysts, the oxidation state and the acidity/basicity of the support are important factors affecting the catalytic activity and selectivity. The activity of Pd is also highly affected by support materials. Hamada et al. [45] summarized data on catalytic materials for $H_2$-SCR. Nevertheless, regarding real engine applications, these results related to catalytic materials have to be handled with care, since the experimental conditions partially vary considerably from real conditions. Moreover, the materials have to be tested for sufficient hydrothermal and mechanical stability.

Since carrying of hydrogen onboard would be too dangerous, hydrogen needs to be produced on demand. Two approaches seem to be possible: electrolysis of water or application of a reformer [40, 56, 57]. Both lead to extra fuel consumption. In case of electrolysis, electrical energy is needed and in case of a reformer, fuel is needed.

Lab-scale results show that SCR of NO with $H_2$ proceeds at relatively low temperatures compared to $NH_3$-SCR. Therefore, $H_2$-SCR could be a promising approach for removal of $NO_x$ of modern lean-burn engines, which exhibit cooler exhaust due to improved thermal efficiency. However, the investigations also showed that in the high-temperature range, the efficiency of $NO_x$ reduction decreases [45]. Moreover, the level of development for suitable catalytic materials is very low, especially for real engine applications. Additionally, safety aspects have to be considered since hydrogen can form highly explosive mixtures in the presence of oxygen.

#### *3.3.1.5 SCR pre-turbo*

The aim of this approach is to use the considerably higher temperature level present upstream of the turbocharger. Gas expansion and energy absorption by the turbocharger cools down the exhaust gas leading to a decreased temperature level downstream of the turbine. However, heat would also be required for the activation of catalysts [58].

In general, a distinction between two approaches can be made: either only AdBlue injection upstream of the turbocharger or injection in combination with SCR catalyst positioned upstream of the turbocharger [59]. The principle of the first approach is an injection of the urea solution already after the outlet valves in order to decompose urea effectively before the downstream heat sinks. In this case, also the DOC has to be placed in front of the dosage location and the turbocharger, in order to avoid oxidation of the produced ammonia at the DOC, see Figure 10 [58].

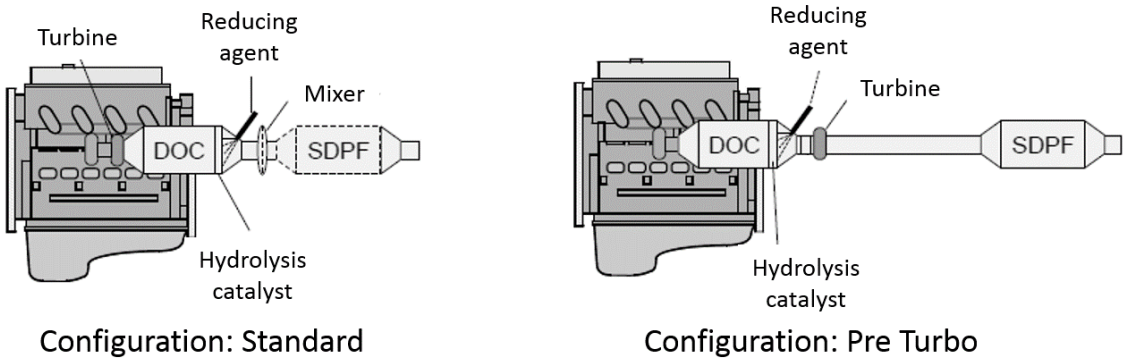


Figure 10: Configurations for standard and pre-turbo dosage investigated by Brück et al. Adapted with permission from [58].

The different configurations shown in Figure 10 were investigated by Brück et al. [58]. There is the standard configuration with the DOC catalysts and urea dosing positioned downstream of the turbine and a setup with a DOC and urea dosing upstream of the turbine. Additionally, a configuration called pre-Turbo “plus” with an extra SCR catalyst has been investigated. A crucial temperature advantage in the new European driving cycle (NEDC) was found at the reducing agent injection position located upstream turbo. In this position, the temperature difference was up to 100 K in the first 800 s during acceleration and up to 125 K afterward [58]. The approach is worth further investigations, especially as the extra fuel consumption (due to back pressure and less energy for the turbocharger) is only 1.5 to 2 % in the NEDC without profound implemented optimization measures. Although the temperatures upstream of the SDPF were identical in each case, the pre-turbo design with dosing in front of the turbocharger achieves better ammonia preparation and uniform ammonia distribution. However, the material of the turbocharger has to withstand reactions with ammonia in order to inhibit damages by corrosive processes [58].

Regarding the second approach, a pre-turbine position of the SCR catalyst without rearranging the DOC and particulate filter, the temperature level in front of the SCR catalyst is even higher. However, in this case, several additional problems occur along with the reduced power of the turbocharger: fast-SCR reaction with $NO_2$ cannot take place since almost only NO is present in the raw exhaust gas. Nearly no passive soot oxidation by $NO_2$ is possible on the DPF, meaning a higher active DPF regeneration frequency is necessary. Additionally, HC/CO poisoning of the SCR catalyst may occur due to exposure to higher amounts of HC/CO. The hydrocarbons may be adsorbed in competition

with $NH_3$ and $NO_x$, and therefore hinder the SCR reaction or may lead to deposits as coke on the zeolite surface or enter the pores, depending on the size. In addition, the high thermal stress of the SCR catalyst has to be expected. Particulate matter is usually too large to enter the zeolite pores but can also be converted. It can also negatively affect the performance by fouling the catalyst surface.

In a study carried out by Günter et al. [59], various reactions including NO/$NH_3$ oxidation, standard and fast SCR have been tested in a temperature range of 180 – 600 °C on a copper-exchanged zeolite (Cu-SSZ-13) catalyst positioned upstream of the turbocharger. The study shows an increased pressure to result in a strikingly higher DeNOx activity, especially under standard-SCR conditions, which is mainly due to higher NO oxidation to $NO_2$ in the gas phase and a higher residence time. The influence of hydrocarbons was also investigated by addition of propene to the feed gas. Even though propene led to a temporary competition between SCR reaction and propene oxidation, the decrease in DeNOx activity can be overcompensated by the higher pressure and temperature within a pre-turbine configuration with no need for regeneration steps. In contrast, $SO_2$ caused severe deactivation at low temperature but had no influence at high temperature.

Thus, an implementation of SCR catalysts upstream of the turbocharger would result in an earlier light-off by avoiding the heat sink turbocharger. As a further benefit, the pressure built up by the turbocharger (typically up to 5 bar) would lead to an increased residence time of the reactants at the catalyst, which would make a smaller total catalyst size possible as well as a decreased back pressure penalty [59, 60]. Altogether, a SCR catalyst positioned upstream of turbocharger leads to a higher temperature level at the SCR functionality, but at the expense of increased thermal stress and reduced flow energy for the turbocharger and increased fuel consumption.

#### *3.3.1.6 SDPF/ SCR active coating on diesel particulate filter (DPF)*

The idea of this technology is the integration of SCR functionality in a diesel particulate filter to enable a positioning closer to the engine and thereby ensuring a higher temperature level. Therefore, the catalyst reaches light-off temperature faster after a cold start [61-64]. SDPF is applied as series technology in various passenger cars [61]. In order to combine the SCR catalyst and DPF, the SCR washcoat is directly applied on the porous wall flow substrate of the DPF. High amounts of SCR washcoat loading increase the SCR efficiency, but also the back pressure, which limits catalyst/filter loading capacity [62, 65]. A trade-off between filtration of soot and $NO_x$ reduction

exists, since efficient soot filtration requires low porosity, while elimination of $NO_x$ is favored by high porosity leading to a higher surface and subsequently higher possible amount of SCR coating [63, 66]. Wylie et al. [64] show that during the NEDC, dosing of AdBlue could be started at about 380 s with a SDPF setup while upon application of a separated filter and SCR catalyst, dosing could not be started until 820 s. As a result, a considerably lower amount of cumulated $NO_x$ was observed. Unlike with SCR solutions downstream of the DPF, by application of a SDPF, the influence of soot on the SCR process has to be taken into account. Fischer et al. [67] concluded that the main impact of soot on the SCR process is caused by affecting the local $NO_2/NO_x$ ratio for the SCR reaction, making the fast SCR reaction more difficult. Moreover, other issues have to be considered when applying SCR on filter systems: high-temperature gradients, making controlled storage of ammonia on the SCR catalyst difficult, a short mixing length, complicating appropriate distribution of the ammonia stream, and increased thermal stress for SCR coating due to filter regenerating events [67]. Besides a higher temperature level, integration of the SCR functionality into the DPF also results in significantly enhanced packaging by improved space and weight utilization [68]. All in all, integrated SCR/DPF systems are promising for an extended exhaust gas temperature range (as required for real driving emissions, RDE) at low $CO_2$ emissions. A combination of a close-coupled SDPF system with a second SCR catalyst and/or a LNT might be promising regarding upcoming emission legislations [62]. In terms of soot aftertreatment, a separate upstream DPF would be advantageous, since passive regeneration of the filter by the engine out $NO_2$, also called CRT effects, is hindered by the reduced amount of nitrogen oxides.

## 3.3.2 Generation of reducing agent

### *3.3.2.1 Coatings to support decomposition of urea*

The decomposition of urea is an important step in the SCR process as it supplies the reducing agent ammonia. Decomposition of urea requires heat, taken from the exhaust gas [69]. Today's SCR catalysts themselves (e.g. metal-exchanged zeolites or vanadia-based catalysts) also exhibit some catalytic activity in decomposing urea [70, 71]. However, many applications include separate heterogeneous hydrolysis catalysts to enhance the decomposition of urea. Nevertheless, also in this case, temperatures of about 200 °C are needed for quantitative conversion of urea to ammonia [72].

The exhaust temperatures of some engine operating points might be significantly lower (e.g. at cold start or low-load phases). Since modern SCR catalysts enable $NO_x$ conversion rates of 90 % at 165 °C, catalytic materials that can decompose urea at lower temperatures would, therefore, allow for

the whole SCR process to proceed at lower temperatures, without influencing fuel consumption [9]. Another crucial problem associated with the incomplete decomposition of urea is the formation of byproducts [70, 73, 74]. These deposits can harm the long-term catalytic performance of the SCR catalyst [71]. The most common way of decomposition at moderate temperatures proceeds in three steps [75]: Since urea is provided as a 32.5 wt% solution in water, water evaporates in the first step. Subsequently, after evaporation of urea, the thermolysis of urea leads to the formation of one equivalent of isocyanic acid and ammonia (equation 9). In the third step, isocyanic acid is hydrolyzed to yield a second equivalent of ammonia and carbon dioxide (equation 10) [72].

*Thermolysis of urea:* $H_2N\text{-}CO\text{-}NH_2 \rightarrow HNCO + NH_3$ (equation 9)

*Hydrolysis of HNCO:* $HNCO + H_2O \rightarrow NH_3 + CO_2$ (equation 10)

Today, commercially employed catalysts for decomposing urea mainly use $TiO_2$ as the catalytically active material. $TiO_2$ catalyzes the hydrolysis of isocyanic acid and the thermolysis of urea [72]. Nevertheless, temperatures of at least 180 - 200 °C are required for quantitative thermolysis. By catalyzing the hydrolysis of isocyanic acid, $TiO_2$ hinders the formation of byproducts [76]. Kröcher and Bernhard investigated the catalytic activity of different materials in decomposing urea [72, 77], see Figure 11.

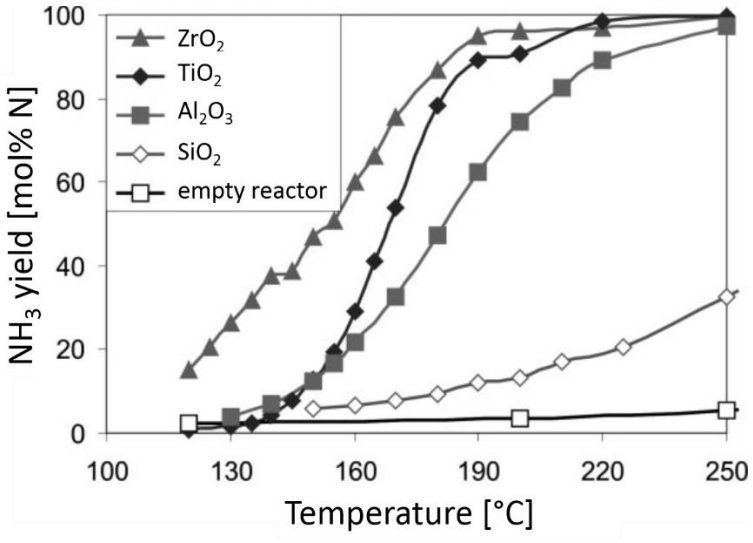


Figure 11: Decomposition of urea in gas phase catalyzed by various materials. Adapted with permission from [77], © Wiley-VCH.

As shown, under the applied experimental conditions $ZrO_2$ exhibits higher efficiency in urea decomposition compared to $TiO_2$. However, real engine tests have to be carried out to ensure sufficient hydrothermal stability and durability of the material. On a lab scale, many more materials have been screened, e.g. a niobium-ceria-based catalytic material [78]. However, it should be noticed that besides catalytic activity, hydrothermal and mechanical stability are important conditions to be considered for real engine applications.

#### *3.3.2.2 $NH_3$ generation outside of exhaust tract*

***Approach 1: Urea preparation in an exhaust bypass***

One way to enable $NH_3$ generation outside of the exhaust tract is the application of an exhaust bypass providing a sufficiently high temperature for decomposition of urea [79-84].

The $BNO_x$ system® of Twintec enables the generation of the reducing agent by using the heat of a partial exhaust flow in an upstream turbo bypass and an electrically heated decomposition catalyst [79].

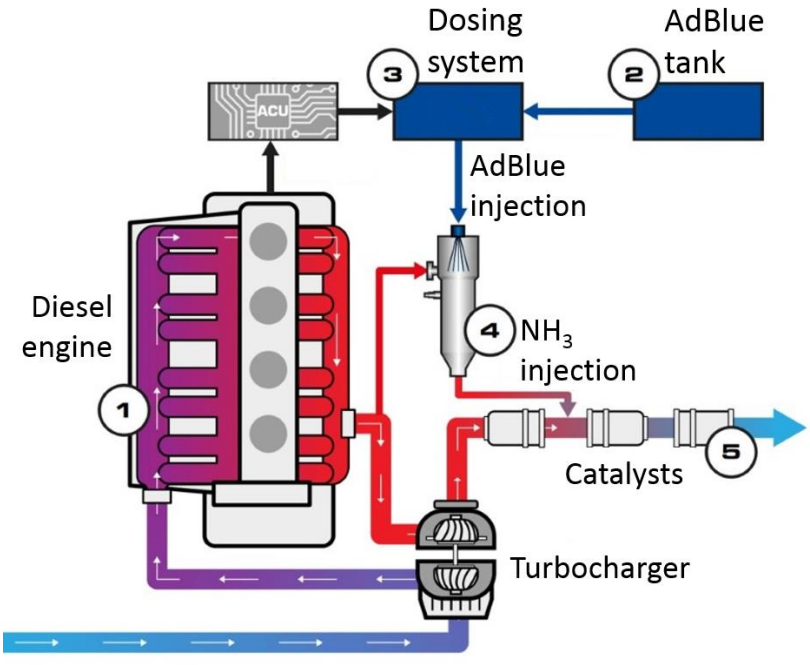


Figure 12: Operating principle of the $BNO_x$ system. Adapted with permission from [85], © Baumot Group AG.

Figure 12 shows a potential implementation of a $NH_3$ generating device into an exhaust aftertreatment system. The partial exhaust flow is taken from upstream the turbocharger, leading to a higher temperature level inside the bypass. The ammonia produced by the $NH_3$ generator, using a partial exhaust flow and a heated hydrolysis catalyst, can directly be injected into the exhaust flow. Thereby, the reducing agent $NH_3$ itself enters the exhaust tract and urea does not have to undergo thermolysis/hydrolysis first [79].

A similar concept was presented by Kowatari et al. [82]. The device consisted of an electrically heated bypass and a hydrolysis catalyst inside the bypass. Engine tests using the bypass system performed at a commercial truck diesel engine with DOC, SCR catalyst and ASC were compared to results derived from a conventional SCR device. In each of the runs, the heated bypass outperformed the conventional device. At 145 °C $NO_x$ conversions of 95 % were obtained, 99 % of nitrogen oxides were reduced at 160 °C. However, the heating process was associated with extra fuel consumption.

Another study on a turbo bypass device for urea decomposition was published by Döring et al. [84]. A hydrolysis catalyst arranged parallel to the turbocharger and a close-coupled NO oxidation catalyst were applied to a heavy-duty engine. Improved hydrolysis was found. Furthermore, the authors mentioned a benefit of the turbocharger bypass concerning deposit formation since the temperatures prior to the hydrolysis catalyst were significantly higher.

***Approach 2: Urea preparation using the enzyme urease***

Besides production of ammonia by heating, other concepts would be conceivable regarding fuel saving. Ureases are biological catalysts (enzymes), which are widespread in nature. Ureases decompose one equivalent of urea to form two equivalents of ammonia, with carbamic acid occurring as intermediate [86]. The property, which makes ureases an interesting alternative for application as part of a SCR system is the fact that ureases can decompose urea already at room temperature. Therefore, patents are known, applying ureases in SCR devices [87-91].

However, the biggest problem associated with the practical use of ureases for $NH_3$ generation, especially in onboard applications, is their very low stability compared to conventional catalysts, normally applied in exhaust aftertreatment. Like other enzymes, ureases can be denatured by various influences. Once urease is denatured, it can no longer catalyze the decomposition of urea. Besides through a high substrate concentration, ureases can be denatured e.g. by high temperatures [92]. In aqueous solutions, ureases as well denature with time, with the speed of denaturation depending on environmental conditions, i.e., pH value and temperature [90].

A way for increasing the stability of ureases is the so-called immobilization technique, in which the enzyme is bound to the surface of a carrier. Immobilization of urease leads to improved operational stability, which allows for several practical applications to be carried out [92]. However, much effort would be required, altering an enzyme for the onboard application.

#### *3.3.2.3 Ammonia storage and delivery system (ASDS)*

The ammonia storage and delivery system (ASDS) of Amminex Emissions Technology stores ammonia chemically within the solid strontium complex $Sr(NH_3)_8Cl_2$, called AdAmmine® [93]. By application of AdAmmine®, ammonia can be released at low temperatures (55 – 80 °C) in a controlled thermal desorption process [94]. Since 1 mole of AdAmmine® contains 8 mol $NH_3$, the volumetric ammonia capacity of AdAmmine® is twice the capacity of AdBlue. By dosing ammonia directly into the exhaust tract, the risk of deposit formation and resulting consequences of increased back pressure can be hindered [94].

AdAmmine® is stored in metal cartridges [95]. The cartridges are equipped with electrical heaters for ammonia desorption. When released from the cartridges, gaseous ammonia flows to the dosing unit. Sassi et al. [90] installed the ASDS system in a 2010 Mercedes C220 CDI equipped with a 2.2 L diesel engine in order to investigate DeNOx performance during the NEDC and real city driving [95].

During NEDC 55 % of $NO_x$ is converted in the case of the ASDS injection strategy, whereas the AdBlue injection strategy reaches 47 %. Both tests were performed with a preloaded ammonia buffer. The improvement results from the ability of ASDS to inject within a larger temperature window and use the conversion capacities of the SCR catalyst below 180 °C.

All in all, this technology brings several advantages: it works as soon as the SCR catalyst reaches light-off temperature, clogging of the exhaust tract can be prevented since AdBlue is not present in the exhaust tract. This goes along with the disadvantages of additional heating requirements for ammonia desorption, entailing extra fuel consumption and increased $CO_2$ emissions. Moreover, depending on the individual application, replacing cartridges is more difficult compared to refilling AdBlue and no infrastructure for AdAmmine® cartridges exists.

#### *3.3.2.4 Alternative precursor for ammonia generation*

This concept focusses on the application of an alternative or second precursor besides urea, which is suitable for onboard generation of ammonia at lower temperatures.

The following alternative precursors have been discussed for onboard application in the literature:

- guanidinium formate [46, 96-99]
- ammonium formate [46, 70, 96]
- ammonium carbamate [96, 100-102]
- ammonium carbonate [101, 102]
- methanamide [46, 96, 103]
- solid urea [46, 102, 104]

For decomposition of guanidinium formate and ammonium formate even higher temperatures are required compared to AdBlue, implying that for low-temperature applications, e.g. a heated bypass system, as described above, has to be applied but again leading to extra fuel consumption [97-99].

Due to the low temperature of decomposition (~60 °C), ammonium carbamate and ammonium carbonate might have the potential for low-temperature applications. In a study by Krüger et al. [105] powdery solid ammonium carbamate is stored as pellets. A heat transfer medium is electrically heated and sprayed from below onto the pellets. The heated ammonium carbamate decomposes to $NH_3$ and $CO_2$. Due to the electrical heating principle, an extra fuel consumption of between 1 - 3.5 % has been observed. A similar setup in which a heat transfer medium was also sprayed from below on solid ammonium carbamate was presented by Lacin et al [106]. The system was tested on a Dodge RAM pickup truck motorized by a 5.9 L 6-cylinder diesel engine. As expected the system showed good $NO_x$ reduction values of 80 - 90 % in transient driving cycles. However, as reported by the authors, much effort is necessary to make the system ready for serial production. Up to now, ammonium carbamate does not seem to be commercially used as ammonia precursor in mobile applications [96]. This might be due to the fact that ammonium carbamate decomposes readily from ambient temperatures to ammonia and carbon dioxide. The ammonia partial pressure of ammonium carbamate is 3 bar already at 80 °C, making storage inside a pressure tank necessary [46].

Kim et al. [102] tested solid ammonium carbonate and solid urea as ammonia precursor. Ammonium carbonate is more suitable for low-temperature vehicle applications due to lower decomposition temperature. They also used a separate reactor in which ammonium carbonate was stored as a solid. By electrical heating, the salt decomposed to a mixture of $NH_3$, $CO_2$ and $H_2O$. The gas mixture can subsequently be injected into the exhaust tract by a dosing module. Steady-state and transient tests were carried out, using a 4-cylinder DI diesel engine. It was found that $NO_x$ amounts were reduced well during the steady and transient mode tests.

Application of solid urea compared to AdBlue might lead to less cooling effects of the exhaust and downstream located components since no water has to be vaporized. Difficulties may arise from the hygroscopic behavior of urea granules [46].

According to Peitz [96], upon application of an $Au/TiO_2$ catalyst, quantitative decomposition of methanamide to ammonia is possible already at 145 °C [80]. Therefore, the application of methanamide for low-temperature applications might be feasible.

In general, the application of alternative precursors leads to several problems:

- dosing of solid precursor is more complicated compared to a liquid,
- no infrastructure exists for any of the presented alternative ammonia precursors,
- low temperature of generating ammonia can entail low thermal stability during handling, storage problems (e.g. ammonium carbamate and carbonate)
- compared to urea toxicity is more problematic for most of the presented precursors.

#### *3.3.2.5 Modification of AdBlue*

The aim of this technique is the addition of additives to AdBlue in order to enhance low-temperature properties of the precursor, e.g. enhancing the evaporation behavior and thereby minimizing deposit formation.

A crucial problem associated with low exhaust temperatures is the incomplete decomposition of urea below 350 °C, leading to the formation of undesired byproducts [69].

As AdBlue is dosed into the exhaust tract, spray impingement leads to cooling of the exhaust pipe by heat transfer and the droplets might form a film on the pipe surface, as shown in Figure 13. The temperature of the pipe might be 80 – 120 °C lower than the exhaust gas temperature, which is too cold to allow complete decomposition [107, 108].

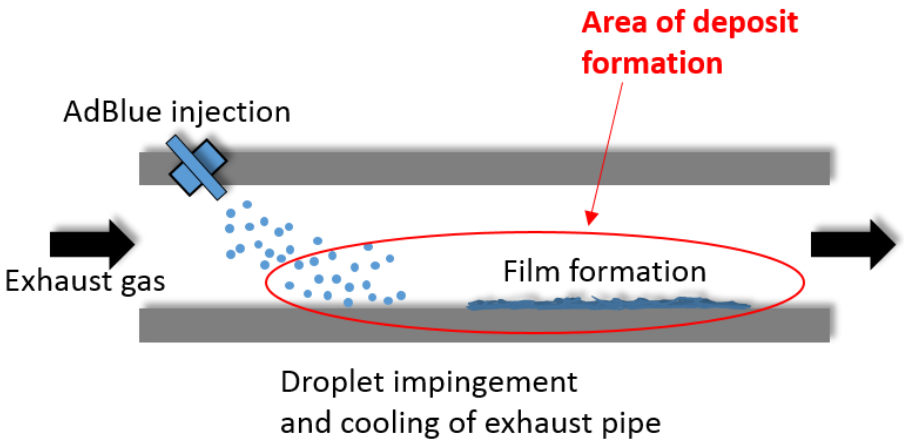


Figure 13: Mechanism of deposit formation inside the exhaust tract. [109]

Thereby, incomplete decomposition of urea and formation of deposits is strongly favored [109, 110]. Deposits inside the exhaust tract can lead to reduced fuel efficiency, particulate filter failure, damage to the SCR catalyst bed and even engine failure as a consequence of the excessively increased back pressure [111].

A possibility for the enhancement of spray properties and thereby reducing potential byproduct formation is the addition of surface-active molecules. Lowering the surface tension, by for example a factor of two, allows a decreased injection pressure by one half for the same degree of AdBlue nebulization, resulting in energy savings [107, 109, 112, 113].

Reduced surface tension is advantageous, as it leads to a better dispersion due to enhanced wettability of the reductant spray in the exhaust tract. Moreover, smaller droplets are formed [112], thereby vaporization and decomposition of the droplets in gaseous ammonia is promoted [114] by increased heat transfer before reaching the colder wall [107]. More precisely, according to Wasow et al. [112], the so-called dynamic surface tension is decisive for enhanced spray properties.

An already commercialized approach of mixing additives to AdBlue is the product Diaxol® from TOTAL. It contains surfactants, which prevent the formation of deposits (mainly cyanuric acid) by enhancing spray properties, in order to avoid clogging of the exhaust tract [109].

TOTAL carried out engine tests and long-term field tests with Diaxol. It was shown that Diaxol significantly reduced white deposit formation. Further tests on DeNOx efficiency in the NEDC were carried out in passenger car SCR systems. Even a small improvement of cumulated $NO_x$ reduction was found for Diaxol with 65 % compared to conventional AdBlue with 64 % $NO_x$ lowering. Therefore, the modified AdBlue is especially recommended for vehicles with a low level of exhaust temperature [109]. Moreover, Ayyappan showed that the addition of small amounts of aldehydes to AdBlue results in the formation of fewer deposits at low exhaust temperatures. Especially formaldehyde showed a positive effect, however, due to its toxicity application of formaldehyde as additive should be avoided [111].

## 3.4 Summary and outlook

Low exhaust temperatures are challenging for the abatement of $NO_x$ emissions since the commercially applied exhaust aftertreatment systems cannot always reach their operating temperature. As a decline of exhaust temperature due to enhanced thermal engine efficiency can be predicted, improvements of the state-of-the-art systems and new technical approaches are necessary. Moreover, since real driving emission tests for type approval will be introduced in the future, the aftertreatment systems have to work in a wider engine operation window. In summary, some promising approaches have been identified and pointed out in the present review. They are promising regarding the improvement of the aftertreatment process of nitrogen oxides at low exhaust temperatures. However, at the current state of the art, no technology is able to completely replace today's DeNOx systems. For some approaches further research is necessary. In the case of $NH_3$-SCR, an efficiency enhancement can mainly be accomplished by an improved and earlier supply of ammonia and a faster catalyst light-off. Some approaches may function as additional measures to conventional systems for achieving higher conversion, but often at the expense of complexity, overall costs and $CO_2$ balance.

Additionally, it should be mentioned that all the approaches presented herein are referred to exhaust aftertreatment strategies. Inner-engine approaches such as the widely applied exhaust-gas recirculation (EGR) or injection of water into the cylinder are also possible [115]. However, as these measures are directly coupled to the engine, efficiency-optimized operation is often hampered.

## 3.5 References


[1] P. Braun, J. Gebhard, H.-P. Rabl, *Low Temperature DeNOx*, Final Report FVV Project 1115, Frankfurt am Main, **2017**.

[2] A. Mackensen, T. Braun, F. Duvinage, *4th IAV Conf. MinNOx*, Berlin, June **2012**.

[3] K. Mollenhauer, H. Tschöke, *Handbuch Dieselmotoren*, 3, Springer, Berlin, **2007**.

[4] G. Cavataio, *23rd North America Catalysis Society meeting*, Louisville, KY, June **2013**.

[5] M. Fu et al., *Catalysis Science & Technology* **2014,** *4 (1)*, 14-25.

[6] J. Li et al., *Catalysis Today* **2011,** *175 (1)*, 147-156.

[7] B. Guan, R. Zhan, H. Lin, Z. Huang, *Applied Thermal Engineering* **2014,** *66 (1)*, 395-414.

[8] I. Nova et al., 3*rd IAV Conf. MinNOx*, Berlin, June **2010**.

[9] Y. Zha et al., *6th IAV Conf. MinNOx,* Berlin, June **2016**.

[10] C. K. Seo et al., *Chemical Engineering Journal* **2012,** *191*, 331-340.

[11] A. Sultana, M. Sasaki, K. Suzuki, H. Hamada, *Catalysis Communications* **2013,** *41*, 21-25.

[12] M. Stanciulescu et al., *Applied Catalysis B: Environmental* **2012,** *123*, 229-240.

[13] Y. J. Kim et al., *Applied Catalysis B: Environmental* **2012,** *126*, 9-21.

[14] G. Cavataio et al., *SAE Technical Paper* Series. **2007, 2007-01-1575**.

[15] H. Yamamoto et al., *6th IAV Conf. MinNOx*, Berlin, June **2016**.

[16] R. Marques, R. Rohe, D. Harris, C. Jones, *4th IAV Conf. MinNOx*, Berlin, June **2012**.

[17] R. Q. Long, R. T. Yang, R. Chang, *Chemical Communications* **2002,** *5*, 452-453.

[18] G. Qi, R. T. Yang, R. Chang, *Applied Catalysis B: Environmental* **2004,** *51, 2*, 93-106.

[19] H. Chang et al., *Catalysis Communications* **2012,** *27*, 54-57.

[20] D. Meng et al., *Applied Catalysis B: Environmental* **2018**, 221, 652-663.

[21] Z. Liu et al., *Applied Surface Science* **2018**, 428, 526-533.

[22] L. Zhang et al., *Industrial & Engineering Chemistry Research* **2018**, 57, 490-497.

[23] Y. Geng et al., *Industrial & Engineering Chemistry Research* **2018,** 57, 856-866.

[24] M. Yoshikawa, A. Yasutake, I. Mochida, *Applied Catalysis A: General* **1998,** *173*, *2*, 239-245.

[25] Q. Zhang et al., *Catalysis Today* **2011,** *175*, *1*, 171-176.

[26] J. P. Chen, R. T. Yang, M. A. Buzanowski, J. E. Cichanowicz, *Industrial & Engineering chemistry research* **1990,** *29*, *7*, 1431-1435.

[27] Z. Wu, R. Jin, Y. Liu, H. Wang, *Catalysis Communications* **2008,** *9*, *13*, 2217-2220.

[28] S. Zheng et al., *RSC Advances* **2018**, 8, 1979-1986.

[29] A. Mackensen, *Ph.D. Thesis*, TU Clausthal **2012**.

[30] J. R. Theis, C. K. Lambert, *Catalysis Today* **2015,** *258*, 367-377.

[31] A. Rubel, J. Stencel, S. Ahmed, in *Symposium on chemistry of flue gas cleanup processes*, Denver **1993**.

[32] Y. Ji, S. Bai, M. Crocker, *Applied Catalysis B: Environmental* **2015,** *170*, 283-292.

[33] A. Funk, *Ph.D. Thesis*, Universität Hannover **2001**.

[34] S. Jones, *Ph.D. Thesis*, University of Kentucky **2016**.

[35] S. Ren et al., *Catalysis Today* **2015,** *258*, 378-385.

[36] C. Henry et al., 17th *Directions in Energy-Efficiency and Emissions Research (DEER) Conference*, Detroit, October **2011**.

[37] K. Hadl et al., *Proc. of the 35th International Vienna Motor Symposium*, Austrian Society of Automotive Engineers, Vienna **2014**.

[38] G. Zikoridse, J. Kopte, U. Hofmann, R. Lindner, *Proc. of the 7. Dresdner Motorenkolloquium*, HTW Dresden **2007**.

[39] H. J. Neußer et al., *Proc. of the 34th International Vienna Motor Symposium, Austrian Society of Automotive Engineers*, Vienna **2013**.

[40] T. Wittka, B. Holderbaum, B. Lüers, T. Körfer, *Proc. of the 22nd Aachen Colloquium Automobile and Engine Technology Aachen Colloquium*, Aachen **2013**.

[41] J. Balland, M. Peters, B. Schreurs, *6th IAV Conf. MinNOx*, Berlin, June **2016**.

[42] J. M. Seo et al., *Proc. of the 24th Aachen Colloquium Automobile and Engine Technology 2015*, Aachen Colloquium, Aachen **2015**.

[43] C. Beidl et al., *Proc. of the 9th International Exhaust Gas and Particulate Emissions Forum*, AVL, Ludwigsburg **2016**.

[44] L. Mussmann et al., *Proc. of the 23rd Aachen Colloquium Automobile and Engine Technology 2014*, Aachen Colloquium, Aachen **2014**.

[45] H. Hamada, M. Haneda, *Applied Catalysis A: General* **2012,** *421*, 1-13.

[46] O. Kröcher, M. Elsener, E. Jacob, *Proc. of the 9th International Exhaust Gas and Particulate Emissions Forum*, AVL, Ludwigsburg **2008**.

[47] T. Nanba et al., *Applied Catalysis B: Environmental* **2003,** *46*, *2*, 353-364.

[48] P. Wu et al., *Catalysis Today* **2010,** *158, 3*, 228-234.

[49] A. M. Efstathiou, C. N. Costa, J. L. G. Fierro, *Patent WO2003068390A1*, **2006**.

[50] C. Costa et al., *Journal of Catalysis* **2002,** *209, 2*, 456-471.

[51] C. Costa, A. Efstathiou, *Environmental Chemistry Letters* **2004,** *2, 2*, 55-58.

[52] B. Wen, *Fuel* **2002,** *81, 14*, 1841-1846.

[53] G. Qi, R. T. Yang, L. T. Thompson, *Applied Catalysis A: General* **2004,** *259*, *2*, 261-267.

[54] G. Qi, R. T. Yang, F. C. Rinaldi, *Journal of Catalysis* **2006,** *237*, *2*, 381-392.

[55] G. L. Chiarello et al., *Journal of Catalysis* **2007,** *252*, *2*, 137-147.

[56] M. Gottschling, A. Horn, B. Hupfeld, *7th Emission Control*, Dresden, May **2014**.

[57] S. Pischinger et al., *5th IAV Conf. MinNOx,* Berlin, June **2014**.

[58] R. Brück et al., *Proc. of the 36th International Vienna Motor Symposium*, Austrian Society of Automotive Engineers, Vienna **2015**.

[59] T. Günter et al., *Applied Catalysis B: Environmental* **2016,** *198*, 548-557.

[60] T. Rammelt, C. Hauck, R. Gläser, O. Deutschmann, *Pre-Turbo SCR*, Final Report FVV Project 1120, Frankfurt am Main, **2013**.

[61] H. Lörch et al., *Proc. of the 22nd Aachen Colloquium Automobile and Engine Technology*, Aachen Colloquium, Aachen **2013**.

[62] S. Stiebels, T. Neubauer, T. Müller-Stach, *4th IAV Conf. MinNOx*, Berlin, June **2012**.

[63] I. Grisstede et al., *Proc. of the 21. Aachen Colloquium Automobile and Engine Technology* Aachen Colloquium, Aachen **2012**.

[64] J. Wylie, D. Bergeal, D. Hatcher, P. Phillips, *5th IAV Conference: MinNOx*, Berlin, June **2014**.

[65] M. Dieterle et al., *4th IAV Conference: MinNOx*, Berlin, June **2012**.

[66] K. Harth et al., *Proc. of the 33rd International Vienna Motor Symposium*, Austrian Society of Automotive Engineers, Vienna **2012**.

[67] M. Fischer et al., *Proc. of the 23rd Aachen Colloquium Automobile and Engine Technology*, Aachen Colloquium, Aachen **2014**.

[68] C. Becker et al., *in 7th Emission Control, D*resden, May **2014**.

[69] P. M. Schaber et al., *Thermochimica Acta* **2004,** *424*, *1*, 131-142.

[70] O. Kröcher, D. Peitz, *4th IAV Conf.: MinNOx*, Berlin, June **2012**.

[71] M. Eichelbaum, R. J. Farrauto, M. J. Castaldi, *Applied Catalysis B: Environmental* **2010,** *97, 1*, 90-97.

[72] A. M. Bernhard et al., *Catalysis Science & Technology* **2013,** *3*, *4*, 942-951.

[73] S. Sebelius, T. T. Le, L. J. Pettersson, H. Lind, *Chemical Engineering Journal* **2013,** *231*, 220-226.

[74] A. Lundström, B. Andersson, L. Olsson, *Chemical Engineering Journal* **2009,** *150*, *2*, 544-550.

[75] C. S. Sluder, J. M. Storey, S. A. Lewis, L. A. Lewis, *SAE Technical Paper Series* **2005**, 0205-01-1858.

[76] A. M. Bernhard et al., *Applied Catalysis B: Environmental* **2012,** *115*, 129-137.

[77] D. Peitz et al., *Chemie Ingenieur Technik* **2013,** *85*, *5*, 625-631.

[78] M. Casapu et al., *Applied Catalysis B: Environmental* **2011,** *103*, *1*, 79-84.

[79] W. S. Doelling et al., *Proc. of SAE-China Congress 2014: Selected Papers*, Springer, Berlin, **2015**.

[80] A. Heubuch, *Ph.D. Thesis*, TU München **2014**.

[81] R. Brück, P. Hirth, T. Häring, *Patent WO2008/040628*, **2008**.

[82] T. Kowatari et al., *SAE Technical Paper Series* **2006**, 2006-01-0642.

[83] A. Nishioka, K. Amou, H. Yokota, T. Murakami, *SAE Technical Paper Series* **2008,** 2008-01-1026.

[84] A. Döring, G. Emmerling, D. Rothe, *Proc. of the 33rd International Vienna Motor Symposium*, Austrian Society of Automotive Engineers, Vienna **2012**.

[85] Baumot Group AG, *BNOx Funktionspronzip*, Glattpark **2017**.

[86] B. Krajewska, *Journal of Molecular Catalysis B: Enzymatic* **2009,** *59*, *1*, 9-21.

[87] W. Münch, L. Walz, R. Hilpert, *Patent DE4425420*, **1995**.

[88] G. Pajonk, L. Hofmann, M. Weigl, G. Wissler, *Patent WO99/56858*, **1999**.

[89] B. Monge-Bonini, F. Dougnier, J. J. Van Schaftingen, *Patent EP 2927452A1*, **2015**.

[90] B. Monge-Bonini, J. J. Van Schaftingen, P. De Man, F. Dougnier, *Patent WO2016/009083A1*, **2016**.

[91] F. Dougnier, D. Madoux, B. Monge-Bonini, J. J. Van Schaftingen, *Patent WO 2015/082675A1*, **2015**.

[92] Y. Qin, J. M. Cabral, *Biocatalysis and Biotransformation* **2002,** *20, 1*, 1-14.

[93] K. F. Hansen et al., *4th IAV Conf. MinNOx*, Berlin, June **2012**.

[94] T. Johannesen, *4th IAV Conf. MinNOx,* Berlin, June **2012**.

[95] A. Sassi et al., *Proc. of the 22nd Aachen Colloquium Automobile and Engine Technology* Aachen Colloquium, Aachen **2013**.

[96] D. Peitz, *Ph.D. Thesis,* ETH Zurich **2012**.

[97] D. Peitz et al., in *Förderkreis Abgasnachbehandlungstechnologien für Dieselmotoren*, FAD Conference, Dresden **2011**.

[98] L. S. Rangel, J. R. de la Rosa, C. J. L. Ortiz, M. J. Castaldi, *Journal of Analytical and Applied Pyrolysis* **2015,** *113*, 564-574.

[99] B. Hammer, H.-P. Krimmer, B. Schulz, E. Jacob, *Patent WO2008077587A1*, **2014**.

[100] B. Ramachandran, A. M. Halpern, E. D. Glendening, *The Journal of Physical Chemistry A* **1998,** *102, 22*, 3934-3941.

[101] G. Fulks et al., *SAE Technical Paper Series* **2009**, 2009-01-0907.

[102] H. Kim, C. Yoon, J. Lee, H. Lee, *SAE Technical Paper Series* **2014**, 2014-01-1535.

[103] O. Kröcher, M. Elsener, E. Jacob, *Applied Catalysis B: Environmental* **2009,** *88*, *1*, 66-82.

[104] S. Käfer, *Ph.D. Thesis,* TU Kaiserslautern **2004**.

[105] M. Krüger, P. Nisius, V. Scholz, A. Wiartalla, *MTZ worldwide* **2003,** 64, 6, 14-17.

[106] F. Lacin et al., *SAE Technical Paper Series* **2011**, 2011-01-2207.

[107] P. Schmelzle, L. Oro-Urrea, S. Escoffier, F. Douce, *Patent CA 2679088C*, **2016**.

[108] J. Han et al., *International Journal of Automotive Technology* **2017**, 18, 6, 951-957.

[109] S. Dumas, M. Lopes, *4th IAV Conf. MinNOx*, Berlin, June **2012**.

[110] Y. Liao et al., *Applied Energy* **2017**, 205, 964-975.

[111] P. Ayyappan, D. Dou, T. M. Harris, *Patent US 8999277B2*, **2015**.

[112] G. Wasow, E. O. Strutz, *Patent WO 2010044676A1*, **2010**.

[113] S. Sebelius, *Patent WO 2011/046491*, **2014**.

[114] G. Hüthwohl, M. Bösing, *8th Emission Control*, Dresden, June **2016**.

[115] R. Strey, L. Bemert, C. Simon, H. Doerksen, *Patent WO2011042432A1*, **2011.**

# 4 EXPERIMENTAL

The individual experimental setups, strategies and approaches applied, as well as a description of the chemicals used for this work are shown in advance of the respective experiments in the results section 5. However, basic strategies are described in the following.

## 4.1 Liquid-phase decomposition

During low-temperature decomposition of urea, the formation of undesired byproducts is problematic [1]. Since local lack of water promotes the formation of byproducts, whereas it can be counteracted by an excess of water [2, 3], the experiments on the decomposition of urea to ammonia described in section 5 were carried out in the liquid phase.

In addition, potentially formed byproducts can be excluded from the exhaust tract by this strategy and potentially occurring problems like increased back pressure and clogging of the exhaust tract can be avoided by that, as well [2].

## 4.2 Ammonia-selective electrode

For determination of the ammonia concentration of individual samples, a $NH_3$-selective electrode, model 6.0506.100 from Metrohm was used. The electrode consisted of two parts. For the detection of ammonia, a pH-glass electrode was used. For separation of ammonia, a so-called membrane module was used, which was screwed from outside on the pH electrode. Before screwing the membrane module on the electrode, the module was filled with 2 ml of a measuring electrolyte. By applying the membrane on the electrode, only ammonia was able to diffuse into the measuring electrolyte, meaning the detected pH shift could be attributed solely to the concentration of ammonia. The electrode is shown in Figure 14.

Figure 14: Ammonia-selective electrode. pH electrode without membrane module (left) and pH electrode with membrane module as used for measurements.

The electrode was connected to a pH meter, which provided the readout of the data from the potentiometric results.

For calibration of the ammonia-selective electrode, ammonium chloride samples of known concentrations were measured and a calibration plot was made, using logarithmically divided concentrations of ammonium chloride. To shift the overall ammonium-ammonia ratio to the side of ammonia, the pH value of the sample solution was shifted to alkaline values of at least 12 by addition of sodium hydroxide solution. Calibration was done every day prior to the measurements. All measurements were carried out at room temperature.

Before and between all measurements, the electrode was equilibrated for at least 10 min in Millipore water. As the electrode was very sensitive, most of the sample solutions were diluted with Millipore water before the measurements.

## 4.3 Conductivity measurement

For determining specific conductivities (κ) in addition to the measurements with the ammonia-selective electrode, measurements of the reaction mixtures were performed in case of the metal oxide experiments using a WTW Cond 3210 conductivity meter. Before the measurements, the conductivity meter was calibrated for determining the cell constant (0.474 $cm^{-1}$) using a 0.01 M potassium chloride solution.

## 4.4 References

[1] T. Lauer, *Chemie Ingenieur Technik* **2018,** *90*, 783-794.

[2] D. Peitz et al., *Chemie Ingenieur Technik* **2013,** *85, 5*, 625-631.

[3] D. Peitz, A. M. Bernhard, M. Elsener, O. Kröcher, *Topics in Catalysis* **2013,** *56*, 19-22.

# 5 RESULTS AND DISCUSSION

## 5.1 Investigations on the liquid-phase decomposition of AdBlue-urea for the SCR process

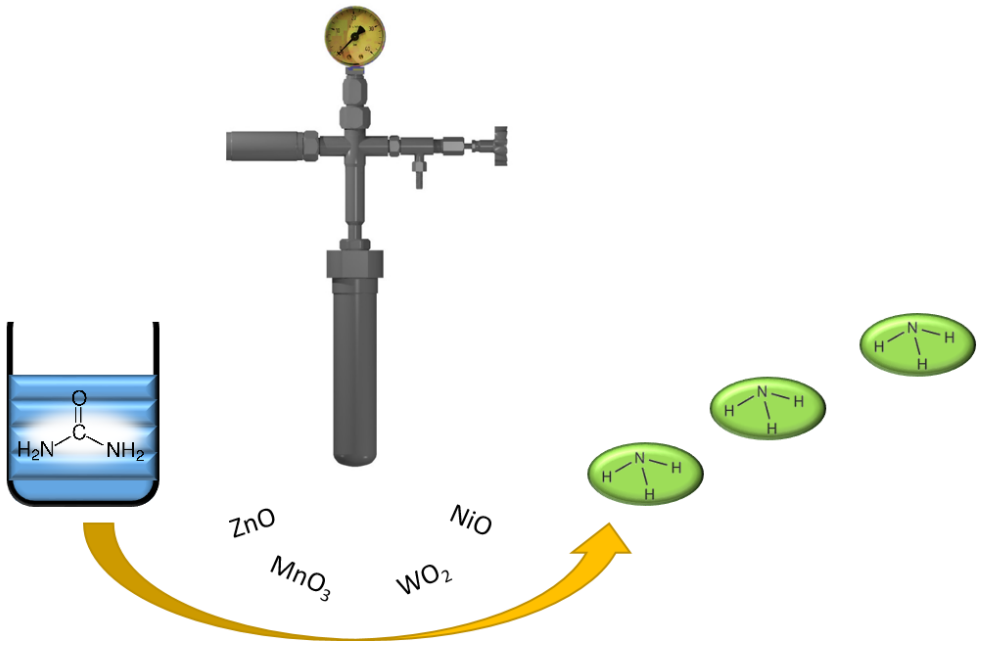


This chapter has been published and adopted from:

Peter Braun, Hans-Peter Rabl and Frank-Michael Matysik,

*Chemie Ingenieur Technik* **2019**, 91, 961-968, DOI: 10.1002/cite.201800055.

**Abstract**

Difficulties in decomposing AdBlue to ammonia limit the applicability of selective catalytic reduction systems at low exhaust temperatures. Investigations on the decomposition of AdBlue in the liquid phase under elevated pressure at temperatures up to 165 °C were carried out. Besides effects of inorganic catalysts, the impact of pH on urea decomposition was examined. After dissolution in aqueous phase, the compounds ZnO, $WO_3$ and $MoO_3$ were found to be effective in liquid-phase AdBlue decomposition. However, the efficiency was dropping significantly over few hours. Decomposition of AdBlue-urea was also found to be favored for alkaline and acidic conditions.

## 5.1.1 Introduction

Under the premise of air pollution control, legal regulations for permitted emissions from combustion engines are becoming continuously more stringent. The allowed limit of pollutants, in particular, the limit value for nitrogen oxides ($NO_x \triangleq NO_2 + NO$), has been lowered significantly in recent years. Due to the harmful effects of nitrogen oxides on human health and the environment, a further reduction of the limit value can be expected for the future [1]. In the case of stoichiometrically operated engines such as gasoline engines, nitrogen oxides can be eliminated effectively by the three-way catalyst. The high share of oxygen in lean-burn engines, such as diesel engines, makes the chemical reduction of $NO_x$ via exhaust aftertreatment much more complex [2, 3]. For passenger car applications, two technologies for reduction of $NO_x$ have evolved over the last years: lean-$NO_x$ trap (also: $NO_x$ storage catalyst) and selective catalytic reduction (SCR) [2-5]. A lean-$NO_x$-trap catalyst has to be regenerated periodically in rich exhaust gas. Therefore, the engine-operating principle is directly coupled to the catalyst working principle [6]. As a consequence, the engine cannot continuously be run at an efficiency- and $CO_2$-optimized operating point [2]. In contrast, SCR systems with the external reducing agent AdBlue, also called diesel exhaust fluid (DEF), can be operated without influencing the engine operating point [7]. Because of that, SCR systems are considered the method of choice for $NO_x$ reduction at lowest $CO_2$ emissions in future, not only in the field of heavy-duty applications but also in case of passenger cars [3, 8-10].

The SCR principle involves two fundamental steps: after injecting the external operating material AdBlue, an aqueous solution of 32.5 wt% urea, into the exhaust tract, in the first step the urea contained in AdBlue gets decomposed by the exhaust-water vapor in a two-step thermo-hydrolysis reaction [3, 11, 12]:

$$H_2N\text{-}CO\text{-}NH_2 + H_2O \rightarrow 2\ NH_3 + CO_2 \qquad \text{(equation 11)}$$

Subsequently, the reducing agent ammonia, generated in this first reaction, is adsorbed and, thus, stored on the surface of the SCR catalyst [13] and can react with the exhaust's $NO_x$ emissions in a second step [2].

Since diesel engines have become more and more efficient over the years, as a result, a decline of exhaust gas temperature was observed [8]. This effect can be expected to become more prevalent in the future, thereby leading to even cooler exhaust gas temperatures. However, this decline is problematic for the SCR process [11]. While modern SCR catalysts show high conversion activity and $N_2$ selectivity already at exhaust temperatures of 165 °C [3, 14, 15], decomposition of AdBlue-urea requires higher temperatures even if hydrolysis catalysts such as $TiO_2$ are used [12]. Moreover, in terms of recently intensified vehicle test conditions of worldwide harmonized light vehicles test procedure (WLTP) and real driving emissions (RDE), the reliable decomposition of urea at low exhaust temperatures is a key aspect for future SCR applications [8].

Therefore, e.g. systems for retrofitting focus on improvement of urea decomposition at low exhaust temperatures to reduce $NO_x$ emissions. Heating devices are used to raise the temperature level [16]. However, the heating process leads to extra fuel consumption, which to a certain extent negatively influences the $CO_2$ emissions of the diesel engine.

Another problem, which is associated with the SCR process in combination with low exhaust temperature, is an undesired byproduct formation from urea [17-19]. These byproducts such as cyanuric acid, biuret and others can lead to deposit formation and clogging inside the exhaust tract. Consequently, increased exhaust back pressure and in the long term even engine failure might occur [20].

Taking these facts into consideration, the overall SCR process could be enabled at lower exhaust temperatures if reliable hydrolysis of AdBlue-urea could be enabled at lower exhaust temperatures [3, 18]. Therefore, in this work, the focus lies on the decomposition of AdBlue-urea at low temperatures. Since byproduct formation during urea hydrolysis is strongly promoted by local lack of water but, as can be derived from equation 11, can as well be counteracted by an excess of water to an even larger extent [21, 22], the studies on decomposition of urea were carried out in liquid phase using elevated pressure.

In this context, liquid-phase urea decomposition was already investigated in some previous studies. Sahu et al. [23] investigated the effect of $TiO_2$, fly ash, mixture of Ni and Fe and $Al_2O_3$ for hydrolysis

of urea solution from 10 to 40 wt% in a semi-batch reactor for flue gas conditioning in thermal power plants. Gangadharan et al. [24] did further studies on the decomposition of urea in presence of $Al_2O_3$ in a batch reactor for application in fly ash removal. Peitz et al. [21, 22] compared the decomposition of AdBlue in the gas phase with the decomposition in the liquid phase under elevated pressure in presence of $TiO_2$, $ZrO_2$ and $Al_2O_3$.

Besides the influence of different inorganic materials on the decomposition efficiency of AdBlue-urea, in the present study also the influence of acidic and alkaline conditions was studied.

## 5.1.2 Experimental

**Chemicals**

For all experiments, Millipore water was used. Urea was purchased from neoFroxx GmbH. $TiO_2$, $ZrO_2$, $Fe_2O_3$, ZnO, $Cr_2O_3$, $WO_3$, $MoO_3$, $Na_2MoO_4 \cdot 2H_2O$, $Na_2WO_4 \cdot 2H_2O$ and $(NH_4)_6Mo_7O_{24} \cdot 4H_2O$ were purchased from Merck, NiO and $Nb_2O_5$ were acquired from ChemPur, $WO_2$ was purchased from Alfa Products and NbO from Ventron GmbH. All chemicals used were of pure grade or higher. Synthetic AdBlue used in the experiments was prepared by dissolving 32.5 wt% urea in Millipore water.

**Experimental setup**

Since AdBlue-urea decomposition in the liquid phase was carried out at temperatures up to 165 °C in the experiments, an autoclave reactor made of stainless steel was applied. By that, experiments at elevated pressures were possible. The autoclave (approx. volume 120 ml) was equipped with a safety valve adjusted to 40 bar, a pressure gauge and a discharge tap. The schematic setup is shown in Figure 15. For heating the autoclave, a heating plate including a magnetic stirrer and an oil bath were used. The temperature required for the individual experiment was adjusted via an electronic contact thermometer, directly connected to the heating plate. The experiments on pH dependence of AdBlue-urea decomposition were performed in centrifuge tubes from VWR since strong acids would have etched the material of the autoclave.

Figure 15: Autoclave reactor used for experiments on the liquid-phase decomposition of AdBlue-urea.

**Experimental procedure**

If not otherwise stated, the standard experiments on liquid-phase urea decomposition were carried out the following way: for all autoclave experiments, except the long-term experiment, 30 g AdBlue (27.5 ml) were used. After addition of AdBlue together with the additives required for the individual experiment into the autoclave, the reactor was sealed. Subsequently, the autoclave was immersed into the oil-bath heated to the temperature required for the experiment. After reaction time had expired, in general, 30 min unless specified otherwise, the autoclave reactor was cooled with water from the outside for further 30 min. Afterward the autoclave reactor was opened again. For the investigations on pH dependence of AdBlue-urea decomposition, the procedure was similar. Here, 5 ml AdBlue pure or with differing concentrations of acid/base depending on the experiment were used inside the centrifuge tubes.

The ammonia content of the resulting reaction mixture was determined by an ammonia-selective electrode, model 6.0506.100 from Metrohm. The electrode was recalibrated daily prior to the measurements with ammonium chloride solutions of known concentrations. To set the overall $NH_3/NH_4^+$ ratio to the side of ammonia, sodium hydroxide solution was added to the sample and the calibration standards prior to the measurements, shifting the pH value into the alkaline region (> 12). In addition to the ammonia concentration measurements with the ammonia-selective

electrode, specific conductivity (κ) measurements of the reaction mixtures were performed in case of the metal oxide experiments with a WTW Cond 3210 conductivity meter. Moreover, the maximum pressure, p(Reactor) inside the autoclave reactor was measured.

For estimation of the amount of ammonia present in the gas phase of the autoclave after reopening the reactor, a calculation was done on the partial pressure of ammonia in the gas volume of the autoclave using its Henry constant $H^{cp}$ [25]. Under the assumption of ideal-gas behavior and the gas-to-liquid volume ratio inside the autoclave reactor of $\frac{V(gas)}{V(liquid)} = 3$, it was found that at the temperature the reactor was opened again (25 °C) less than 1 % of overall ammonia was present in the gas phase, which is negligible in terms of overall measuring accuracy.

## 5.1.3 Results and discussion

### *5.1.3.1 Investigations on metal oxides as potential decomposition catalysts*

#### 5.1.3.1.1 Screening of metal oxides

First, a screening of metal oxides was carried out. The experiments were performed according to the protocol described in 5.1.2 with an amount of metal oxide equal to a concentration of 100 mM in AdBlue. The reaction temperature was set to 165 °C since modern SCR catalysts show significant activity in $NO_x$ reduction at this temperature, but hydrolysis of urea is problematic [8, 12, 14, 15]. The following substances were investigated: titanium(IV) oxide, zirconium(IV) oxide, iron(III) oxide, zinc(II) oxide, tungsten(IV) oxide, tungsten(VI) oxide, niobium(II) oxide, niobium(V) oxide, chromium(III) oxide, molybdenum(VI) oxide, and nickel(II) oxide. The ammonia concentration measured with the ammonia-selective electrode, the conductivity of the resulting reaction mixture and the pressure inside the reactor after 30 min reaction time are shown in Figure 16. Since the pressure inside the autoclave was raising for all the experiments even as the reaction time of 30 min had expired, it can be concluded that a thermodynamic equilibrium was not reached during the investigated reaction time.

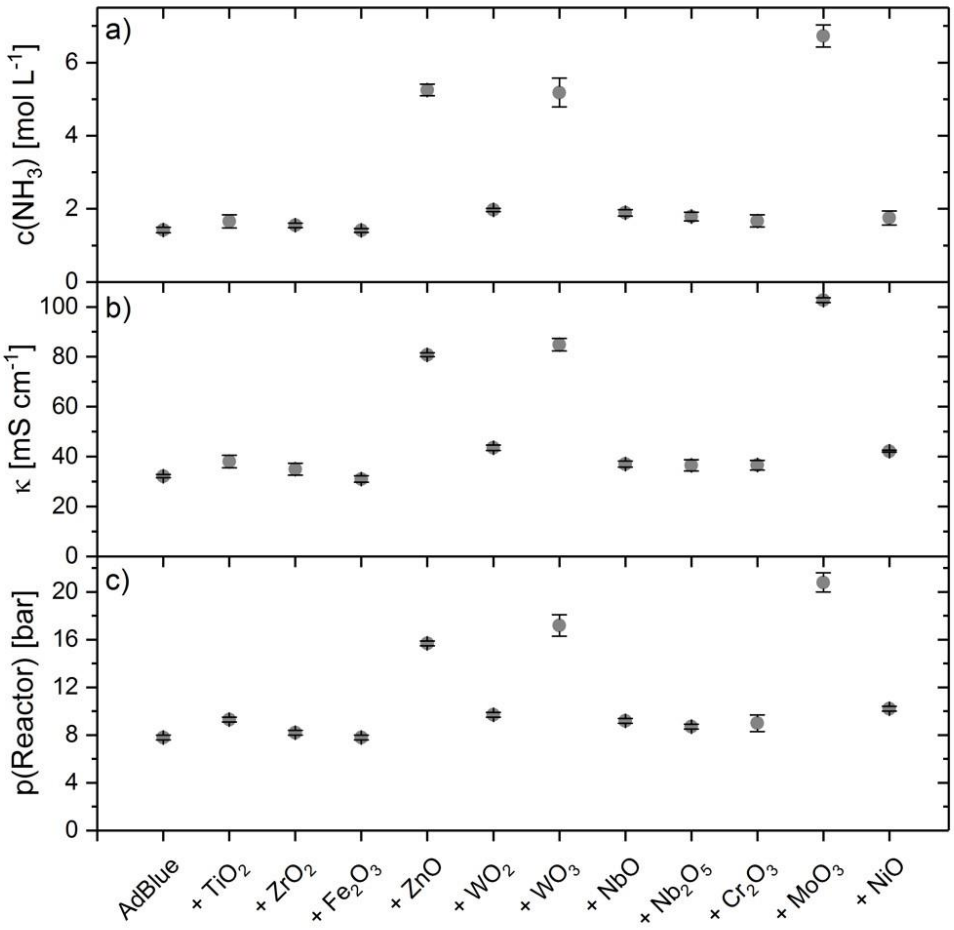


Figure 16: Results of metal oxide screening for AdBlue-urea decomposition at 165 °C in liquid phase: a) ammonia concentration measured with ammonia-selective electrode, b) conductivity of reaction mixture and c) max. pressure inside autoclave reactor after 30 min.

From the results, it can be seen that three of the screened materials showed significant catalytic activity in AdBlue-urea decomposition under the applied conditions: ZnO, $WO_3$ and $MoO_3$. However, in contrast to the other investigated materials, the three oxides were not suspended in the reaction mixture any more after the experiment but were dissolved. Tungsten oxide and molybdenum oxide were already reported in the literature regarding urea decomposition, however, no experimental results were presented so far [23]. In the experiments with all the other compounds, the ammonia concentration was not remarkably increased after 30 min at 165 °C. Also, $TiO_2$ and $ZrO_2$, which were shown to be active in the decomposition of urea in the gas phase [21], did not show remarkable catalytic activity in the liquid-phase decomposition. This observation goes along with findings of

Peitz et al. [21, 22] who could find only very low catalytic effects for these materials in the liquid phase. The reason for the high activity of the metal oxides being dissolved in the reaction mixture might be explained by the hydrophilicity of urea. By dissolution, the Zn, W and Mo species became homogeneous catalysts in the liquid phase and, therefore, were present in the same phase compared to the co-dissolved urea. This seemed to result in increased accessibility to urea.

Moreover, from the results, it can be seen that the values observed by the conductivity of the reaction mixture and the prevalent pressure inside the autoclave reactor fitted together well. In case of conductivity measurements of the ZnO, $WO_3$ and $MoO_3$ samples, a small part of the measured value was due to the dissolution of the screened material.

#### 5.1.3.1.2 Influence of temperature on catalyst decomposition activity

After having found catalytic activity of these three materials, the influence of the reaction temperature inside the autoclave on the catalytic activity of these materials was examined. Therefore, experiments with 100 mM ZnO, $WO_3$ and $MoO_3$ according to the protocol described in 5.1.2 were carried out additionally at 145 °C and 155 °C. The results in comparison to the values at 165 °C are shown in Figure 17.

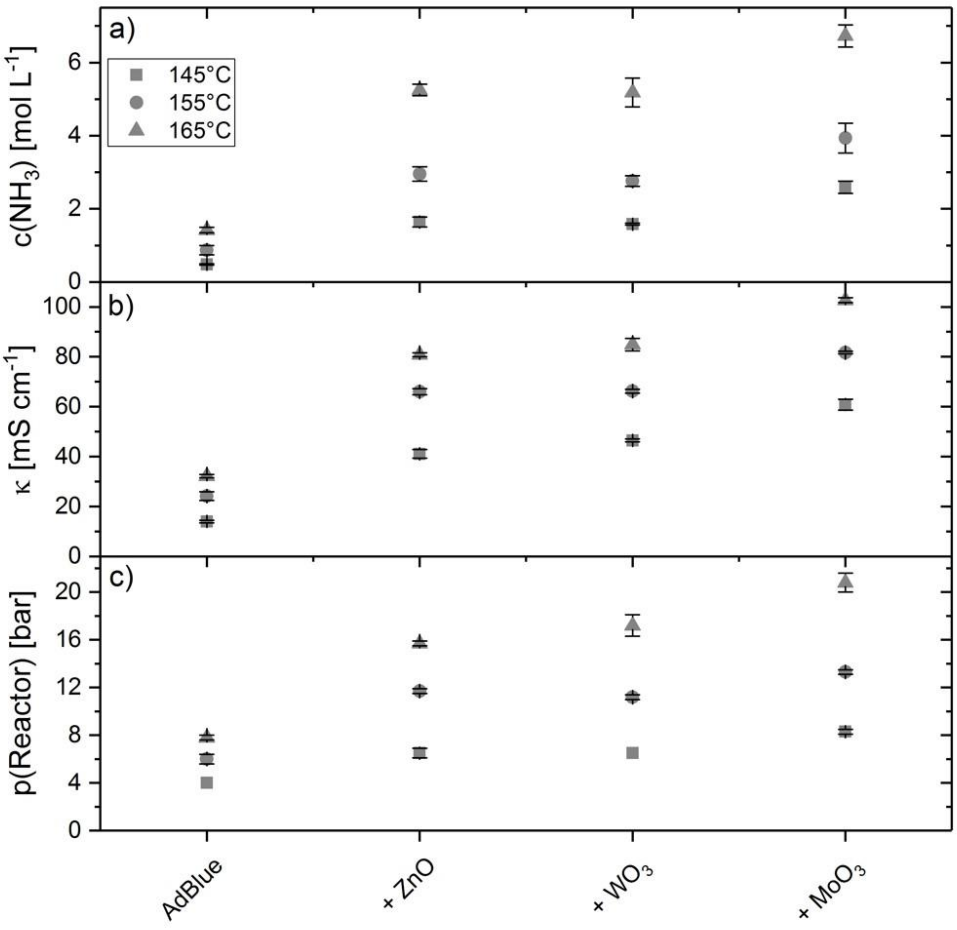


Figure 17: Influence of reaction temperature on the decomposition of AdBlue-urea in the liquid phase with and without metal oxides: a) ammonia concentration measured with ammonia-selective electrode, b) conductivity of reaction mixture and c) max. pressure inside autoclave reactor after 30 min.

As expected, the amount of AdBlue-urea decomposition and ammonia formation was increased with raising reaction temperature. Raised temperature led to enhanced thermal decomposition, but also the urea decomposition attributed to the catalyst increased at higher temperatures as can be seen in Figure 17. This observation was again supported by the compliance of the three investigated parameters.

#### 5.1.3.1.3 Influence of the amount of catalyst on decomposition activity

To investigate the influence of the concentration of catalyst, a series of experimental studies was performed with varying amounts of ZnO, $WO_3$ and $MoO_3$. The experiments were carried out at 165 °C according to the protocol described in 5.1.2. The results of the experimental series are shown in Figure 18.

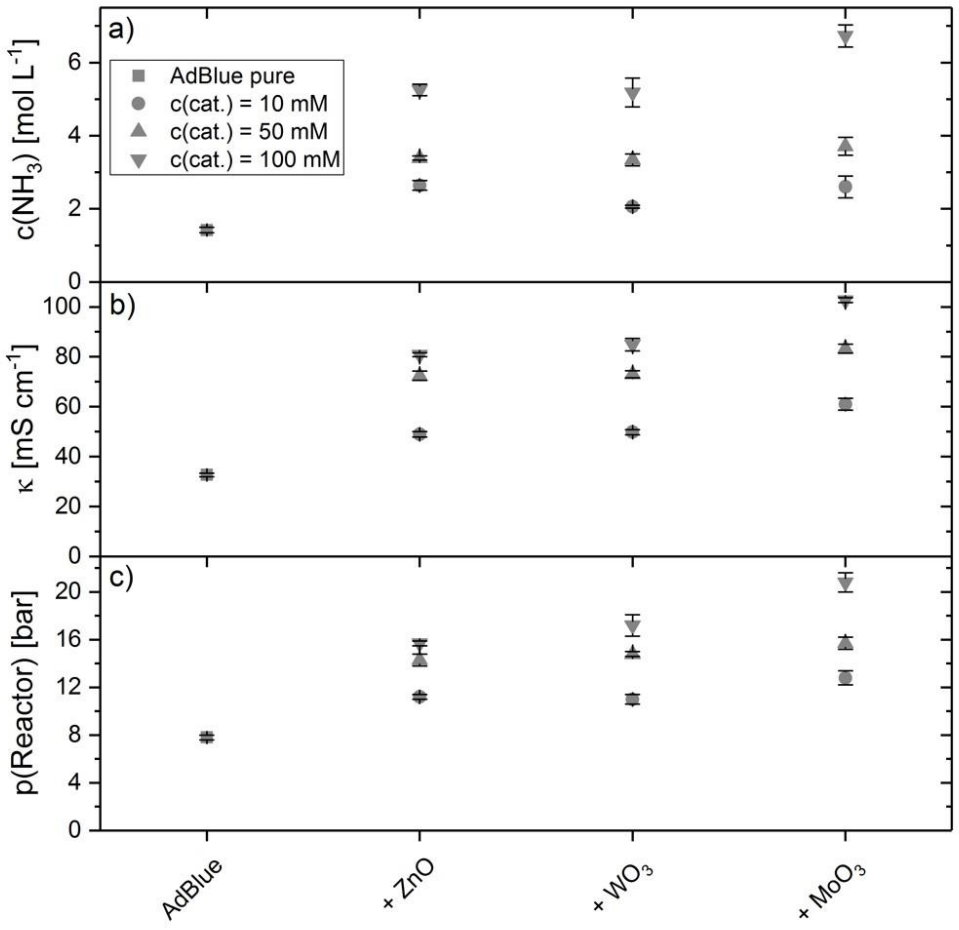


Figure 18: Influence of catalyst amount on the decomposition of AdBlue-urea in the liquid phase with and without metal oxides at 165 °C: a) ammonia concentration measured with ammonia-selective electrode, b) conductivity of reaction mixture and c) max. pressure inside autoclave reactor after 30 min.

As expected, the results derived from ammonia concentration measured by the ammonia-selective electrode, conductivity and maximum pressure showed that by increasing the amount of catalyst, the urea decomposition and ammonia generation within 30 min increased as well. This makes sense

since more catalytically active molecules present in the reaction mixture can interact with the urea molecules at the same time and thus higher conversion of urea is observed per time.

#### 5.1.3.1.4 Stability of dissolved species

Since the three screened materials showing significant catalytic activity in AdBlue-urea decomposition were dissolved in the reaction mixture and were not suspended at the end of the experiments, the question appeared, if the species formed in solution was the catalytically active one and if it was stable. Therefore, a long-term experiment was set up: 1 M urea solution was filled into the autoclave in one case with an amount equal to 100 mM $MoO_3$ and in the other case without $MoO_3$ addition. The autoclave reactor was then immersed into the oil bath at 155 °C and kept at this temperature for 90 min. Afterward, the autoclave reactor was cooled as described before. Subsequently, the reactor was opened and a 0.5 ml sample was taken from the overall reaction mixture and then an amount equal to 1 M urea was added. Afterward, the autoclave was sealed again, and the procedure was repeated two more times, each for 90 min at 155 °C. The lower concentrated 1 M urea solution was used instead of AdBlue to avoid solubility problems of the reaction products. After the experiment, the ammonia content of the samples taken after 90 min, 180 min and 270 min was measured with the ammonia-selective electrode. The results of the experiments are shown in Figure 19.

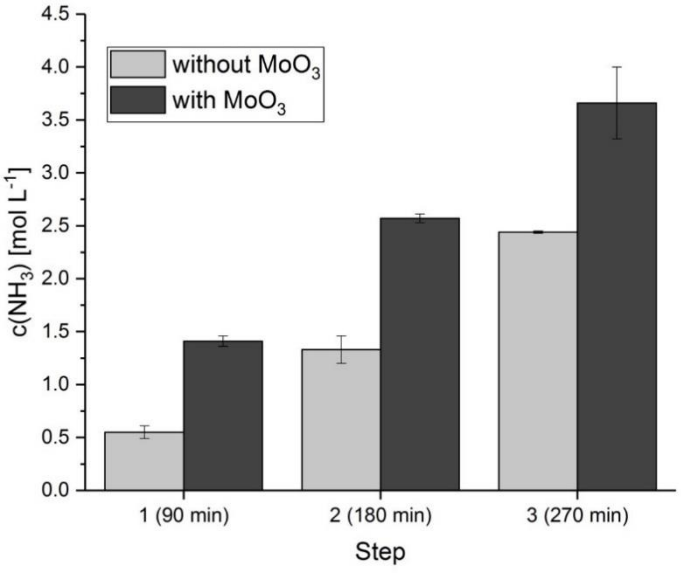


Figure 19: Ammonia concentrations during long-term experiment with and without $MoO_3$ after 90 min, 180 min and 270 min measured with ammonia-selective electrode.

To get information on the stability of the species formed in solution, a detailed evaluation of the experimental results was done. For that reason, a calculation on the conversion of available urea in each of the three steps was set up for both runs, with $MoO_3$ and without $MoO_3$. The calculation considers the quantity of urea present before each step by taking into account the addition of urea after 90 min and 180 min and the removal of the individual samples after each step. The results of this evaluation are shown in Figure 20.

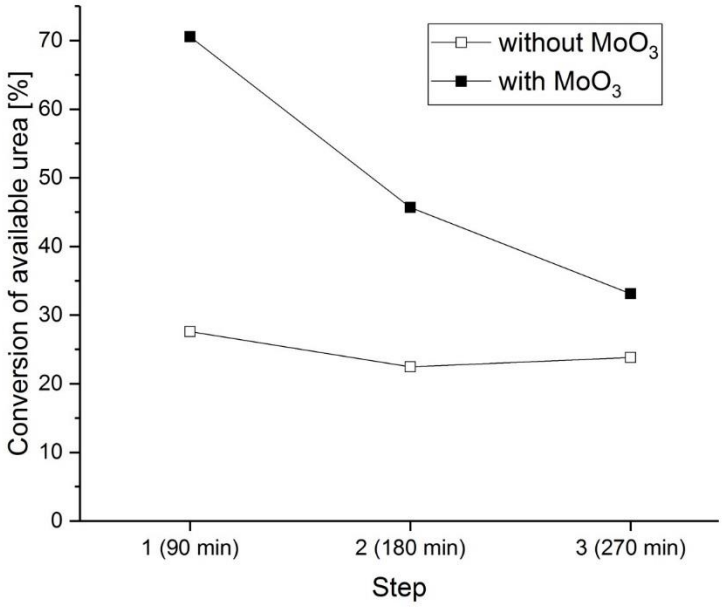


Figure 20: Evaluation of long-term experiment with and without $MoO_3$: conversions of available urea after 90 min, 180 min and 270 min measured with ammonia-selective electrode.

As clearly visible in Figure 20, there was a significantly higher conversion activity at the beginning of the experiment with $MoO_3$ addition in contrast to the sample without $MoO_3$. In the case of $MoO_3$, in the first 90 min, more than 70 % of the available urea got decomposed in solution. In step 2, the decomposition activity dropped down to approximately 45 % to decrease further in step 3 to about 33 %. On the other side, the decomposition activity in case of the sample without $MoO_3$ stayed relatively constant at approximately 25 % over the whole 270 min of the experiment, which was due to the thermal decomposition of urea without catalytic support. This observation showed that the catalytically active species was inactivated in solution over time.

#### 5.1.3.1.5 Comparison of the results with molybdate (aq.) and tungstate (aq.)

As the metal oxides ZnO, $WO_3$ and $MoO_3$ are in general not soluble in water, some soluble species must have formed. From literature, it is known that the three investigated active materials get dissolved via formation of metallate anions in alkaline solution [26]. Thus, it was investigated if the metallates show similar activity in urea decomposition. For this purpose, an experiment described in 5.1.2 was carried out again with sodium molybdate, ammonium heptamolybdate and sodium tungstate at 155 °C. In contrast to the other materials, the amount of ammonium heptamolybdate used was adjusted to 1/7 of the other materials, since one unit of the compound contains seven Mo-units. Additionally, the same experiment with sodium chloride and sodium sulfate was carried out, to exclude that the sodium cation causes catalytic activity. The results of the experiments are shown in Figure 21.

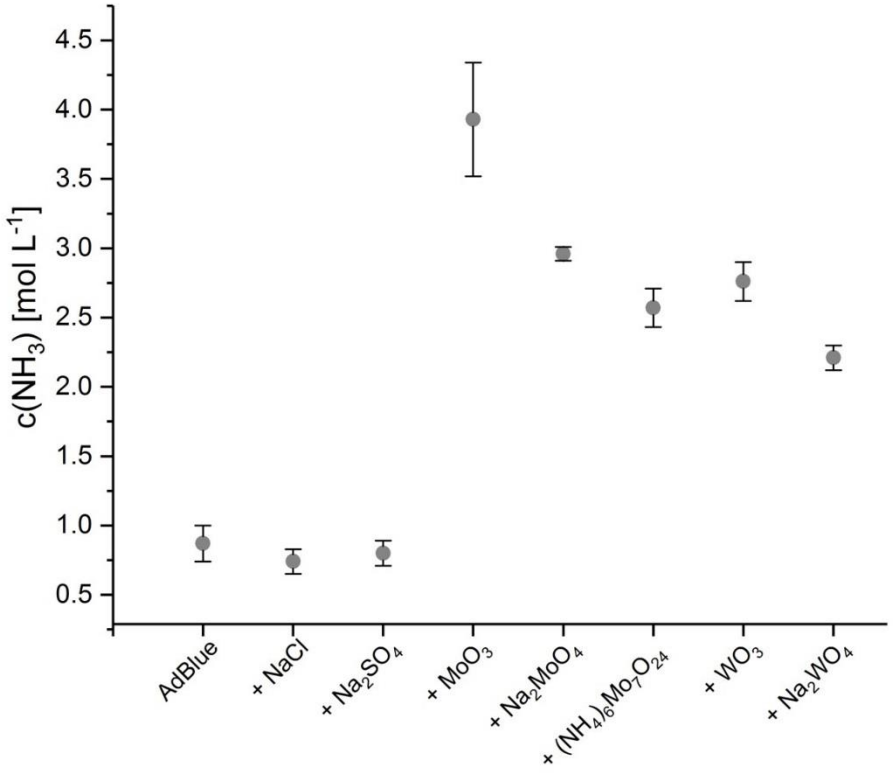


Figure 21: Comparison of results for AdBlue-urea decomposition with different additives (100 mM, except ammonium heptamolybdate: 14.3 mM) in liquid phase. Ammonia concentration measured with ammonia-selective electrode.

It can be seen from Figure 21 that in the case of sodium molybdate, ammonium heptamolybdate and sodium tungstate a certain catalytic activity for urea decomposition was existing. In case of sodium chloride and sodium sulfate, no catalytic activity could be observed. This observation

showed that the dissolved anionic metallates molybdate and tungstate were catalytically active in the decomposition of AdBlue-urea in the liquid phase and were responsible for catalytic effects which were detected in case of the metal oxide screening in point 5.1.3.1.1. However, as prevalent in Figure 21, the amount of ammonia formed was about 20 % lower in the case of the pre-dissolved anionic metallates. This effect might be explained by additional effects occurring during the dissolution process of $MoO_3$ and $WO_3$. Nevertheless, as it was shown in 5.1.3.1.4, the metallates get inactivated over time.

#### *5.1.3.2 Investigations on pH-dependent AdBlue-urea decomposition*

Since the decomposition of urea in solution was described to be promoted in alkaline [27, 28] and acidic [29, 30] media, in the following part, the AdBlue-urea decomposition upon addition of acid or base was investigated. The stainless steel autoclave reactor described in the experimental part could not be applied for these experiments since a strong acid, needed for the required pH shift, would have etched the stainless steel material of the reactor. Therefore, the experiments were carried out in centrifuge tubes with 2 M acid/base in AdBlue, as described in 5.1.2. In a first experiment, the temperature dependence at pH values of < 1 and > 13 in AdBlue was investigated, with the results being shown in Figure 22. In Figure 22 a), the experiments with 2 M sulfuric acid and 2 M sodium hydroxide solution are shown and in Figure 22 b), the experiments with 2 M hydrochloric acid and, for improved comparability, the same values for sodium hydroxide are shown. The values at pH 8.5 represent the experiments with pure AdBlue, without any addition of acid or base as a reference point.

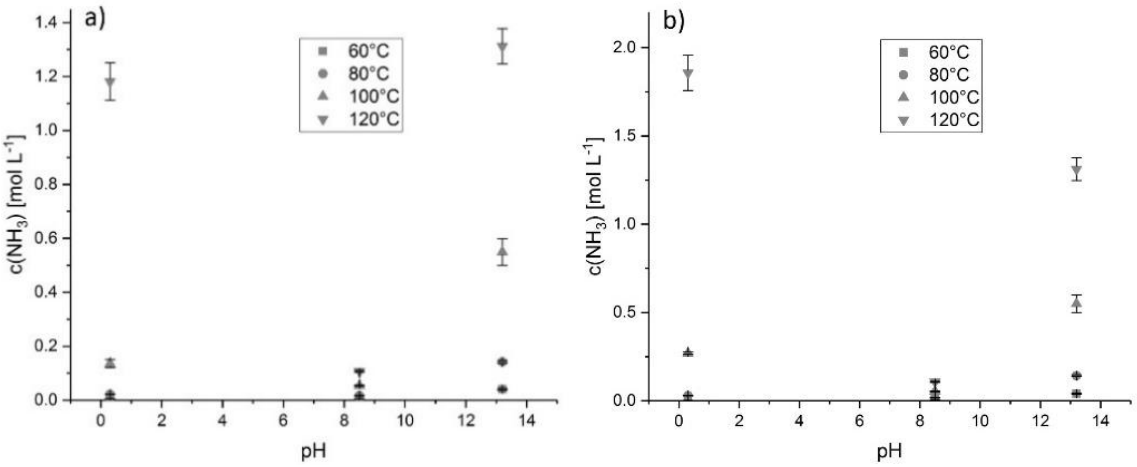


Figure 22: Influence of temperature on decomposition of AdBlue-urea at strongly alkaline (2 M sodium hydroxide) and acidic (2 M sulfuric acid/hydrochloric acid) pH values in liquid phase measured with ammonia-selective electrode: a) sodium hydroxide/sulfuric acid, b) sodium hydroxide/hydrochloric acid.

In Figure 22, the significantly enhanced decomposition efficiency at strongly alkaline and strongly acidic conditions at each temperature investigated in comparison to AdBlue without acid or base addition is visible. Moreover, the extent of enhancement in the case of hydrochloric acid was higher compared to sulfuric acid at a similar pH value. An increase in temperature led to an increase of ammonia production also at the extreme pH values investigated.

Additionally, the effect of acid or base concentration on ammonia generation was investigated, as shown in Figure 23.

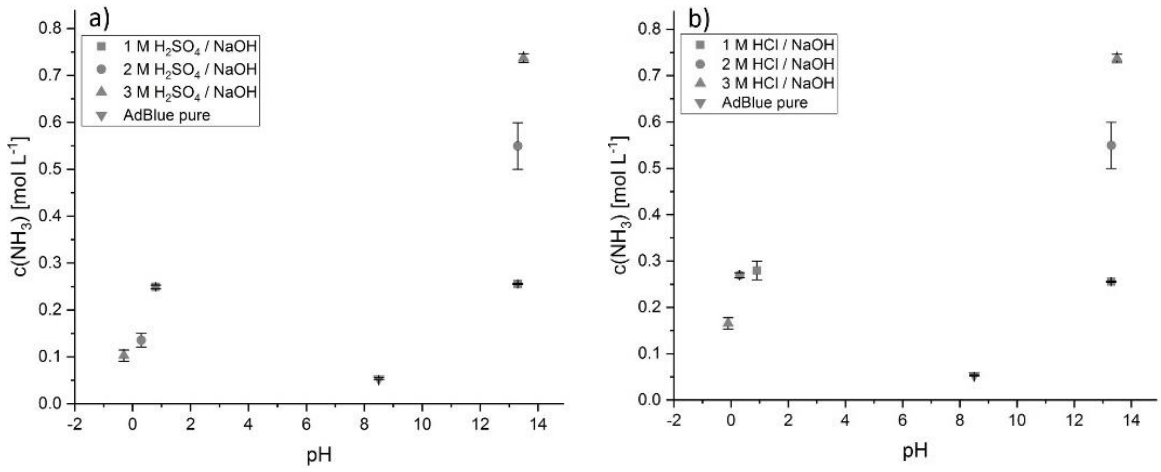


Figure 23: Influence of acid/base concentration on the decomposition of AdBlue-urea at strongly alkaline (sodium hydroxide) and acidic (sulfuric acid/hydrochloric acid) pH values in the liquid phase at 100 °C measured with ammonia-selective electrode: a) sodium hydroxide/sulfuric acid, b) sodium hydroxide/hydrochloric acid.

The experiments were carried out at 100 °C with a) 1 M, 2 M and 3 M sulfuric acid/sodium hydroxide solution and b) 1 M, 2 M and 3 M hydrochloric acid/sodium hydroxide solution. For acidic and alkaline conditions, a different behavior was observed: while higher concentrations of sodium hydroxide led to significantly increased ammonia generation, in case of the experiments with acidic pH value, higher concentrations of acid led to less ammonia generation. This effect was observed for both acids studied, hydrochloric acid and sulfuric acid. A decrease of the urea-decomposition rate at strongly acidic pH values was also described in literature [27, 28]. According to Blakeley [27], the drop of ammonia formation at increased acid concentration and, thereby, more acidic pH of < 2 can be explained by the protonation of urea, thereby inhibiting its decomposition reaction.

In general, there are some possible explanations for decreased stability of urea at acidic and alkaline pH values. Panyachariwat et. al [30] suggested the reversibility of the equilibrium between urea and ammonium cyanate to be relevant since $H^+$ as well as $OH^-$ promote the conversion of cyanate to ammonia thereby hampering the reverse reaction of cyanate to urea [31]:

$$CNO^- + 2\ H^+ + 2\ H_2O \rightarrow NH_4^+ + H_2CO_3 \qquad \text{(equation 12)}$$

$$CNO^- + OH^- + H_2O \rightarrow NH_3 + CO_3^{2} \qquad \text{(equation 13)}$$

This explanation is in agreement also with findings of Warner et al. [30, 31].

According to Blakeley [27], the increase of ammonia formation at alkaline pH above 12 might be explained by a specific base catalysis of urea decomposition [32, 33]:

$$H_2\text{-N-CO-}NH_2 + OH^- \rightarrow HN\text{-CO-}NH_2^- + H_2O \qquad \text{(equation 14)}$$

$$HN\text{-CO-}NH_2^- + H_2O \rightarrow HNCO + NH_3 + OH^- \qquad \text{(equation 15)}$$

### *5.1.3.3 Comparison of pH-induced urea decomposition with metal oxide-/metallate-effected decomposition*

Finally, a comparison between the pH-induced AdBlue-urea decomposition efficiencies and the decomposition efficiencies observed with metallates was performed. For this purpose, the pH-induced urea decomposition with sodium hydroxide at different concentrations at 145 °C was carried out, being equal conditions at which the experiments on the metal oxides/metallates have been performed. For this purpose, the autoclave reactor system described in 5.1.2 was used again. In Figure 24, the results of this study are shown.

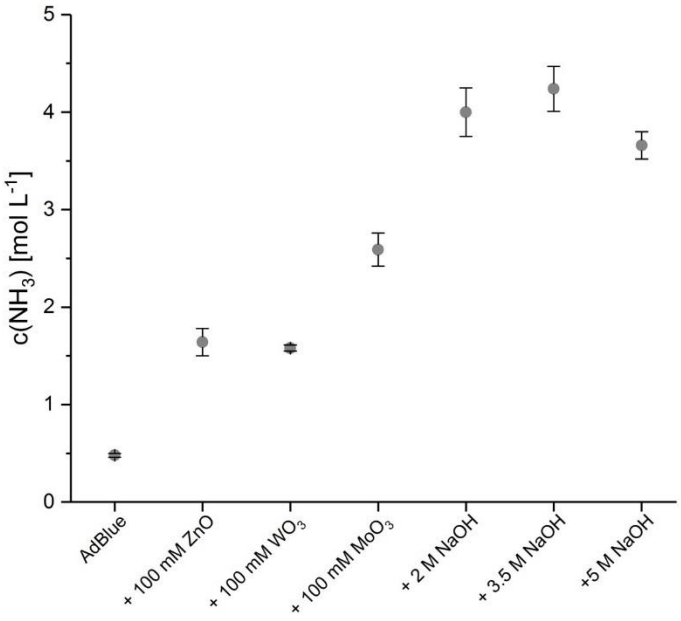


Figure 24: Comparison of decomposition of AdBlue-urea at 145 °C in strongly alkaline conditions with decomposition catalyzed by metal oxides / metallates in the liquid phase. Ammonia concentration measured with ammonia-selective electrode.

As can be seen, the urea decomposition was more pronounced in case of the alkaline experiments with 2 M, 3.5 M and 5 M sodium hydroxide solution compared to the values observed with metallates for urea decomposition. However, the pH value in case of the experiments with 2 M, 3.5 M and 5 M sodium hydroxide solution dropped during the experiments from approximately 14 to < 12, i.e., the strongly alkaline conditions were mitigated during the experiment due to the formation of ammonia and the associated pH effects. The investigation of higher concentrations of sodium hydroxide was not possible since problems with precipitation already occurred with the 5

M sodium hydroxide in AdBlue. This was presumably also a reason for the decrease in ammonia concentration in case of 5 M sodium hydroxide since in all other experiments higher sodium hydroxide concentration resulted in an increased ammonia buildup.

### 5.1.4 Conclusion and outlook

Since modern SCR catalysts show high conversion efficiencies and $N_2$ selectivities already at temperatures of 165 °C, the overall SCR process in the low-temperature range is limited by difficulties in decomposing AdBlue to ammonia. In the screening of metal oxides, three candidates showing catalytic efficiency for the decomposition of AdBlue-urea in the liquid phase were found: ZnO, $WO_3$ and $MoO_3$. However, it was shown that the actually active species were anionic metallates, e.g. molybdate, formed from the metal oxides in alkaline solution. By dissolution, the Zn, W and Mo species became homogeneous catalysts in aqueous phase, which seemed to have improved access to the co-dissolved urea. The behavior of catalytic activity for molybdate was investigated over 270 min. A drastic decrease of catalytic activity was found during the experiment. Therefore, stabilization of the active species in solution is urgently required for potential real engine application. If a significant long-term stabilization of the found catalytic materials could be achieved, this approach would present a possible alternative for the onboard generation of ammonia for SCR. Additionally, the influence of strongly alkaline and acidic pH values on the decomposition of AdBlue-urea was investigated. Acidic as well as alkaline conditions were found to significantly destabilize urea in AdBlue thereby enhancing ammonia production in solution. Since the external onboard addition of acid or base into AdBlue is difficult to achieve in practice, for technical application e.g. an in-situ generated pH shift would present an interesting technical implementation of the presented principle.

### 5.1.5 References


[1] K.-H. Kim, S. A. Jahan, E. Kabir, *Environment International* **2013,** *59*, 41-52.

[2] K. Mollenhauer, H. Tschöke, *Handbuch Dieselmotoren*, 3, Springer, Berlin **2007**.

[3] P. Braun, J. Gebhard, F.-M. Matysik, H.-P. Rabl, *Chemie Ingenieur Technik* **2018,** 90, 762-773.

[4] T. V. Johnson, *SAE International Journal of Engines* **2015,** *8*, *3*, 1152-1167.

[5] P. Forzatti, L. Lietti, I. Nova, E. Tronconi, *Catalysis Today* **2010,** *151*, 202-211.

[6] C. Shi et al., *Applied Catalysis B: Environmental* **2012,** *119-120*, 183-196.

[7] J. Jiang, D. Li, *Applied Energy* **2016,** *174*, 232-244.

[8] P. Braun, J. Gebhard, H.-P. Rabl, *Low Temperature DeNOx*, Final Report FVV project 1155, Frankfurt am Main, **2017**.

[9] R. Marques, R. Rohe, D. Harris, C. Jones, *4th IAV Conf. MinNOx*, Berlin, June **2012**.

[10] C. P. Cho et al., *Applied Thermal Engineering* **2017,** *110*, 18-24.

[11] B. Guan, R. Zhan, H. Lin, Z. Huang, *Applied Thermal Engineering* **2014,** *66*, 395-414.

[12] A. M. Bernhard et al., *Catalysis Science & Technology* **2013,** *3*, 942-951.

[13] T. Feng, L. Lü, *Journal of Industrial and Engineering Chemistry* **2015,** *28*, 97-109.

[14] Y. J. Kim et al., *Applied Catalysis B: Environmental* **2012,** *126*, 9-21.

[15] L. Qiu et al., *Catalysis Letters* **2015,** *145*, 1500-1509.

[16] W. S. Doelling et al., *Proc. of SAE-China Congress 2014: Selected Papers*, Springer, Berlin, **2015**.

[17] M. Goldbach et al., *Chemical Engineering & Technology* **2017,** *40*, *11*, 2035-2043.

[18] A. Roppertz, S. Füger, S. Kureti, *Topics in Catalysis* **2017,** *60*, 199-203.

[19] P. M. Schaber et al., *Thermochimica Acta* **2004,** *424*, 131-142.

[20] S. Dumas, M. Lopes, *4th IAV Conf. MinNOx,* Berlin, June **2012**.

[21] D. Peitz et al., *Chemie Ingenieur Technik* **2013,** *85*, *5*, 625-631.

[22] D. Peitz, A. M. Bernhard, M. Elsener, O. Kröcher, *Topics in Catalysis* **2013,** *56*, 19-22.

[23] J. N. Sahu, A. V. Patwardhan, B. C. Meikap, *Asia-Pacific Journal of Chemical Engineering.* **2010,** *5*, 533-543.

[24] P. Gangadharan, J. N. Sahu, B. C. Meikap, *Journal of Chemical Technology & Biotechnology* **2011,** *86*, 1282-1288.

[25] R. Sander, *Atmospheric Chemistry and Physics* **2015,** *15*, 4399-4981.

[26] N. Wiberg et al., *Lehrbuch der Anorganischen Chemie*, 102, de Gruyter, Berlin, **2007**.

[27] R. L. Blakeley, A. Treston, R. K. Andrews, B. Zerner, *Journal of the American Chemical Society* **1982,** *104*, 612-614.

[28] A. N. Alexandrova, W. L. Jorgensen, *Journal of Physical Chemistry B* **2007,** *111*, 720-730.

[29] K. J. Laidler, J. P. Hoare, *Journal of the American Chemical Society* **1950,** *72*, 2489-2494.

[30] N. Panyachariwat, H. Steckel, *International Journal of Cosmetic Science* **2014,** *65*, 187-195.

[31] R. C. Warner, *Journal of Biological Chemistry* **1942**, 705-723.

[32] L. W. Dittert, T. Higuchi, *Journal of Pharmaceutical Science* **1963**, 52, 852-857.

[33] M. L. Bender, R. B. Homer, *Journal of Organic Chemistry* **1965**, 30, 3975-3978.

## 5.2 Investigations on the electrochemically induced decomposition of AdBlue-urea using nickel-based electrodes

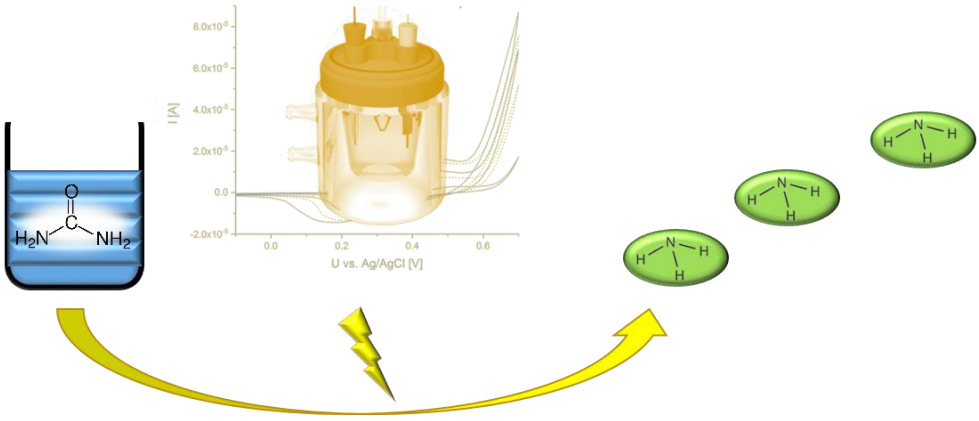

### 5.2.1 Introduction

In order to act against air pollution, emission legislation is progressively limiting the allowed emissions of exhaust gases from internal combustion engines. Nitrogen oxides, $NO_x$, the sum of nitrogen monoxide NO and nitrogen dioxide $NO_2$, have lately attracted attention in connection with the “dieselgate”. Diesel engines are, in contrast to stoichiometrically-driven engines, operated with a lean combustion mixture with the consequence that, related to the amount of fuel, a stoichiometric excess of oxygen is present inside the combustion chamber [1]. Regarding the reduction of $NO_x$, difficulties arise thereof, since the potential reducing agents in the raw exhaust gas react with the excess of oxygen present in the exhaust gas. Therefore, vehicles operated by diesel engines, are equipped with an additional technology for the reduction of $NO_x$ emissions to meet the EURO VI standard and the stricter $NO_x$-limit value enacted thereby. The selective catalytic reduction (SCR) process is the most commonly used strategy for reduction of $NO_x$ emissions from lean exhaust gas [2]. The SCR process requires an external reducing agent, ammonia, which must be carried onboard as additional operating material. As ammonia is a toxic gas at ambient conditions, the reducing agent is carried onboard in form of the precursor urea. Therefore, urea as 32.5 wt% solution in water (AdBlue or DEF) is used as reducing agent. Consequently, the process of urea decomposition to ammonia must go ahead of the process of $NO_x$ reduction. While today’s SCR catalytic coatings reach 90 % $NO_x$ reduction at exhaust temperatures of 165 °C [2], in case when ammonia is available, the decomposition of urea to ammonia requires temperatures of at least 180 - 190 °C even when an additional hydrolysis catalyst is applied (e.g. $TiO_2$) [3]. Since diesel engines have become progressively more efficient over the last years, a decline of exhaust-gas temperature was observed as a consequence [4]. As a result, in the case of city traffic or other low-load driving situations, the decomposition process of urea to ammonia limits the applicability of the overall SCR system. Strategies which enable the preparation of ammonia from urea at lower temperatures would, therefore, lead to a reduction of $NO_x$ emissions of diesel vehicles at low exhaust temperatures [5].

One electrochemical approach for decomposing urea in the liquid phase at low temperatures was presented by Lu et al. [6]. In their study, they showed that a nickel-based electrode was able to increase the rate of ammonia generation by a factor of ~28 in comparison to the thermal hydrolysis of urea at a temperature as low as 70 °C. The investigations were carried out in AdBlue containing 7 M KOH. In a further publication, the same authors presented mechanistic studies on this electrochemically induced conversion of urea to ammonia [7]. They concluded that nickel oxyhydroxide, NiOOH, is the species catalytically active in the decomposition of urea on the nickel

surface [8]. However, since all these studies were carried out in urea solutions containing potassium hydroxide at relatively high concentrations, the experiments represent an approach which is difficult to implement in practice. The most desirable approach in terms of practicability would be to use AdBlue without any variations or, in general, without changing its composition. Along with the decomposition of urea in aqueous solution, in addition to the formation of ammonia, the evolution of carbon dioxide takes place. Due to the aqueous environment, an ammonium carbonate solution is formed by dissolution.

Because of that, in this study, the electrochemical behavior of a nickel electrode in ammonium carbonate solutions was investigated by cyclovoltammetric (CV) studies and compared to the behavior of the nickel electrode in sodium hydroxide solution. In addition, experiments were carried out to investigate the influence of the species formed on the nickel surface on the concentration of ammonia in AdBlue solutions.

## 5.2.2 Experimental

### Reagents and chemicals

Urea, purity “>99.5 %”, was from Roth. Sodium hydroxide, purity “p.a.”, was purchased from Merck. Ammonium carbonate, purity “pure food grade”, was purchased from AppliChem. Millipore water was used throughout the experiments. The AdBlue used in all experiments was prepared by dissolving the appropriate amount of urea in Millipore water.

### Instrumentation

An in-house made nickel-disc electrode was used in the CV experiments. A nickel wire (diameter 0.5 mm) was embedded into the tip of a glass pipette, using epoxy resin. The nickel disc electrode is shown in Figure 25.

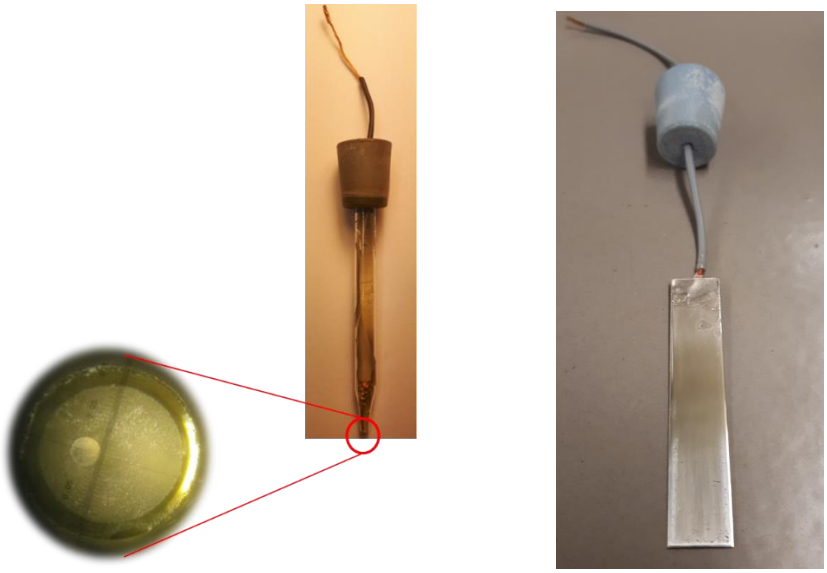

Figure 25: Left: applied nickel disc-electrode with zoom on the bottom. Surface of nickel wire can be seen. Right: applied nickel sheets for experiments on ammonia formation.

For the CV studies, a three-electrode configuration was applied consisting of the working electrode (nickel-disc electrode) which was polished before each experiment, the auxiliary electrode (platinum wire electrode) and the reference electrode (Ag/AgCl/3 M KCl).

The schematic setup is shown in Figure 26.

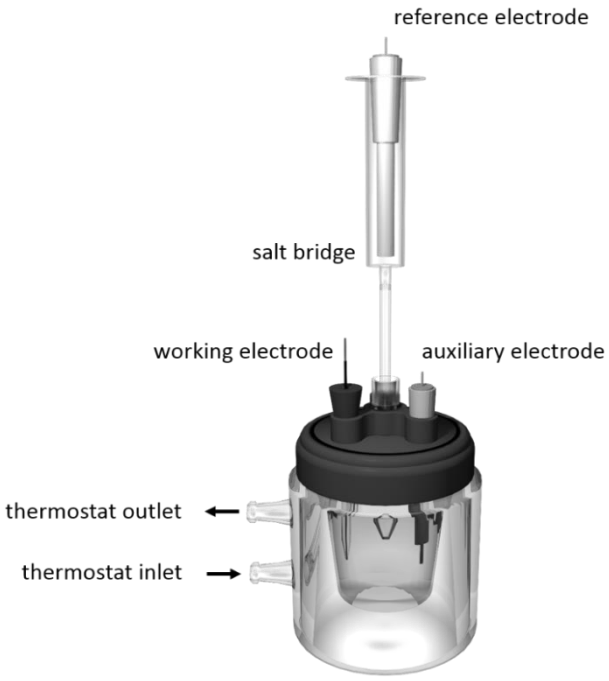


Figure 26: Schematic setup of the electrochemical cell configuration used for CV studies.

For investigations of the influence of the species, formed at the nickel surface, on the formation of ammonia, nickel sheets, exhibiting a larger surface compared to the disc electrode, were used as working and auxiliary electrode to apply different currents. One nickel sheet is exemplarily shown in Figure 25.

A 797 VA Computrace of Metrohm was used as potentiostat. To enable CV experiments at elevated temperatures, a reaction vessel with a thermostat jacket and a Haake D8 thermostat were used. To keep the reference electrode at a constant temperature and thereby enable comparability of the potentials in the different experiments, the reference electrode was placed in an external compartment, connected to the reaction vessel via a salt bridge filled with 3 M KCl. The experiments were performed with the following voltammetric parameters: sweep rate: 50 mV $s^{-1}$, voltage step: 0.001 V, number of sweeps: 30.

### 5.2.3 Results and discussion

For the investigations of the electrochemical behavior of the nickel electrode, cyclovoltammetric (CV) experiments were performed. Since the signals in the CVs of ammonium carbonate were growing during the experiments, CVs in both electrolytes were repeated 30 times and the 30th sweep of each experiment is shown in Figures 27 and 28.

First, the electrochemical behavior of the nickel electrode in sodium hydroxide solutions of different concentrations (0.1 M, 0.5 M, 1.0 M, 2.0 M and 4.0 M) was investigated at 25 °C and 40 °C. The results of each CV experiment are shown in Figure 27.

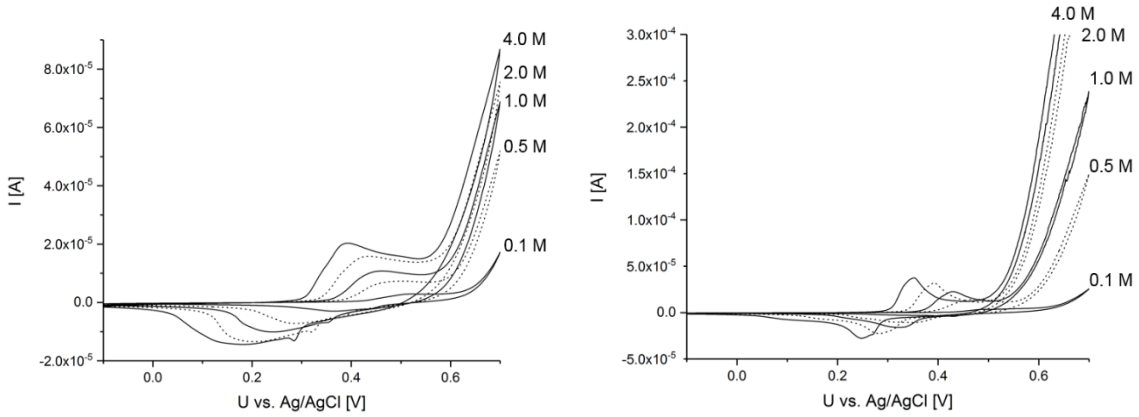


Figure 27: Cyclic voltammograms of a nickel-disc electrode (d = 0.5 mm) in sodium hydroxide solutions of various concentrations, left: at 25 °C, right: at 40 °C.

As it can be seen for all investigated concentrations at 25 °C and 40 °C, a signal of oxidation and reduction for the nickel surface was observed. According to the literature, the process can be attributed to the oxidation of $Ni^{2+}$ to $Ni^{3+}$ [9] by

$$Ni(OH)_2 + OH^- \rightarrow NiOOH + H_2O + e^- \qquad \text{(equation 16)}$$

thereby forming NiOOH, which was shown to be catalytically active concerning the decomposition of urea [7].

In the next step, the CV experiments were carried out in ammonium carbonate solutions of different concentrations (0.1 M, 0.5 M, 1.0 M and 2.0 M). The experiments were again carried out at 25 °C and 40 °C. The results of these experiments are shown in Figure 28.

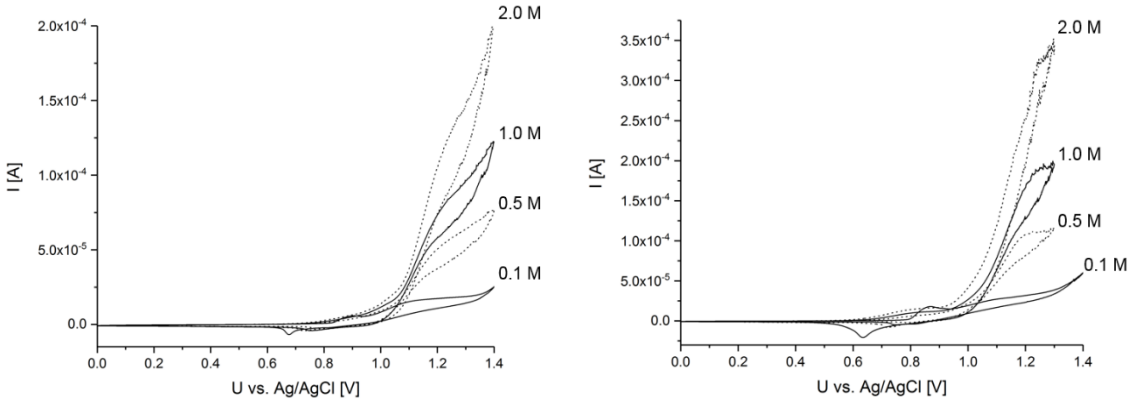


Figure 28: Cyclic voltammograms of a nickel-disc electrode (d = 0.5 mm) in ammonium carbonate solutions of various concentrations, left: at 25 °C, right: at 40 °C.

Regarding the 0.1 M ammonium carbonate solution, two oxidation signals at potentials of about 0.9 V and 1.1 V and one reduction signal at about 0.65 V were found during the CV experiments for both temperatures. The reduction signal was of similar size like the oxidation peak at 0.9 V. The oxidation, as well as the reduction signal, were growing with the number of sweeps during the experiment, meaning the signals did not reach a steady-state even after the recording of 30 CVs. As can be seen in Figure 28, the intensity of the signals at 0.65 V and 0.9 V was most pronounced in the experiments with low ammonium carbonate concentrations. In the experiments with 0.5 M, 1.0 M and 2.0 M ammonium carbonate at 25 °C and 40 °C, these signals were much smaller. This finding could additionally be confirmed by an experiment with a 0.05 M ammonium carbonate solution. Literature indicates that these signals can possibly be related to the transition $Ni^{2+}/Ni^{3+}$ [10]. However, as visible in Figure 28, the intensity of the second oxidation peak increased by increasing the ammonium carbonate concentration, which can be an indication that the oxidation process at 1.1 V is due to oxidation of ammonia on the nickel surface [10]. Besides the experiments shown in Figure 28, the CV experiment with 0.1 M ammonium carbonate was also carried out with the upper vertex potential being 1.0 V instead of 1.4 V. In this case, the signals at 0.65 V and 0.9 V could not be detected. This observation shows that this process cannot proceed independently of processes occurring at potentials >1.0 V. One possible explanation might be a local acidic pH shift at the nickel electrode, which is associated with the formation of oxygen at high potentials with progressing experiment.

To check the influence of urea on the voltammetric experiments, solutions containing 0.1 M sodium hydroxide and 0.1 ammonium carbonate with differing amount of urea were investigated. The results are shown in Figure 29.

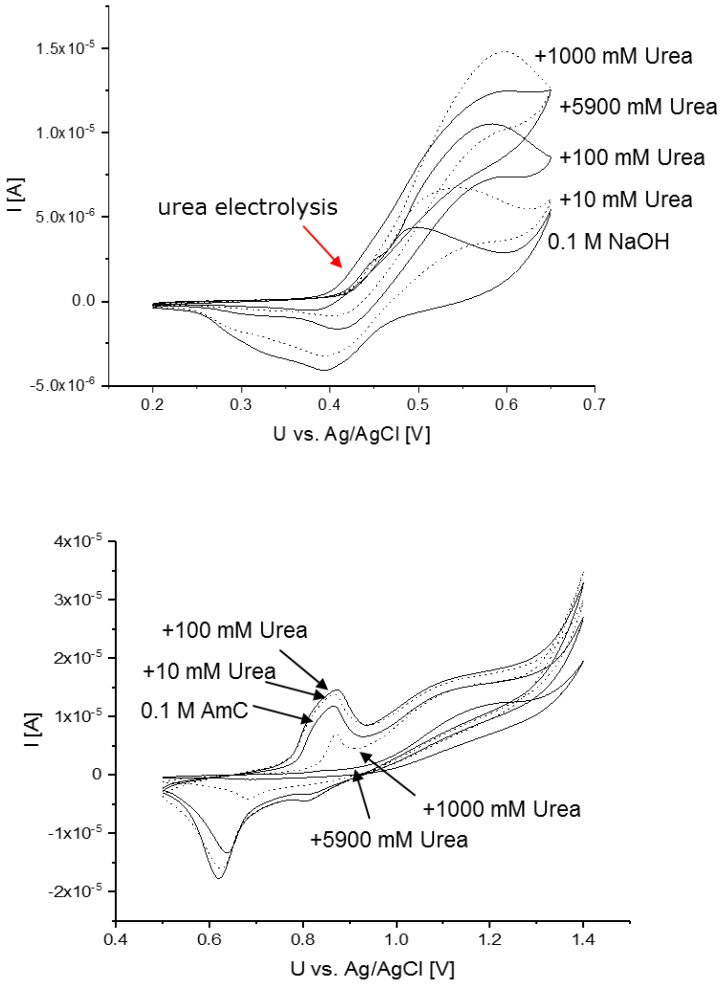


Figure 29: Influence of urea concentration on cyclic voltammograms of nickel surface in 0.1 M sodium hydroxide (top) and 0.1 M ammonium carbonate (bottom) at 25 °C.

As shown in Figure 29, electrolysis of urea was observed concurrently to nickel surface oxidation. To investigate the influence of the species formed at the nickel surface during the electrochemical processes detected by cyclic voltammetry on the formation of ammonia, experiments were set up the following way: 0.1 M sodium hydroxide or 0.1 M ammonium carbonate in AdBlue was stirred in the electrochemical cell and nickel sheets (Figure 25, right) were used as working and auxiliary electrode to apply different potentials within a three-electrode configuration. The resulting electrochemical cell is shown in Figure 30.

Figure 30: Electrochemical cell configuration with nickel sheets used as working and auxiliary electrode.

The potential was applied for 60 min and the amount of ammonia dissolved in the solution after the experiment was measured using an ammonia-selective electrode. The cyclic voltammogram with the different potentials applied and the resulting variation of ammonia concentration for the experiments with 0.1 M NaOH in AdBlue are shown in Figure 31.

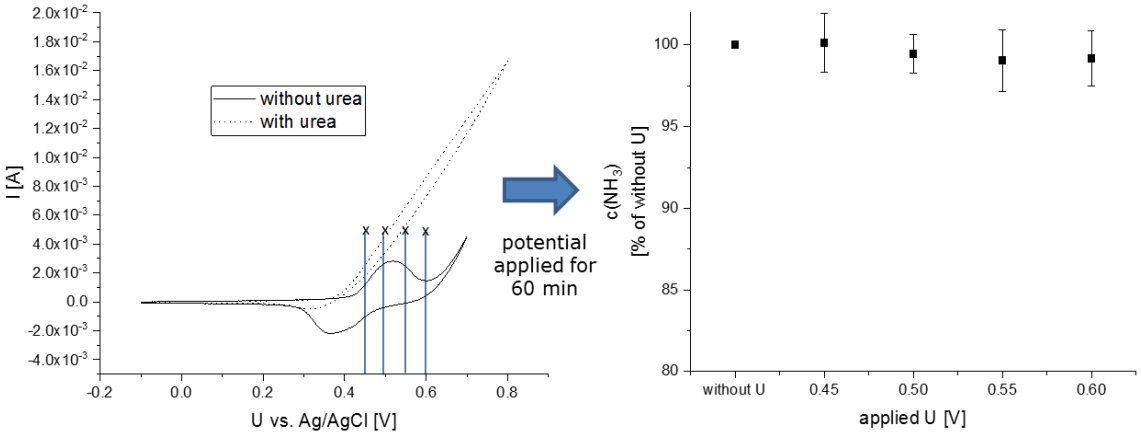


Figure 31: Cyclic voltammogram with the different potentials applied and the resulting variation of ammonia concentration for the experiments with 0.1 M NaOH in AdBlue after 60 min at ambient temperature.

As it gets obvious from Figure 31, within the standard deviation of the measurements there was no variation of the ammonia concentration detected for any of the applied potentials in case of the sodium hydroxide addition. Thus, the applied potential seemed to have no influence on the ammonia concentration.

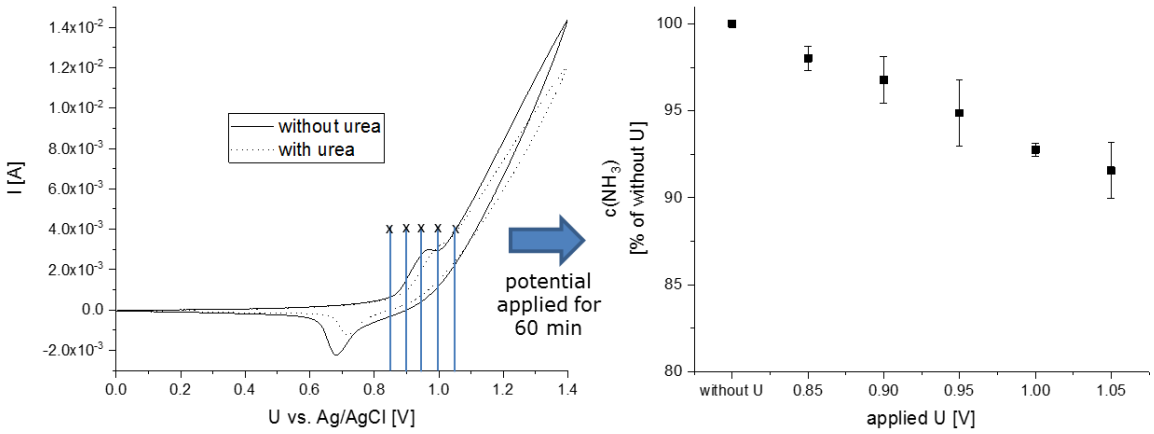


Figure 32: Cyclic voltammogram with the different potentials applied and the resulting variation of ammonia concentration for the experiments with 0.1 M ammonium carbonate in AdBlue after 60 min at ambient temperature.

The experiment was also performed with ammonium carbonate in the AdBlue solution. The results for the measurement with 0.1 M ammonium carbonate in AdBlue are shown in Figure 32. Here, the detected amount of ammonia differed with the applied potential. The higher the applied potential in the experiment, the lower was the detected concentration of ammonia. So, other effects seemed to influence ammonia concentration. Since in case of ammonium carbonate, in general, a higher potential was applied compared to the sodium hydroxide solution, the oxidation of ammonia at these higher voltages can be more pronounced. The performed experiments could not confirm the formation of ammonia in the case of ammonium carbonate in AdBlue and room temperature conditions. The NiOOH promoting effect on ammonia concentration suggested in literature was not detectable due to ammonia oxidation effects.

### 5.2.4 Conclusion

Electrochemically induced decomposition of AdBlue-urea using a nickel electrode in the presence of ammonium carbonate and sodium hydroxide was investigated in the presented study. For that, CV experiments with an in-house made nickel electrode were carried out and subsequent experiments on ammonia concentration upon applying currents in the two different electrolytes were done.

The results showed that the behavior of the nickel electrode studied by CV experiments changes significantly by changing the electrolyte from sodium hydroxide to ammonium carbonate. Oxidation of the nickel surface might have also occurred in the ammonium carbonate solutions. However, this could not finally be proven. Experiments on the influence of the applied potential on the amount of ammonia dissolved in AdBlue/ammonium carbonate solutions showed a reduction of the ammonia concentration for the applied currents, thereby covering any potentially occurring ammonia-formation effects. The reason for that might be the higher potential applied in the case of the ammonium carbonate in AdBlue compared to sodium hydroxide in AdBlue and the higher amount of ammonia present in the AdBlue/ammonium carbonate solution. Suitable separation approaches should be applied to avoid oxidation effects of ammonia at the electrode surface. Further studies would be necessary for the evaluation of the effects at higher temperatures since earlier studies on the behavior of a nickel surface in sodium hydroxide have shown that the ammonia-formation effects are favored by elevated temperatures.

### 5.2.5 References

[1] K. Mollenhauer, H. Tschöke, *Handbuch Dieselmotoren,* 3, Springer, Berlin, **2007**.

[2] P. Braun, J. Gebhard, F.-M. Matysik, H.-P. Rabl, *Chemie Ingenieur Technik* **2018**, 90, 762-773.

[3] A. M. Bernhard et al., *Catalysis Science & Technology* **2013**, 3, 942-951.

[4] P. Braun, J. Gebhard, H.-P. Rabl, *Low Temperature DeNOx,* Final Report FVV project 1155, Frankfurt am Main, **2017**.

[5] A. Roppertz, S. Füger, S. Kureti, *Topics in Catalysis* **2017**, 60, 199-203.

[6] F. Lu, G. G. Botte, *ECS Electrochemistry Letters* **2015**, 4, 10, E5-E7.

[7] F. Lu, G. G. Botte, *Electrochimica Acta* **2017**, 246, 564-571.

[8] D. A. Daramola, D. Singh, G. G. Botte, *Journal of Physical Chemistry A* **2010**, 114, 11513-11521.

[9] F. Hahn, D. Floner, B. Beden, C. Lamy, *Electrochimica Acta* **1987**, 32, 11, 1631-1636.

[10] G. Zheng, H. Cao, L. Zheng, *Journal of Applied Electrochemistry* **2007**, 37, 799-803.

## 5.3 Investigations on the decomposition of AdBlue-urea in the liquid phase at low temperatures by an electrochemically induced pH shift

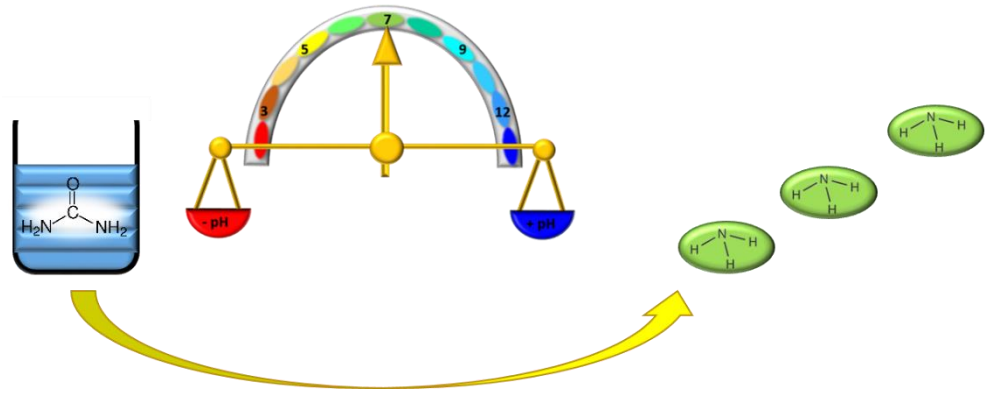


---

This chapter has been published and adopted from:

Peter Braun, Bernhard Durner, Hans-Peter Rabl and Frank-Michael Matysik,

*Monatshefte für Chemie – Chemical Monthly* **2019,** in press, DOI: 10.1007/s00706-019-02406-6.

**Abstract**

Ammonia-based selective catalytic reduction (SCR) systems are the most widely used technology for reduction of nitrogen oxide emissions from lean-burn engines such as diesel engines. However, at low exhaust temperatures, the SCR process is limited by difficulties in the decomposition of the ammonia precursor urea, which is carried onboard using an aqueous solution AdBlue. In this study, the decomposition of AdBlue-urea induced by electrical current and the resulting associated pH shifts was investigated in a divided cell configuration in the liquid phase. The decomposition was found to be favored in both electrochemical compartments, anodic and cathodic, at temperatures of 60 – 80 °C compared to a reference without electrochemical treatment. In addition to the determination of ammonia contents using an ammonia sensor, IC/HPLC analyses were carried out for each sample. Different byproducts such as biuret, nitrate, cyanuric acid, ammelide, and others were formed. In the anodic compartment, nitrate formation could be observed due to oxidation of ammonia at the electrode surface.

## 5.3.1 Introduction

To counteract environmental air pollution, legislation worldwide increasingly limits the permitted amounts of exhaust gases from internal combustion engines [1]. Nitrogen oxides ($NO_x$), meaning the sum of nitrogen monoxide NO and nitrogen dioxide $NO_2$, have attracted attention in recent years regarding the discussions about the so-called “dieselgate”, concerning the engine’s $NO_x$ emissions [2, 3].

In contrast to gasoline engines, diesel engines are in general operated with a lean combustion mixture, meaning that a stoichiometric excess of oxygen compared to the amount of fuel is present inside the combustion chamber [4]. For this case, the onboard chemical reduction of $NO_x$ is a complex process due to undesired reactions of exhaust’s reduced species (unburned hydrocarbons, carbon monoxide) with the oxygen present in the lean exhaust gas [4, 5]. Therefore, vehicles operated by diesel engines require an additional technology for the reduction of $NO_x$ emissions, at least since the introduction of the EURO 6 standard [6]. Besides the lean-$NO_x$-trap catalyst, which is mainly used for light-duty applications, the selective catalytic reduction (SCR) process is the most commonly used technology for the elimination of $NO_x$ emissions from lean exhaust gas [5-12]. The SCR process requires ammonia as an external reducing agent, which needs to be carried onboard as additional operating material. However, as ammonia is a toxic gas at ambient conditions, a precursor of the reducing agent, namely urea, is carried onboard. Here, urea as eutectic, 32.5 wt% solution in

water (AdBlue or DEF) is used as an external reducing agent [13]. The process of $NO_x$ reduction is thus preceded by the process of urea decomposition to ammonia. While modern SCR-catalytic coatings reach 90% $NO_x$ reduction at exhaust temperatures of 165 °C [7] for the case of available ammonia, the decomposition of urea to ammonia requires temperatures of at least 180 °C - 190 °C even when applying a hydrolysis catalyst (e.g. $TiO_2$) [7, 14]. Since modern diesel engines have become more and more efficient over the last years, a decline of exhaust temperature could be observed concurrently [5, 15]. Hence, in the case of low-load driving, like in city traffic, the decomposition process of urea to ammonia limits the applicability of the overall SCR system. Consequently, methods enabling preparation of ammonia are desired to reduce $NO_x$ emissions of diesel vehicles at low exhaust temperatures [7, 16].

In the literature, improved urea decomposition in the liquid phase at high or low pH was reported [17-20]. In previous studies on the liquid-phase decomposition of AdBlue-urea, a facilitated decomposition of urea into ammonia at low temperatures under alkaline and acidic conditions inside AdBlue was found. The results showed that alkaline, as well as acidic conditions, led to an increased formation of ammonia at low temperatures. However, since the addition of an acid or base would not present a feasible technical approach for onboard applications, the focus of this study was to investigate the influence of an in situ generated pH shift in AdBlue on the formation of ammonia at low temperatures. The generation of local pH shifts was achieved by electrolysis of solutions containing urea.

In general, electrochemistry of urea is currently a relevant topic [21-23]. A lot of research is carried out, e.g. in connection with the generation of hydrogen and the application of fuel cells [24-27].

In addition to the determination of the produced amounts of ammonia by an ammonia-selective electrode, an IC/HPLC method was used to study the formation of byproducts [28, 29]. Byproducts can be a problem in case of decomposing urea at low temperatures, e.g. leading to clogging of the exhaust tract [30-33].

The idea in this study was to exploit the increase of pH in the cathodic compartment as well as the decrease of pH in the anodic compartment associated with the electrolysis. This strategy enables high system dynamics that allow the system to react quickly to changes in the engine operating point and associated variations in ammonia demand.

## 5.3.2 Experimental

**Chemicals**

Urea and biuret, both purity “p.a.”, and sodium carbonate, purity “> 99 %”, were purchased from Roth. Anhydrous sodium sulfate, purity “extra pure”, was obtained from Acros Organics. Sodium formate, sodium acetate, sodium nitrite, sodium cyanate and sodium nitrate, purity “p.a.” were purchased from Merck. Sodium hydroxide solution 50 %, purity “p.a.” was obtained from Fluka and conc. sulfuric acid, purity “analytical reagent grade”, was purchased from Fisher Scientific. Melamine, purity “99 %”, cyanuric acid and ammelide, both purity “analytical standard”, were obtained from Sigma-Aldrich. Millipore water was used throughout all experiments. Synthetic AdBlue was prepared by dissolving 32.5 wt% urea in Millipore water.

**Instrumentation**

For most of the experiments, an electrochemical cell consisting of three chambers, which were separated from each other by frits, was used. To avoid mixing during the experiment, cathode and anode were each placed in the outer chambers of the cell, to ensure kind of “buffer zone” between the two electrochemical compartments. In addition, the sample solution was filled in the electrochemical cell in a way that it was the same height in all three chambers, resulting in equal hydrostatic pressure. In the anodic and the cathodic compartment, 10 ml of sample solution was used and in the buffer zone between the electrode compartments, 23 ml was used. To enable experiments at elevated temperatures an external water bath was used for heating. The overall experimental setup is shown in Figure 33.

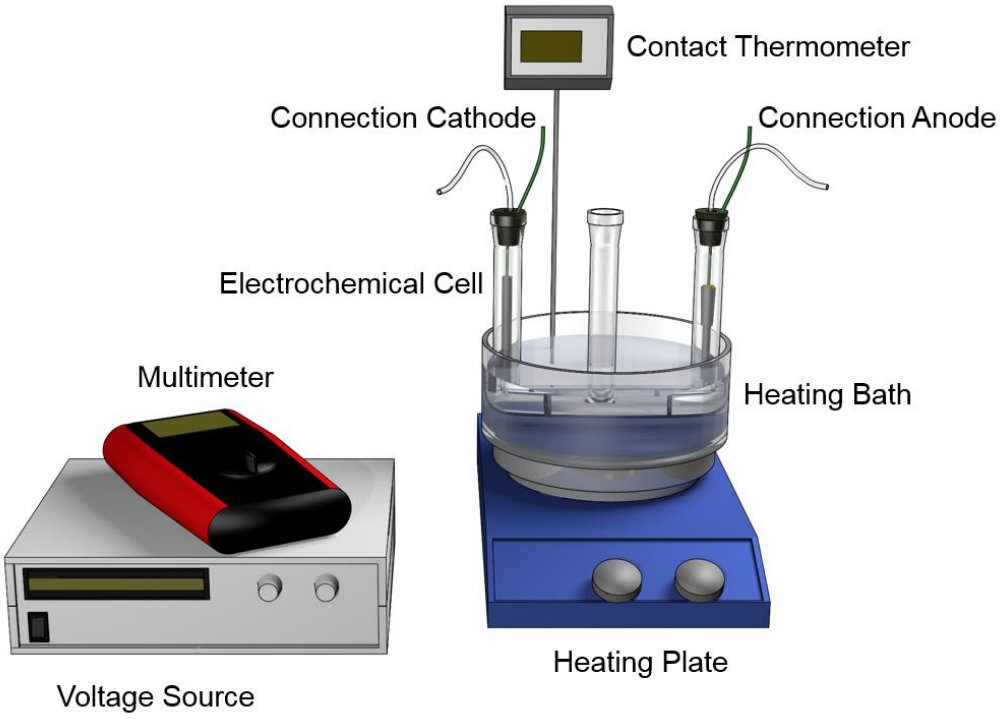


Figure 33: Overall setup for experiments with separated electrochemical compartments.

A reference sample without any electrochemical treatment was generated using a separated reaction vessel inside the heating bath (10 ml). As voltage source, a Voltcraft “HPS 13015” was applied. For monitoring the current for the experiments, a UNI-T “UT71D” multimeter was used. If not noted otherwise, a Pt wire electrode from Metrohm was used as the anode and a Ni cylinder was used as the cathode. Since ammonia can evaporate from the solution, the gases generated during the experiment were collected with glass bottles, but the concentration of ammonia subsequently measured in the liquid acid trap was below the detection limit for all the experiments. To enable high currents without any electro-osmosis effects inside the reaction mixture, an auxiliary electrolyte, 0.5 M sodium sulfate in most of the experiments, was added to the synthetically made AdBlue ($\kappa$ = ~39 mS/cm). After the experiments, the samples inside the outer chambers and the reference sample were collected and the concentration of ammonia in the liquid phase was measured using a $NH_3$-selective electrode “6.0506.100” from Metrohm. Due to the high sensitivity of the electrode, the samples were diluted before the measurement. In addition, the pH value was determined by a pH glass electrode from Schott. For investigating the effect of the electrolytic treatment on the formation of byproducts in solution, an IC/HPLC analysis of the individual samples was carried out. For that, the procedure described by Koebel et al. [28, 29] was used with few adaptations. The measurements were carried out on a “Thermo Fisher Vanquish HPLC” system using

an anion exchange column “Waters IC-Pak WAT026770 ANION HC 4.6 x 150” and an UV/Vis detector “Thermo Fisher UV HighSense Flow Cell” set to a measuring wavelength of 197 nm. An excerpt of an exemplary chromatogram observed for byproduct determinations up to retention time of 25 min is shown in Figure 34. No analytes were found at longer retention times.

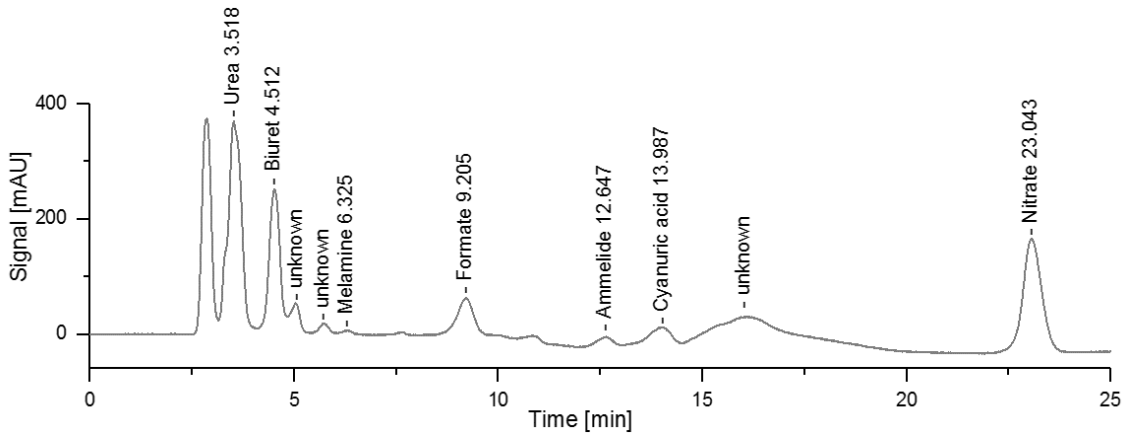


Figure 34: Example of a chromatogram for byproduct analysis of a sample from an anodic compartment. Experimental conditions: 6.5 V (50 mA), 80 °C, 20 min, see Figure 36.

As eluent, a 5 mM phosphate buffer with pH 10.4 was used and a gradient elution was applied the following way:

Table 2: Applied gradient elution for IC/HPLC analysis

| *t* / min | *Flow* / ml |
|---|---|
| 0 – 10 | 0.5 |
| 10 - 12 | 0.5 → 1.0 |
| 12 - 18 | 1.0 |
| 18 - 25 | 1.0 → 2.0 |
| 25 - 37 | 2.0 |
| 37 - 37.5 | 2.0 → 0.5 |
| 37.5 - 39 | 0.5 |

The applied sample volume was 20 µl. For quantitative analysis standard samples were used to construct calibration plots for various substances.

## 5.3.3 Results and discussion

### *5.3.3.1 Influence of temperature*

Using the divided cell configuration described in the experimental section, first the influence of the reaction temperature on the formation of ammonia in the two electrochemical half-cells was investigated. To avoid evaporation effects of the sample solution, the upper-temperature limit for the experiments was set to 80 °C.

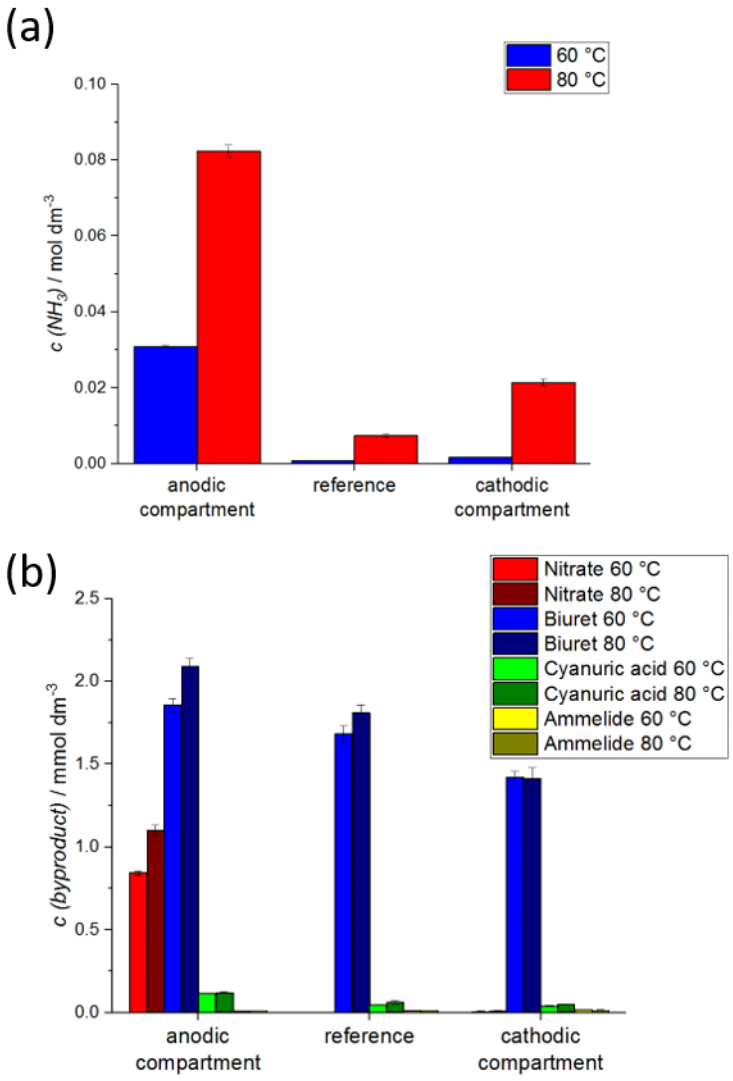


Figure 35: Influence of the reaction temperature on the formation of ammonia (a) and byproducts (b). Experimental conditions: 10 ml of 0.5 M sodium sulfate in AdBlue in cathodic and anodic compartment, 12 V (60 °C) or 10 V (80 °C), 100 mA, 20 min.

The experiments were carried out for 20 min at a current of 100 mA. As expected, an increase from 60 °C to 80 °C adjusted by external heating resulted in an increase in ammonia formation for both electrochemical compartments, anodic and cathodic (see Figure 35 a). The same observation was made for the reference, which was obtained without any electrochemical treatment, meaning solely thermal decomposition. The amount of ammonia generated at 60 °C and 80 °C in the anodic as well as in the cathodic compartment was higher compared to the reference sample. At 80 °C after 20 min a ~3-fold increase of ammonia concentration was observed in the cathodic compartment compared to the reference and in the anodic compartment, even a ~11-fold increase was detected. The ammonia formation in the cathodic compartment increased more strongly than in the anodic region with increasing the temperature. The pH values measured after the experiments were similar for 60 °C and 80 °C with 2.5 and 2.9 in the case of the anodic compartment and with 13.6 and 13.5 in the cathodic compartment. An excerpt of the byproduct formation investigated by an IC/HPLC method [28, 29] is shown in Figure 35 b. A decrease of biuret concentration in the order anodic compartment > reference > cathodic compartment for both temperatures investigated was obtained. In the anodic compartment, a formation of nitrate was detected. In the reference and the cathodic sample, nitrate formation was not found. The detection of nitrate might be due to electrochemical oxidation of ammonia. Few amounts of cyanuric acid and ammelide were also found in the reaction mixture with the amount of cyanuric acid being the lowest again in the cathodic compartment.

Since a higher degree of decomposition was generally observed at 80 °C, the following experiments were carried out at 80 °C.

#### *5.3.3.2 Influence of the current*

In a next step, the influence of the current applied to the sample was investigated. The results of the experiments are shown in Figure 36.

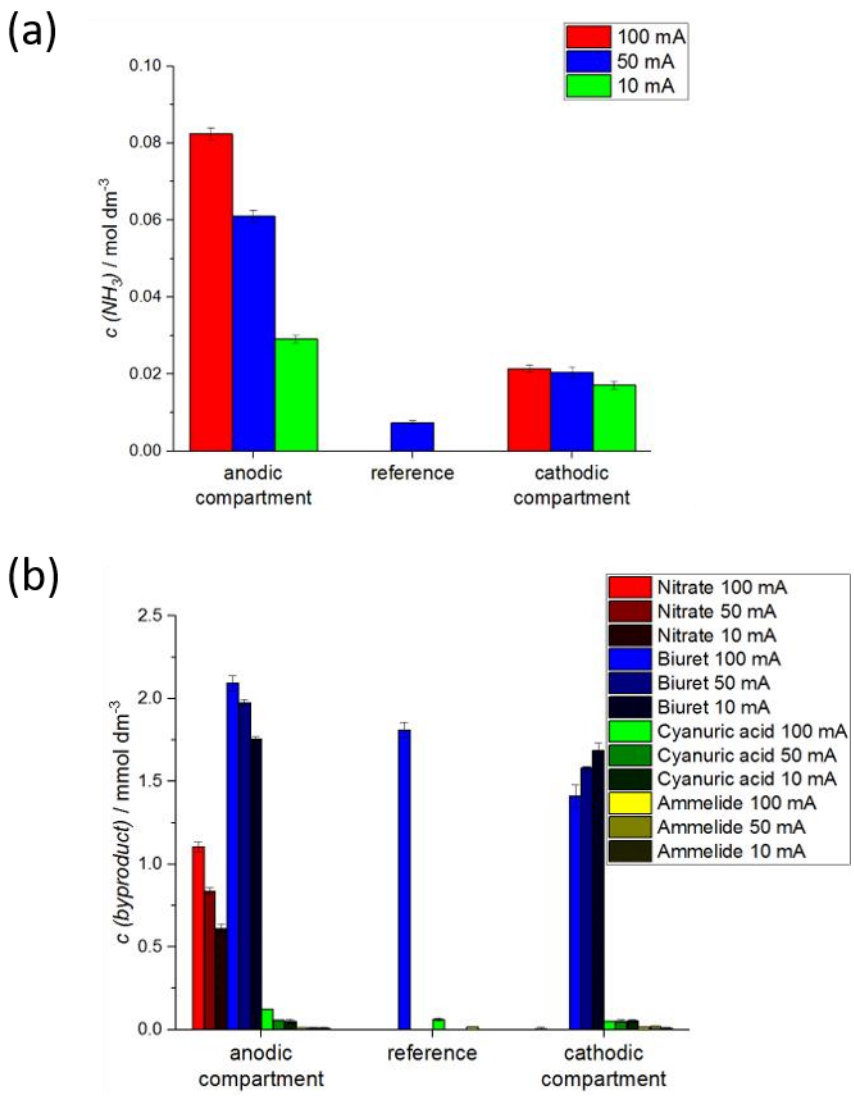


Figure 36: Influence of the current on the formation of ammonia (a) and byproducts (b). Experimental conditions: as in Figure 35, 6.5 V (50 mA) or 4.0 V (10 mA), 80 °C.

Again, the experiments were carried out for 20 min at 80 °C. In both half-cells, the ammonia formation increased by raising the applied current. The degree of increase was significantly more pronounced in the case of the anodic compartment (see Figure 36 a). The observed shift of pH was related to the degree of electrolysis and to the formation of ammonia. From 10 mA, 50 mA to 100 mA, the pH dropped in the anodic compartment from 7.3, 5.8 to 2.9 and in the cathodic compartment the pH raised from 10.6, 13.3 to 13.5 respectively. This means that ammonia formation increased the more alkaline or acidic the sample solution was. As it can be seen in Figure 36 b, for the biuret formation, the concentration in the cathodic compartment was again lower compared to the reference and the anodic compartment. Interestingly, with increasing current, the biuret formation increased in the case of the anodic but decreased in the cathodic

compartment. Nitrate formation, which was only found in the anodic compartment, increased with increasing current. Low levels of cyanuric acid and ammelide were detected. With increasing current, the amount of cyanuric acid increased in the anodic compartment but decreased in the cathodic compartment.

#### *5.3.3.3 Influence of the reaction time*

In the next step, the aim was to check the influence of the reaction time. Therefore, the experiments at 80 °C and 50 mA were carried out additionally for 40 min. The results in comparison to the 20 min experiments are shown in Figure 37.

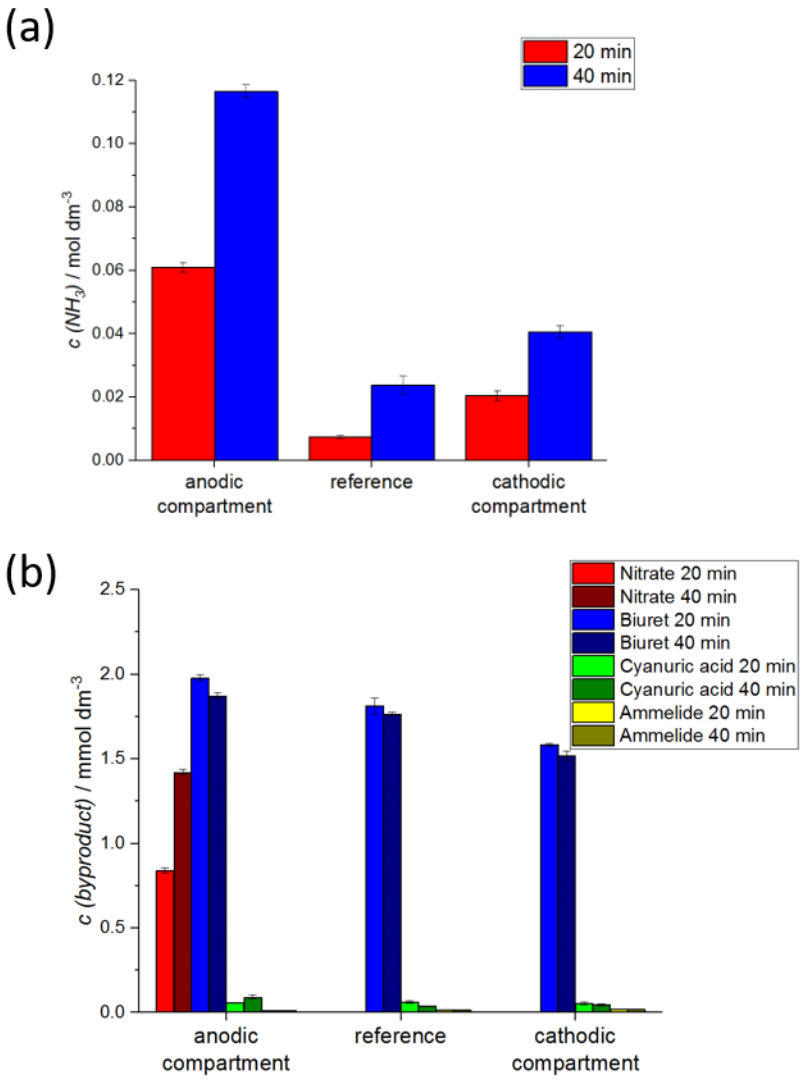


Figure 37: Influence of the reaction time on the formation of ammonia (a) and byproducts (b). Experimental conditions: as in Figure 36, 6.5 V (50 mA), 80 °C.

The results show that an increase in the reaction time by a factor of 2 resulted in almost a doubling of ammonia formation. The pH values observed in the electrochemical compartments after the experiments were comparable for both reaction times (20 min and 40 min). However, in contrast to the ammonia concentration, the concentrations of the byproducts biuret, cyanuric acid and ammelide, except cyanuric acid in the anodic compartment, have not increased but slightly decreased with the reaction time 40 min instead of 20 min. This indicates no linear buildup of these species with time during the experiment. Nevertheless, an increase of nitrate formation in the anodic compartment was observed in the case of the 40 min experiments.

#### *5.3.3.4 Influence of the auxiliary electrolyte*

The influence of the auxiliary electrolyte was checked by an experiment in which sodium sulfate was replaced by sodium nitrate. The experiments were carried out for 20 min at 80 °C and the results are shown in Figure 38.

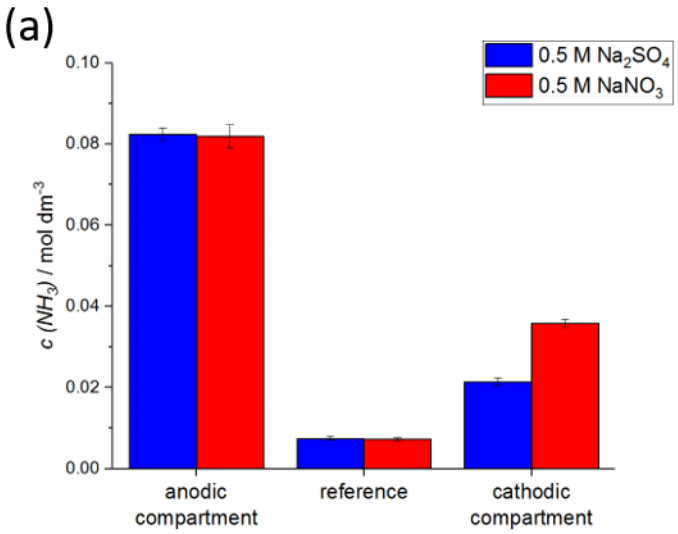

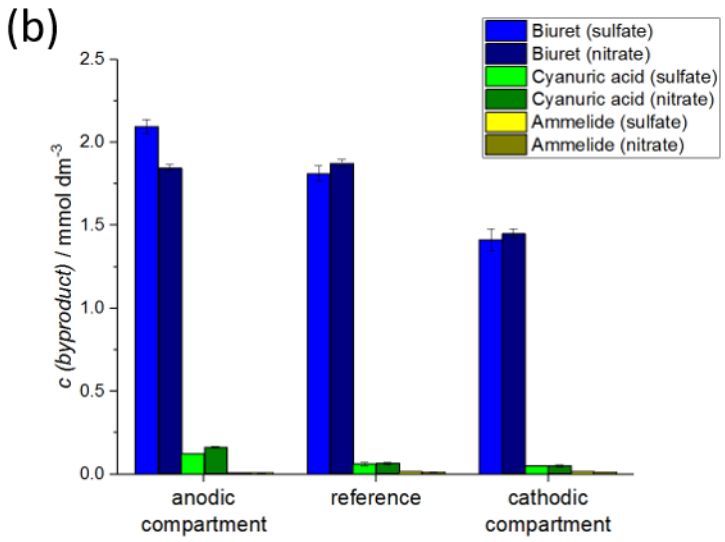


Figure 38: Influence of the auxiliary electrolyte on the formation of ammonia (a) and byproducts (b). Experimental conditions: as in Figure 35, 10 ml of 0.5 M sodium sulfate or sodium nitrate in AdBlue in cathodic and anodic compartment, 13 V (100 mA) for $NaNO_3$, 20 min, 80 °C.

As can be seen in Figure 38, the auxiliary electrolyte showed no influence in case of the reference and the anodic compartment. However, in the cathodic compartment, a higher amount of ammonia was detected. In general, sodium sulfate is the more inert electrolyte [34]. Thus, this effect might be explained by side reactions, e.g. the reduction of nitrate to nitrite according to Eq. (1) at the electrode surface and the additional formation of $OH^-$ associated therewith.

$$NO_3^- + 2\ e^- + H_2O \rightarrow NO_2^- + 2\ OH^- \qquad \text{(equation 17)}$$

The influence of the auxiliary electrolyte on the byproduct formation is shown in Figure 38 b.

### *5.3.3.5 Influence of the current density and the electrode material*

To investigate the influence of current density and/or the influence of the electrode material, the experiments at 100 mA and 80 °C were additionally carried out with two platinum electrodes instead of the nickel cathode and the platinum anode which was used by default.

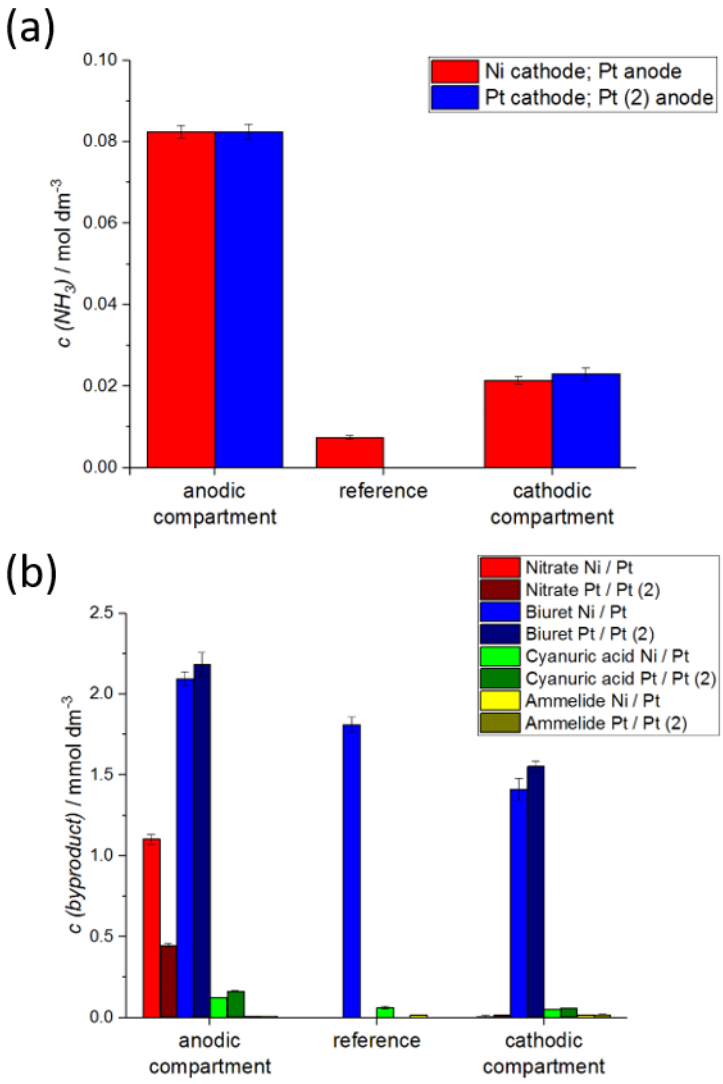


Figure 39: Influence of the current density and/or the electrode material on the formation of ammonia (a) and byproducts (b). Experimental conditions: as in Figure 35, 11.5 V (100 mA) for Pt cathode; Pt (2) anode, 80 °C.

As shown in Figure 39 a, the two different electrodes led to the formation of equal amounts of ammonia after 20 min. The observations show that current density and/or electrode material had no significant impact on the formation of ammonia in the two electrochemical compartments. As shown in Figure 39 b, the most significant difference between the two experiments can be found in the formation of nitrate in the anodic compartment. While in the case of the Pt anode used by default, ~1.2 mM nitrate could be detected, the application of an alternative Pt anode with smaller electrode surface led to the formation of only ~0.5 mM. This is a lowering by a factor of > 2. Consequently, the nitrate formation could be influenced by the current density and/or the specific material of the electrode tested. Due to the increased current density, a locally more acidic region around the electrode surface can be expected. Thereby the $NH_3/NH_4^+$ ratio is shifted to the side of

the ammonium ion. As can be found in previous studies from literature [35], it is more difficult to oxidize the ammonium ion compared to the non-ionic species ammonia, which can be an explanation for the lower nitrate amount detected in case of the alternative Pt (2) anode. Besides that, influences of the specific material of the platinum electrodes are also possible.

#### *5.3.3.6 Influence of separated electrochemical compartments*

Additionally, experiments were carried out using an electrochemical cell without a separation of the two electrochemical half-cells. A comparison to the experiments with separated compartments is shown in Figure 40.

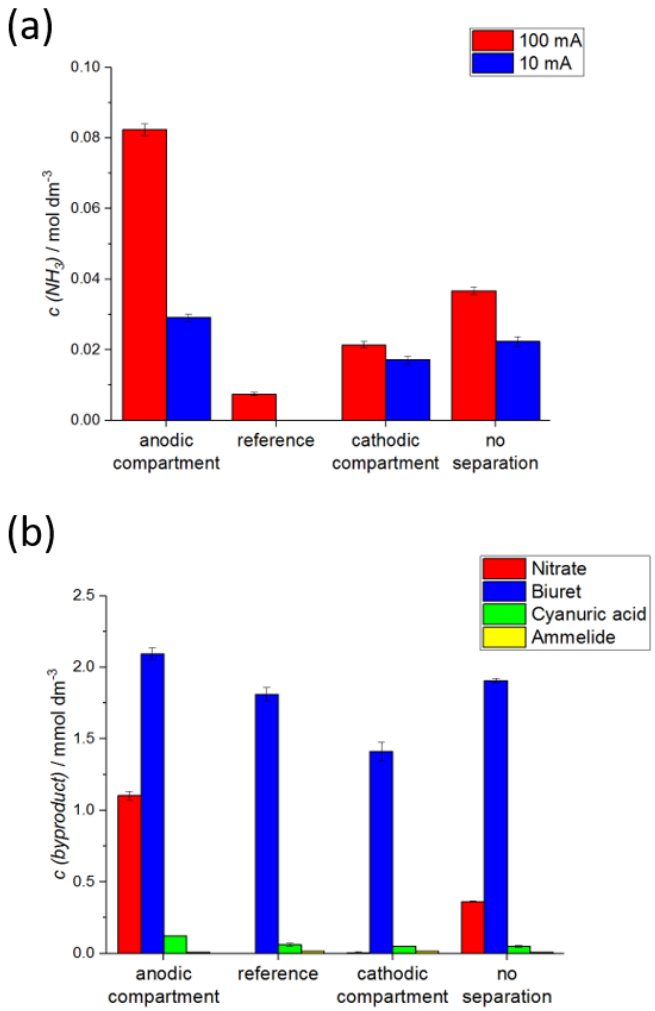


Figure 40: Influence of separated compartments and the current on the formation of ammonia (a) and byproducts (at 100 mA) (b). Experimental conditions: 20 min, 80 °C, for separated compartments: as in Figure 35, 10 ml in cathodic and anodic compartment and in case of no separation: 20 ml of 0.5 M sodium sulfate in AdBlue, 3.0 V (10 mA) or 6.0 V (100 mA).

The performed experiments showed that the ammonia concentration in the experiments without separation lies in between the ammonia concentrations found in the two half-cells for both currents investigated of 10 mA and 100 mA. The same was observed for the byproduct formation, which is shown in Figure 40 b.

#### *5.3.3.7 Comparison of results to externally acidified and alkalized samples*

In a next measurement, a comparison was done between the in-situ pH shifted experiments and sample solutions to which some amount of acid or base was added. The amount of acid and base added was in a way that the pH value after 20 min reaction time was similar to the pH observed at the end of the in-situ pH shifted experiments. For the anodic and cathodic compartment, the pH value was 2.9 and 13.5. For the experiments with acid/base addition, the pH was 2.7 and 13.5. The measured ammonia concentrations are shown in Figure 41 a.

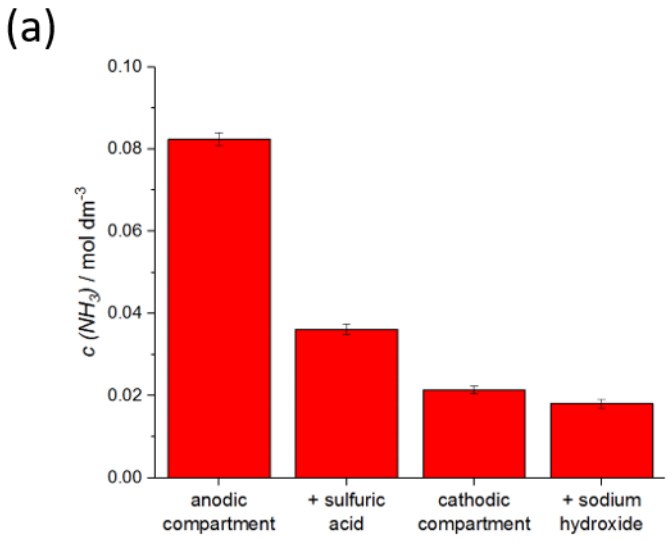

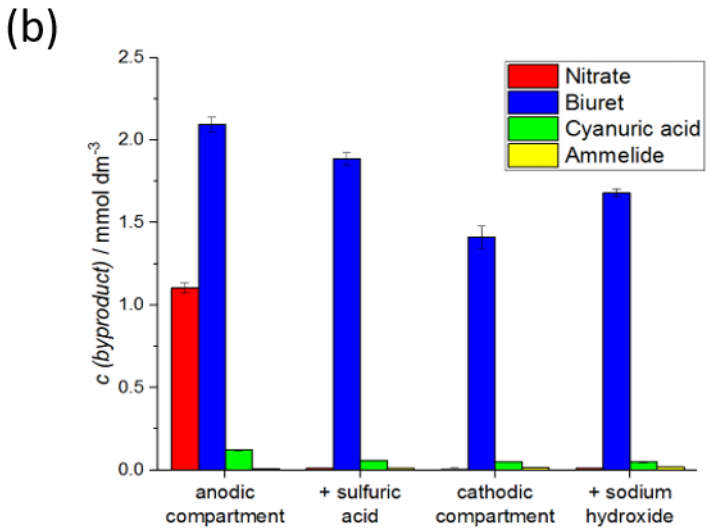


Figure 41: Comparison of anodic with acidic conditions and cathodic with alkaline conditions on the formation of ammonia (a) and byproducts (b). Experimental conditions: 10 ml of 0.5 M sodium sulfate in AdBlue with or without 0.05 M sulfuric acid/sodium hydroxide, 20 min, 80 °C, in case of applied current: as in Figure 36, 10 V (100 mA).

The results show that the ammonia formation in the case of the electrochemical experiments was in both compartments higher than for the one of acid/base addition into AdBlue. A possible explanation is the high local pH shift in close vicinity to the electrodes accelerating the ammonia formation. Figure 41 b shows that the nitrate formation in the anodic compartment was likely due to the oxidation of ammonia on the electrode surface since in the acidified sample nearly no nitrate was detected. Another hint for this is the fact that nitrate formation was growing linearly with the reaction time (see Figure 37 b). The concentration of biuret seemed to be generally reduced in alkaline conditions.

#### *5.3.3.8 Tests with commercial AdBlue*

Moreover, the electrochemically induced pH shift experiments were also carried out with commercial AdBlue which was taken from the tap of a commercial petrol station. Samples of three different petrol stations were compared by their specific conductivities. The following values were found:

Table 3: Specific conductivities of the commercial AdBlue samples from different petrol stations.

| Sample | κ / mS cm$^{-1}$ |
|---|---|
| 1 | 1.90 |
| 2 | 1.78 |
| 3 | 2.22 |

The specific conductivities of the three investigated samples were similar. However, for the following experiment, sample 3 having the highest conductivity was chosen to be tested. As described above, the experiments were carried out on the one hand in an electrochemical cell with separated compartments and on the other hand with an undivided cell. In the case of separated compartments, the low conductivity of the commercial samples (~2 mS/cm vs. ~39 mS/cm with sodium sulfate addition) led to strongly pronounced electro-osmosis effects meaning there was a transport of the liquid from one compartment to the other. Because of that, the experiments could only be performed at a low current of 10 mA. The results together with the experiments without separation of the electrochemical compartments are shown in Figure 42.

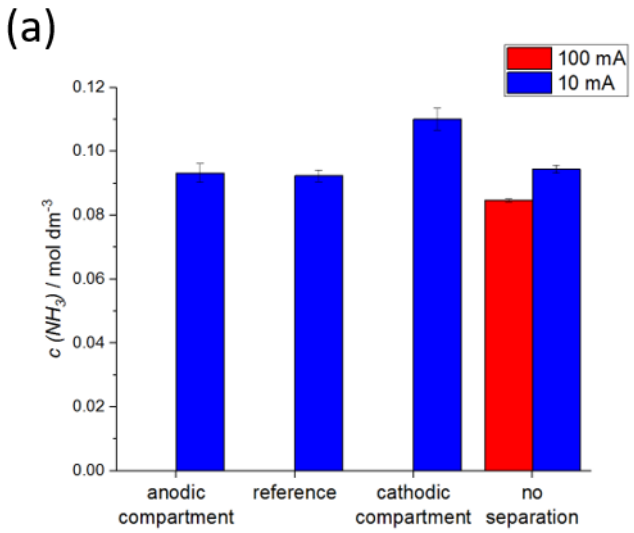

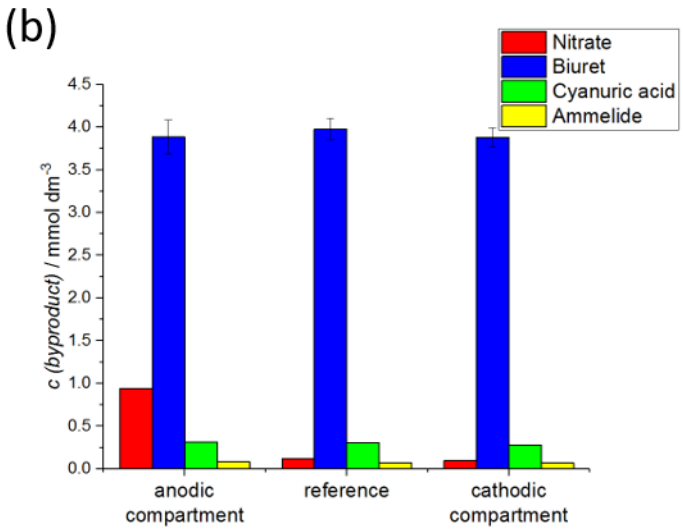


Figure 42: Influence of the in-situ pH shift experiments with commercial AdBlue. Influence on formation of ammonia (a) and byproducts (for separated cathode and anode) (b). Experimental conditions: as in Figure 40, commercial AdBlue, 20 min, 80 °C, 5.7 V (10 mA) or 30 V (100 mA) in case of non-separated cell, 11 V (10 mA) in case of separated half-cells.

Firstly, a significantly higher concentration of ammonia in the reference sample was found compared to the experiments with freshly prepared synthetic AdBlue. A partial decomposition of urea in AdBlue in aged samples is the reason for that. Further, it can be seen that anodic treatment did not result in significantly higher ammonia formation, which is in contrast to the results shown above. The same was observed for the experiment at 10 mA in the undivided cell. Due to the lower conductivity of the commercial AdBlue, a higher voltage was needed in this case for enabling a current of 10 mA. In the case of the cathodic compartment, an increase of ammonia concentration at 10 mA was observed. When the current was increased to 100 mA in case of the undivided cell experiments, even a decrease in the formation of ammonia was obtained. The reason can only be the higher degree of ammonia oxidation. It can be assumed that the high background level of the commercial AdBlue seemed to act like a buffering system. Consequently, the pH shift could not propagate from the electrode's diffusion layer into the bulk solution and thus not improve urea decomposition.

Regarding the byproduct determinations, the substances shown, biuret, cyanuric acid, and ammelide are known for their behavior to form undesired deposits in the exhaust tract [36, 37]. It should be noticed that decomposition in the cathodic compartment, in general, led to the formation of a lower variety of byproducts. In contrast, in the case of anodic decomposition, the variety of byproducts was increased at the temperatures investigated compared to the reference samples.

One broad signal, which was found at retention time of ~15 min in the IC/HPLC analyses of the reference and the cathodic sample, but not in the anodic ones, could not be identified. The peak was also found in the experiments with added sodium hydroxide, showing the promoting effect of alkaline conditions. It was found to increase with time since it was more pronounced in the 40 min experiments compared to the 20 min experiments. Formate was also found especially in the anodic compartment but also in the reference. However, an increase in anodic current reduced its detected amount. At constant current formate was found to build up with reaction time. Cyanate, the anion of the urea decomposition intermediate isocyanic acid was also found. Maybe the signal with a retention time of ~15 min is related to a species associated with the cyanate ion, which had a similar retention time. Nitrite was found coexisting with nitrate. Melamine, ammeline and acetate could not be detected or only be found in traces amounts for all the experiments carried out.

Considering the widely accepted two-step mechanism of urea decomposition, with thermolysis and subsequent hydrolysis [14], in general, anodic treatment might have the following advantage for liquid-phase decomposition: isocyanic acid which is formed from urea in the thermolysis reaction together with a first equivalent of ammonia has a pKs value of 3.7 [38]. In case of acidic conditions isocyanic acid is present as protonated species and not as its anion cyanate. Since isocyanic acid can be hydrolyzed more easily in excess of water, the low pH value should promote further decomposition of it and thereby improve ammonia formation.

During the electrolysis, of course, hydrogen is produced in the cathodic compartment. As different studies on a "$H_2$-assisted $NH_3$-SCR" have shown a promoting effect of hydrogen in the exhaust gas on the $NH_3$-SCR efficiency, the production of hydrogen can be seen as advantageous for the SCR process. In addition to the $NH_3$-SCR promoting effect, a $H_2$-based SCR pathway was observed to proceed e.g. on a Cu-SSZ-13 [39-42].

As, in general, $H_2$-SCR is discussed at the moment as an alternative or complement to the existing $NH_3$-SCR approaches, the experimental results shown in this chapter indicate the potential of the presented strategy [7].

### 5.3.4 Conclusion

The decomposition of AdBlue-urea influenced by electrical current and the associated pH shifts was studied in the liquid phase. In order to investigate the influence of anodic and cathodic half-cell reactions separately, an electrochemical cell was used, in which the two compartments were separated from each other by frits. For currents between 10 mA and 100 mA at temperatures up to 80 °C, the level of detected ammonia was found in the order: anodic compartment > cathodic compartment > reference, meaning the ammonia formation was promoted in the acidic anodic compartment and also in the alkaline cathodic compartment. Higher temperature, in general, led to higher concentrations of ammonia. A current increase led to more acidic or alkaline pH values, which promoted the formation of ammonia.

In addition to the measurement of ammonia, determinations of byproducts were carried out using an IC/HPLC method [28, 29]. Different byproducts such as biuret, nitrate, cyanuric acid, ammelide, formate and others were detected. In the anodic compartment, electrochemical oxidation of ammonia led to the formation of nitrate and nitrite. However, in the experiments using an alternative platinum electrode, nitrate formation at the anode was shown to be reduced by increased current density and/or the specific material of the platinum electrode. Separation approaches should be applied for avoiding anodic ammonia and urea oxidation on the electrode surface, e.g. by using selective-membrane techniques. Since in earlier studies byproduct formation was shown to be reduced at higher temperatures, for real applications a higher temperature level for this strategy would be advantageous [30].

All in all, the study showed that an in-situ pH shift effected by electrolysis can be applied for increased ammonia formation in liquid AdBlue. However, strategies for reducing byproduct formation would be advantageous. The produced hydrogen might be used for further $NO_x$ reduction.

### 5.3.5 References


[1] J. Li, H. Chang, L. Ma, J. Hao, R. T. Yang, *Catalysis Today* **2011**, 175, 147-156.

[2] M. Frigesi di Rattalma, *The Dieselgate,* Springer, **2017**.

[3] T. Koch, *Diesel - eine sachliche Bewertung der aktuellen Debatte*, Springer, **2018**.

[4] K. Mollenhauer, H. Tschöke, *Handbuch Dieselmotoren*, 3, Springer, Berlin, **2007.**

[5] Y. J. Kim,H. J. Kwon, I. Heo, I. S. Nam, B. K. Cho, J. W. Choung , M. S. Cha, G. K. Yeo, *Applied Catalysis B: Environmental* **2012**, 126, 9-21.

[6] H. J. Neußer, J. Kahrstedt, R. Dorenkamp, H. Jelden, *Motortechnische Zeitschrift* **2013***,* 74, 440-447.

[7] P. Braun, J. Gebhard, F.-M. Matysik, H.-P. Rabl, *Chemie Ingenieur Technik* **2018**, 90, 762-773.

[8] T. V. Johnson, *SAE International Journal of Engines* **2015**, 8, 1152-1167.

[9] B. Guan, R. Zhan, H. Lin, Z. Huang, *Applied Thermal Engineering* **2014**, 66, 395-414.

[10] B. Thirupathi, P. G. Smirniotis, *Journal of Catalysis* **2012**, 288, 74-83.

[11] Y. Wan, W. Zhao, Y. Tang, L. Li, H. Wang, Y. Cui, J. Gu, Y. Li, J. Shi, *Applied Catalysis B: Environmental* **2014**, 148-149, 114-122.

[12] L. Qiu, J. Meng, D. Pang, C. Zhang, F. Ouyang, *Catalysis Letters* **2015**, 145, 1500-1509.

[13] International ISO-Standard: Diesel engines - NOx reduction agent AUS 32: ISO 22241-1:2006 **2006.**

[14] A. M. Bernhard, D. Peitz, M. Elsener, T. Schildhauer, O. Kröcher, *Catalysis Science and Technology* **2012**, 3, 942-951.

[15] H. Hamada, M. Haneda, *Applied Catalysis A: General* **2012,** *421*, 1-13.

[16] A. Roppertz, S. Füger, S. Kureti, *Topics in Catalysis* **2017**, 60, 199-203.

[17] R. L. Blakeley, A. Treston, R. K. Andrews, B. Zerner, *Journal of the American Chemical Society* **1982**, 104, 612-614.

[18] A. N. Alexandrova, W. L. Jorgensen, *Journal of Physical Chemistry B* **2007**, 111, 720-730.

[19] K. J. Laidler, J. P. Hoare, *Journal of the American Chemical Society* **1950**, 72, 2489-2494.

[20] N. Panyachariwat, H. Steckel, *Journal of Cosmetic Science* **2014**, 65, 187-195.

[21] F. Lu, G. G. Botte, *Electrochimica Acta* **2017**, 246, 564-571.

[22] A. Schranck, R. Marks, E. Yates, K. Doudrick, *Environmental Science & Technology* **2018**, 52, 8638-8648.

[23] R. K. Singh, A. Schechter, *Electrochimica Acta* **2018**, 278, 405-411.

[24] B. K. Boggs, R. L. King, G. G. Botte, *Chemical Communications* **2009**, 32, 4859-4861.

[25] K. Ye, G. Wang, D. Cao, G. Wang, *Topics in Current Chemistry* **2018**, 376, 42-80.

[26] N. Senthilkumar, G. G. Kumar, A. Manthiram, *Advanced Energy Materials* **2018**, 8, 1702207.

[27] X. Zhu, X. Dou, J. Dai, X. An, Y. Guo, L. Zhang, S. Tao, J. Zhao, W. Chu, X. Cheng Zeng, C. Wu, Y. Xie, *Angewandte Chemie International Edition* **2016**, 55, 12465-12469.

[28] M. Koebel, M. Elsener, *Journal of Chromatography A* **1995**, 689, 164-169.

[29] A. M. Bernhard, I. Czekaj, M. Elsener, A. Wokaun, O. Kröcher, *Journal of Physical Chemistry A* **2011**, 115, 2581-2589.

[30] D. Peitz, A. M. Bernhard, M. Mehring, M. Elsener, O. Kröcher, *Chemie Ingenieur Technik* **2013**, 85, 625-631.

[31] A. M. Bernhard, D. Peitz, M. Elsener M, A. Wokaun, O. Kröcher, *Applied Catalysis B: Environmental* **2012**, 115, 116, 129-137.

[32] G. Zheng, A. Fila, A. Kotrba, R. Floyd, *SAE Technical Paper* **2010**, 2010-01-1941.

[33] V. O. Strots, S. Santhanam, B. J. Adelman, G. A. Griffin, E. M. Derybowski, *SAE International Journal of Fuels and Lubr* **2010**, 2, 283.

[34] P. P. Trigueros, F. Sagues, J. Claret, *Physical Review E* **1994**, 49, 4328-4335.

[35] S. H. Lin, L. Wu, *Water Research* **1996**, 30, 715-721.

[36] P. M. Schaber, J. Colson, S. Higgins, D. Thielen, B. Anspach, J. Brauer, *Thermochimica Acta* **2004**, 424, 131-142.

[37] M. Lecompte, J. Obiols, J. Cherel, S. Raux, *SAE International Journals of Fuels and Lubricants* **2017**, 10, 864-876.

[38] D. J. Belson, A. N. Strachan, *Chemical Society Reviews* **1982**, 11, 41-56.

[39] Y. Zheng, M. P. Harold, D. Luss, *Catalysis Today* **2016**, 264, 44-54.

[40] K. Shimizu, A. Satsuma, *Journal of Physical Chemistry C* **2007**, 111, 2259-2264.

[41] N. A. Sadokhina, D. E. Doronkin, G. N. Baeva, S. Dahl, A. Y. Stakheev, *Topics in Catalysis* **2013**, 56, 737-744.

[42] D. E. Doronkin, S. Fogel, P. Gabrielsson, J.-D. Grunwaldt, S. Dahl, *Applied Catalysis B: Environmental* **2014**, 148-149, 62-69.

## 5.4 AdBlue additivation for low-temperature applicability enhancement

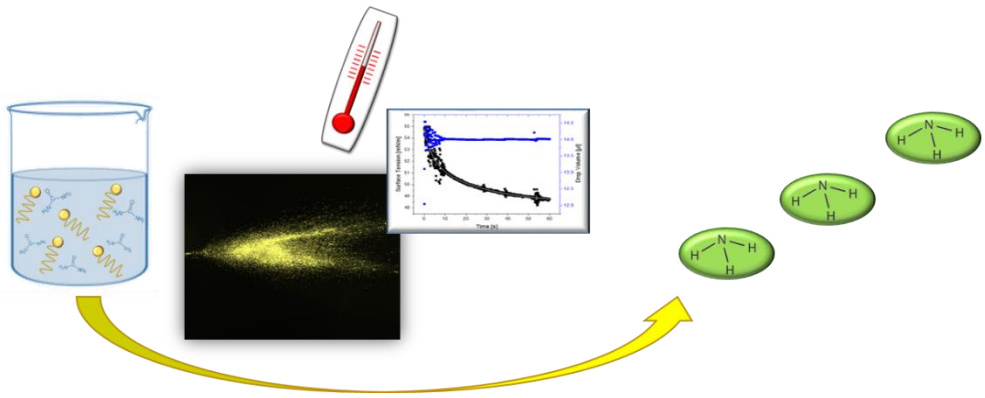

### 5.4.1 Introduction

The SCR process presents the most frequently applied technology for exhaust aftertreatment of nitrogen oxide emissions of diesel engines [1-6]. The SCR principle brings the advantage of a not-influenced engine operation, as it is the case with a $NO_x$-trap for $NO_x$ reduction. Thus, an efficiency-optimized operation can be ensured over the entire engine map [5]. However, commercial SCR systems require an external reducing agent, which reacts selectively with the toxic nitrogen oxides. Ammonia is used as the reductant, but, as it is also a toxic gas at ambient conditions, cannot be carried onboard. Therefore, an ammonia precursor, namely urea, is used. AdBlue or DEF, a solution of 32.5 wt% urea in water, is carried onboard and used as an additional operating material in order to reduce the nitrogen-oxide emissions [2, 3, 6, 7]. The liquid reductant precursor is injected into the exhaust tract of the diesel engine. After decomposition of urea to ammonia, the latter can selectively react with $NO_x$ to form non-toxic nitrogen and water.

The concentration of urea in commercial AdBlue corresponds to an eutectic aqueous solution, meaning at the concentration of 32.5 wt% urea the freezing point of the binary mixture reaches a minimum. Therefore, the freezing point of AdBlue is located at -11.5 °C [7, 8]. However, in a moderate climate's winter term as well as in colder regions of the world, ambient temperature can be, at least temporarily, significantly lower than -11.5 °C. At these temperatures, the SCR process cannot proceed. Because of that, modern SCR systems are equipped with external electrical heating systems in order to avoid freezing of the precursor liquid and hence avoid damage of the exhaust aftertreatment system [9]. The electrical heating requires electrical energy, which negatively influences the high fuel efficiency of the diesel engine. Besides that, the implementation of the heating system itself brings along additional costs, requires additional installation space and presents a potential source of error by increased technical complexity [10]. Taking the mentioned points into consideration, a lowering of the precursor's freezing point would be advantageous for both, the vehicles manufacturer as well as for the customer.

A product, which is already commercially available, uses the addition of ammonium formate to an urea solution to decrease the freezing point of the precursor solution. The product, which consists of 24 % ammonium formate, 20 % urea and 56 % water, is known as Denoxium -30 [10-12]. However, ammonium formate has the disadvantage that after injection into the exhaust tract, formic acid is formed, which is a highly corrosive acid and can, therefore, lead to damage of the exhaust system. In addition, ammonium formate is more expensive compared to urea [10, 12, 13].

Moreover, due to its high decomposition temperature, ammonium formate is not suitable for low-temperature applications [5, 10].

Another crucial aspect regarding the injection of AdBlue at low temperatures is the formation of undesired byproducts which appear as white solid crystals [3-5, 14]. These deposits can consist of a number of species such as cyanuric acid, biuret, ammelide, ammeline or melamine [3, 14, 15]. They have been observed in heavy-duty diesel engines, but also for light-duty diesel engines [4]. The deposits inside the exhaust tract can be found at the injector nozzle, at the mixing element and even downstream of the mixing element [4]. As the temperature during urea decomposition becomes too low, formation of deposits can be observed, which can cause catalyst passivation [1] and, in the worst case, can lead to a clogging of the exhaust tract and over a long time even bring engine failure by increased engine back pressure [3, 4]. Eakle et al. even observed corrosion of stainless steel initiated by compounds derived from urea decomposition [4, 16]. Mechanistically, as described in chapter 3, formation of byproducts is initiated by splashing of AdBlue droplets on the surface of the exhaust pipe and subsequent cooling of it [3, 14]. The temperature of the exhaust-pipe wall was found to be 80 - 120 °C cooler at an exhaust temperature in the range of 220 - 350 °C [14, 17, 18]. Due to cooling, arising from evaporation effects of the liquid film on the wall, temperatures can become even lower [3, 17, 19, 20]. Since the formation of deposits starts below a critical temperature, as wall wetting sets in, instead of droplet rebound or thermal breakup, a cooling of the wall is problematic. In literature, values in the range of between 243 °C and 273 °C are reported. Here, wall film formation by liquid deposition and formation of deposits begins [3, 17, 21, 22]. Subsequent reaction of urea with isocyanic acid, occurring as intermediate product during the urea decomposition, can be seen as the starting point for undesired deposit formation [3, 4, 14]. Lecompte et al. summarize the deposit formation mechanism the following way [4, 23]:

droplet impingement → liquid film formation → deposit nucleus formation → deposit accumulation

Investigations have shown that by the optimization of the aqueous AdBlue spray properties, meaning the formation of smaller droplets, the tendency to form deposits inside the exhaust tract can be reduced [2, 4, 24, 25]. In principle, the spray at a given exhaust temperature and mass flow can possibly be optimized by two approaches. On the one hand, a modified injection setup could be used to form smaller droplets [4, 20, 24]. On the other hand, surfactants dissolved in AdBlue can be used to improve the spray properties [4, 14]. Due to their amphiphilic character, surfactants tend to go to interfaces. By accumulating at the interface, the interfacial tension can be reduced

significantly, depending on the type of the surfactant [26]. In the present case, the interface is between the aqueous AdBlue solution and the surrounding air meaning the term surface tension is more appropriate. A lower surface tension of the aqueous solution corresponds to a smaller energy necessary to increase the interfacial area meaning smaller droplets can be created with a smaller effort. Compared to the spray improvement using modified injection pressure or alternative injectors, the application of surfactants has the advantage to be able to be used not only in upcoming SCR applications but also with the already existing hardware. Since the additivated AdBlue can be used just instead of conventional AdBlue, no retrofitting is necessary. In addition, it presents a more cost-efficient solution. Applications of surfactant addition are already commercially known from some products on the market, as there are Diaxol from TOTAL, PowerBlue from Deutz, CleanR MAX from Renault Trucks Oils or Air 1 OptiSpray from Yara [4]. However, no research on the physical-chemical background of the addition of surfactants to the AdBlue solution is available. Moreover, the parameter “surface tension” needs to be evaluated in dependence of time, meaning the dynamic surface tension needs to be considered.

In this study, both approaches are examined. First, different solvents and salts for reducing the freezing point of the urea solutions are investigated. Second, the influence of the addition of surface-active substances on the spraying behavior of the precursor solution is studied. The direct influence of the additivation on the diameter of the droplets formed inside the spraying cone is checked by an injection-test bench designed for this purpose.

## 5.4.2 Experimental

**Chemicals**

Urea (purity: "> 99.5 %, p.a.") and ammonium bicarbonate (purity: "p.a.") were purchased from Roth. Ammonium carbonate (purity: "pure Food grade") was bought from AppliChem. Ammonium acetate (purity: "p.a.") was from Merck. Decanoic acid (purity: "> 98 %"), sodium dodecylsulfat (purity: "> 99.9 %") and Polyoxyethylene-sorbitane monostearate were from Sigma-Aldrich. Polyoxyethylene-10-decyl ether and Polyoxyethylene-14-decyl ether were provided from BASF. Polyoxyethylene-sorbitane-monooleate was from Fluka and Dowanol TPM was from Dow Chemicals.

The AdBlue used in all experiments was prepared by dissolving the appropriate amount of urea in Millipore water.

**Experimental setup**

For the experiments on the lowering of the freezing point of AdBlue, the test samples were filled in 10 ml glass tubes and sealed. The temperature needed for the individual experiments was adjusted by a cryostat "ALPHA RA 8" from LAUDA. The cryostat was used to cool an oil bath into which the tubes containing the samples were placed. The experiments started at a temperature of -11 °C and were carried out down to a device-limited temperature of -25 °C. The temperature reduction was performed in intervals of 1 °C after giving the system a time of 30 min to equilibrate during the temperature steps. To ensure correct temperature settings, a contact thermometer was used in addition to the temperature controller of the cryostat. To guarantee nucleation inside the samples as temperature of inhomogeneity is reached, boiling granules were used. Each sample was tested at least three times and the average value was taken for evaluation.

For the determinations of the dynamic surface tension of additivated AdBlue, the so-called pendant-drop method was applied [27, 28]. The pendant-drop tensiometer "PAT1M" from Sinterface was used for all measurements. The shape of a pendant drop is dependent on the interplay between gravity and surface tension. An optical analysis of the drop shape according to the Young−Laplace equation (see equation 18) can, therefore, be used to determine the surface tension.

$$\boldsymbol{\Delta P = \gamma \left(\frac{1}{R_1} + \frac{1}{R_2}\right)} \qquad \text{(equation 18)}$$

In the equation, $\Delta P$ stands for the Laplace pressure difference between the bubble interior and exterior (capillary pressure), $\gamma$ stands for the surface tension and $R_1$ and $R_2$ are the principal radii of drop curvature [29, 30].

All measurements were performed at 25 °C. All investigated samples were prepared by weighing the appropriate mass of the pure surfactant into the AdBlue solution. The samples were shaken and left for some hours for equilibration. Each sample was measured three times with washing steps between the measurements.

For the visual characterizations of the spray cone and the determinations regarding the droplet size after injection of the additivated AdBlue, an in-house built injection-test bench was applied (see Figure 43). According to literature, the droplet diameters of sprays during the injection are determined by measurements with laser optical techniques, such as laser diffraction or phase Doppler anemometry. In contrast, the shape of the spray is determined by high-speed imaging [3].

In this study, however, for optical shape analysis and determination of the droplet diameters inside the injection spray, a single imaging approach for gathering both the optical information and the numerical information on the droplet diameters, was applied.

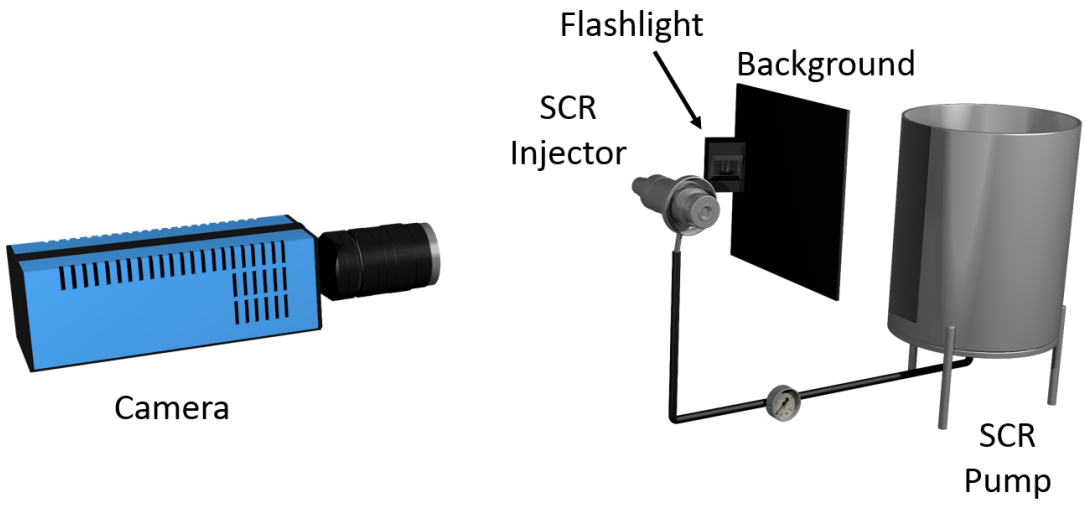


Figure 43: In-house built experimental setup for investigations on droplet size after injection.

The setup of the imaging-test bench is shown in Figure 43 and consisted of the following parts:

- Commercial SCR pump

  The submersible membrane pump was removed from the commercial AdBlue tank and placed in a custom-made pump vessel, in order to reduce the individual sample volume required for the experiments. The pump ensured a constant injection pressure of 8.5 bar. The power supply was done by a 12 V-voltage source.

- Prototype SCR injector, one-hole application

  For injection and atomization, a one-hole SCR injector was used. The injector was connected by a pressure-resistant tube to the SCR pump. The injector was controlled by 12 V-voltage pulses by which the injection could be started and stopped. Thus, the injection volume could also be controlled.

- Flashlight

  To ensure sufficient brightness and contrast of the sample droplets, flashlight was used to illuminate the spray during recording. The flashlight was triggered shortly before the images were recorded.

- High-resolution CCD camera

  A camera of the type “pco.2000” from pco imaging was used to take pictures of the flashlight-illuminated spray droplets. The camera had a resolution of 4 MP. To ensure high contrast, a black photo background was chosen. Greyscale pictures were recorded.

The entire setup was mounted on a laboratory tripod (not shown in Figure 43) in order to ensure comparability of the recorded photos. The overall setup was controlled by the software Arduino, which was used to trigger sample injection, flashlight and camera in well-defined time delays. By choosing suitable delays, optimum pictures could be enabled. For all images shown, a dwell time of 5 ms was chosen between injection and imaging and the exposure time of the CCD camera was set to 1 µs.

In order to make a numerical evaluation - besides the optical evaluation - of the recorded spray pictures possible, the size of the droplets was determined. For that, the image evaluation software Image J was applied to the recorded images. The software counts the single droplets and gives out the size of the droplets in pixels. As the size of the picture section and the number of pixels of an image is known, the size of droplets can be indicated in µm. It was assumed that the droplets have circular shape. Using equation 19,

$$\boldsymbol{A = \pi \left(\frac{d}{2}\right)^2} \qquad \text{(equation 19)}$$

in which *A* is the area of the droplet, the diameter of a droplet *d* was calculated.

For the investigations on the deposit formation after drop-surface interaction, a defined volume of 2 x 50 µl was dropped on a hot surface (microscope slide or stainless steel plate) from a fixed height of 15 cm with an Eppendorf pipette. The surface was weighed before and after the experiments. Via this method, the deposited mass could be calculated by subtraction.

## 5.4.3 Results and discussion

### *5.4.3.1 Addition of alternative solvents*

In a first experimental series, the idea was to substitute a certain amount of the AdBlue solution by a solvent known to have a lower melting point. The formation of an eutectic mixture can possibly decrease the freezing point of the AdBlue solution [31]. This is already known for several binary systems like water and short-chain alcohols [32]. The following additives were investigated:

- methanol (melting point: - 97 °C [33])
- ethanol (melting point: - 114 °C [33])
- propanol (melting point: - 126 °C [33])
- glycerin (melting point: 18 °C [34])
- solketal (melting point: - 27 °C [34])

First, ternary-phase diagrams of mixtures with the solvent, urea and water were established at a temperature of 25 °C to get information on the solubility of different mixture compositions. A lower solubility of urea in the mixtures compared to pure water was observed. The reason for this was the already smaller solubility of urea in the pure solvent. No additional co-solvent effects for the mixture were observed. For a first impression of the freezing point or the temperature of precipitation of the mixtures, differential scanning calorimetry (DSC) was used. From the DSC curves, a hint towards a shift to lower freezing points by adding an additional solvent was found. The associated peak of melting was shifted with increasing amount of solvent. However, to confirm the DSC results, optical tests were carried out in a larger volume scale. Therefore, various mixtures of urea, water and solvent were put into a cryostat and kept at different temperatures as described in 5.4.2. Here, no freezing of the liquid sample along with the AdBlue reference was found. However, urea began to precipitate from the mixture. Precipitation already occurred at temperatures > -11 °C. These experiments showed that the addition of alternative solvents did not result in a usability of the precursor solution at lower temperatures compared to AdBlue. The reason was the lower solubility of urea in the investigated solvents.

### *5.4.3.2 Addition of alternative ammonia precursor*

Another strategy to lower the freezing point of the precursor solution is the influence of the addition of a salt to the aqueous solution. The effect is known for pure water and therefore tested with practically useful salts, meaning salts containing an ammonia source [31]. Thus, different ammonium salts, namely ammonium bicarbonate ($NH_4HCO_3$), ammonium carbonate ($(NH_4)_2CO_3$) and ammonium acetate ($NH_4Ac$) were investigated as additives to AdBlue. As both, ammonium carbonate and ammonium bicarbonate, already present decomposed urea in aqueous solution ($NH_3$ + $CO_2$), the application of these additives also brings along an improved low-temperature applicability. $NH_4Ac$ also brings some advantages compared to ammonium formate, applied in the Denoxium -30. First, the acetate salt is significantly cheaper compared to formate. Another advantage is the fact that after injection into the exhaust system, the less acidic species acetic acid is formed. Acetic acid is less acidic by a factor of 10 compared to formic acid, which is observed in case of ammonium formate [34]. Thus, ammonium acetate is less corrosive to the exhaust tract compared to ammonium formate. In addition, the solubility of $NH_4Ac$ in water is higher by a factor of > 2 compared to ammonium formate [34], thereby avoiding solubility problems. However, it should be noticed that ammonium acetate can form other undesired products upon reaction, meaning e.g. catalytic support for decomposition would be advantageous [35].

In a first experiment, the general freezing point depression of pure ammonium acetate in water was investigated. For that, ammonium acetate solutions of 10 wt%, 20 wt%, ... , 60 wt% in water were put into the cryostat as described in 5.4.2 and the state of the samples was optically analyzed. Using the cryostat, temperatures down to -25 °C could be tested. The results of the experimental series are shown in Figure 44.

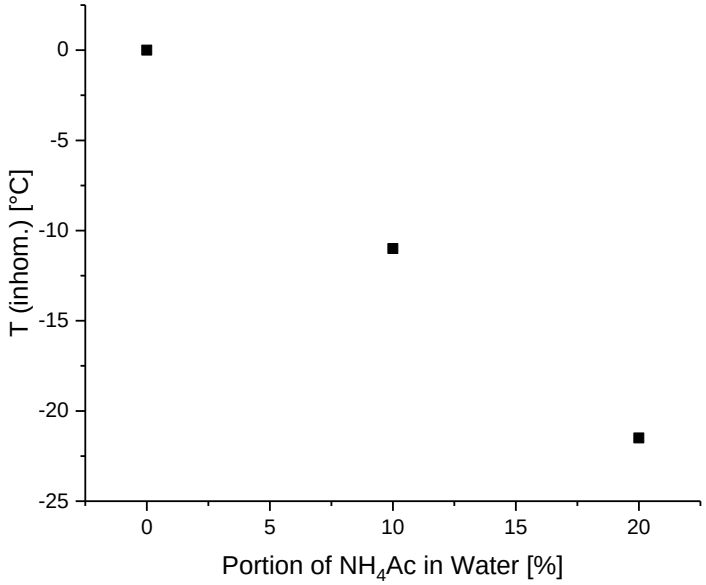


Figure 44: Temperature of inhomogeneity for ammonium acetate solutions of different concentrations in water. Solutions with 30 wt%, 40 wt%, 50 wt% and 60 wt% $NH_4Ac$ were clearly liquid without crystallization down to -25 °C.

After having found a significant freezing point depression of ammonium acetate in water, test solutions containing both, urea and $NH_4Ac$, were investigated. The solutions were prepared in a way that the ammonia content per mass of the samples was equal to the ammonia content per mass of the commercial AdBlue solution.

The temperatures of inhomogeneity of the samples were again optically analyzed. The results of the experiments are shown in Figure 45.

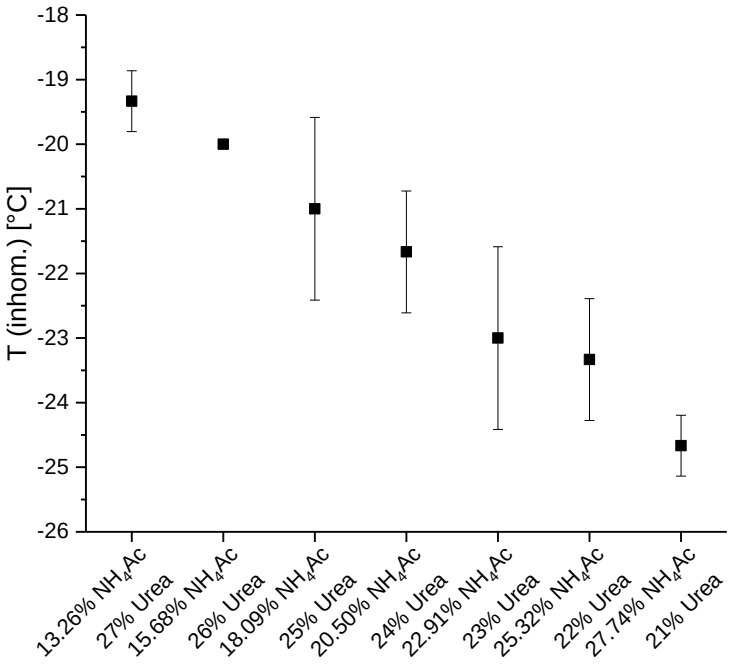


Figure 45: Temperature of inhomogeneity for urea/ammonium acetate/water mixtures of different compositions. Samples with a higher mass percentage of ammonium acetate were clear and homogeneous down to -25 °C.

From the results shown in Figure 45, it can be seen that the temperature of inhomogeneity decreases with increasing the portion of ammonium acetate in the solution. The test solutions with a portion of 27.7 wt% ammonium acetate or higher were clearly liquid down to temperatures of -25 °C. Due to this observation, replacing the urea from AdBlue by ammonium acetate can be applied as an efficient way to significantly decrease the temperature of inhomogeneity of the solution. However, the formation of undesired species upon heating from ammonium acetate has to be avoided, meaning catalytic support for decomposition might be necessary.

The tests on the reduction of the temperature of inhomogeneity were also carried out using ammonium carbonate and ammonium bicarbonate. The results of the studies are shown in Figures 46 and 47. Again, the amount of additive and urea was chosen in a way that the sample's ammonia content per mass was the same as it is in AdBlue.

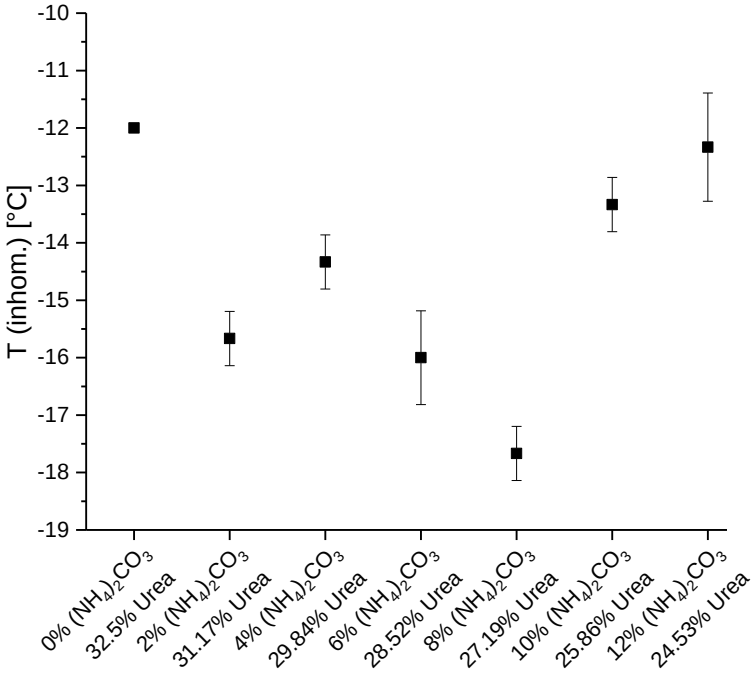


Figure 46: Temperature of inhomogeneity for urea/ammonium carbonate/water mixtures of different compositions measured as described in 5.4.2.

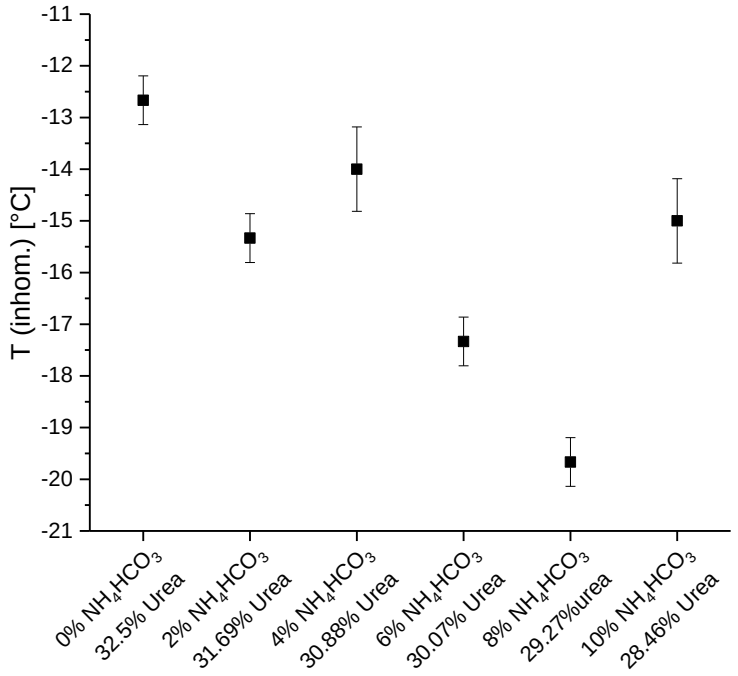


Figure 47: Temperature of inhomogeneity for urea/ammonium bicarbonate/water mixtures of different compositions measured as described in 5.4.2.

The substitution of some amount of urea by ammonium carbonate or ammonium bicarbonate led to a reduction of the temperature of inhomogeneity as it can be seen in Figures 46 and 47. The results for ammonium carbonate and ammonium bicarbonate addition looked similar. This observation can be explained by the fact that ammonium carbonate gets decomposed already at room temperature to ammonium bicarbonate and the ammonium carbonate used was already partly decomposed to ammonium bicarbonate [34]. In the experiments, the lowest temperature of inhomogeneity was observed for an amount of 8 wt% ammonium carbonate or –bicarbonate with the corresponding amount of urea. Thereby, the applicability of the additivated solution would be enabled down to -18 °C or -20 °C, as shown in the Figures above. At a higher amount of additive, the temperature of inhomogeneity was again shifted to higher values. This effect can be explained by the lower solubility of the ammonium salts compared to urea and thus additive precipitation at higher temperatures.

Of course, in the case of the carbonate or bicarbonate addition, the thermal stability of the solutions is lowered. However, commercial SCR injectors are cooled during conventional operation. Therefore, the lowered stability of the solutions should not pose a critical problem. Taking into account that the applicability at low exhaust temperatures is also improved, due to the less concentrated urea solution and thereby lower tendency to form byproducts, the presented additivation of AdBlue could present an approach relatively easy to be implemented, not only for new vehicles but also for use in already existing vehicles.

#### *5.4.3.3 Addition of surfactant for lowering droplet diameter after injection*

For the correct working of the SCR device, the system needs continuous supply with the external reducing agent ammonia. Therefore, the liquid precursor solution has to be brought into the gas flow of the exhaust tract. Basically, injectors of different layouts and different injection pressures are used for this purpose [4, 10, 24]. Since the trend in SCR-setup layout goes away from underfloor implementations to the so-called close-coupled strategies, the corresponding building parts of the setup move closer to the engine to make use of the higher temperature level [5]. By such a sophisticated packaging, the available space for injection of the precursor liquid and mixer placing for equal ammonia dispersion is problematic [3, 4]. As the SDPF technology has evolved as a standard technology for passenger cars, deposits can increase the back pressure even more significantly as in case of an open SCR catalyst [4].

As subsequently to injection, evaporation and decomposition of the precursor to ammonia should be finished already in the mixing section for optimum conversion inside the SCR catalyst, the process of AdBlue injection is of high importance for the functionality of the overall system [3, 24].

The formation of solid byproducts was found to preferentially proceed at low exhaust temperatures and at high dosing rate of AdBlue. This is because, at these conditions, AdBlue tends to form liquid films at the surface of the exhaust pipe or for example on the surface of a mixing element, applied for better ammonia distribution [3]. A possibility to lower the tendency of deposit formation in the exhaust tract is the surfactant addition to AdBlue [4].

In general, surfactants are defined as amphiphilic compounds meaning they consist of a hydrophilic (head group) and a hydrophobic (tail) structural part [36]. Due to this structure, in the case of an aqueous solution like AdBlue, they tend to move to interface and orientate with their hydrophobic tails towards the hydrophobic air phase. This results in a lowering of the normally high surface tension of water of 72 mN/m to smaller values, which depend strongly on the type of the surfactant [37]. The differentiation of surfactants is done regarding their hydrophilic head group. It can be distinguished between anionic, cationic, nonionic and zwitterionic surfactants [36]. Regarding the lowering of the surface tension, anionic and especially nonionic surfactants are most efficient [38].

In the literature, the trend of lower surface tension of AdBlue leading to a reduced amount of formed deposits in the exhaust tract was found. Therefore, the correlation of low surface tension leading to less deposits was assumed. However, at the same level of surface tension, a relatively high spread of the deposit reduction was found [4, 14]. More precisely, as the processes of injection occur on a millisecond time scale, the value of the surface tension in equilibrium should not be the decisive parameter for observing a spray, which consists of small droplets. In this case, the processes right after the creation of the droplet surface are the interesting aspect. This is qualified by the dynamic surface tension of a surfactant. It describes the behavior of the surfactant molecules in the bulk phase when a new interfacial area is formed. Depending on the velocity and the tendency of the surfactant molecule to move to the interface, the value of the surface tension decreases more or less fast. Consequently, it is the dynamic surface tension, which should be of decisive importance for the process of AdBlue injection. Therefore, in this study, a correlation between the dynamic surface tension of an AdBlue-surfactant mixture and the average droplet size formed during the injection process is investigated.

#### 5.4.3.3.1 Dynamic surface tension of AdBlue-surfactant mixtures

In order to get an impression of the surfactant's potential of high surfactant dynamics, the investigations started with experiments on the dynamic surface tension of differently additivated AdBlue mixtures. As it is a simple and fast method, the pendant-drop technique was chosen for this investigation as it is described in 5.4.2. Here, the surface tension of an aqueous sample in a pendant drop is measured as a function of time. Going out from investigations of Hofmann et al. [39], the following substances, given in Table 4, were chosen to be tested as additives to AdBlue.

Table 4: Investigated surface-active substances with the pendant drop measurement as described in 5.4.2.

| Applied substance | Abbreviation | cmc in water at 25 °C |
|---|---|---|
| Decanoic acid | | 20 mM [40] |
| Sodium dodecylsulfate | SDS | 9 mM [40] |
| Nonyl dimethyl phosphine oxide | C9DMPO | 4.66 mM [41] |
| Polyoxyethylene-10-decyl ether | Lutensol 100 | 2.4 mM |
| Polyoxyethylene-14-decyl ether | Lutensol 140 | 2.3 mM |
| Polyoxyethylene-sorbitane-monostearate | Tween 60 | 0.021 mM [42] |
| Polyoxyethylene-sorbitane-monooleate | Tween 80 | 0.012 mM [43] |
| Tripropylene-glycol-methyl ether | Dowanol TPM | no cmc |

First, the surface tension of pure AdBlue was measured by the pendant drop technique. The results are shown in Figure 48. As expected, the surface tension of the pure AdBlue sample stayed constant over the entire time of the experiment. Since the commercial AdBlue solution only consists of dissolved urea in pure water, no surface-active substances were present in the solution, which could have an influence on the measured surface tension. A constant value of 75 mN/m was measured. This fits to the reported data in literature where a slight increase of surface tension for urea as additive is reported [44, 45].

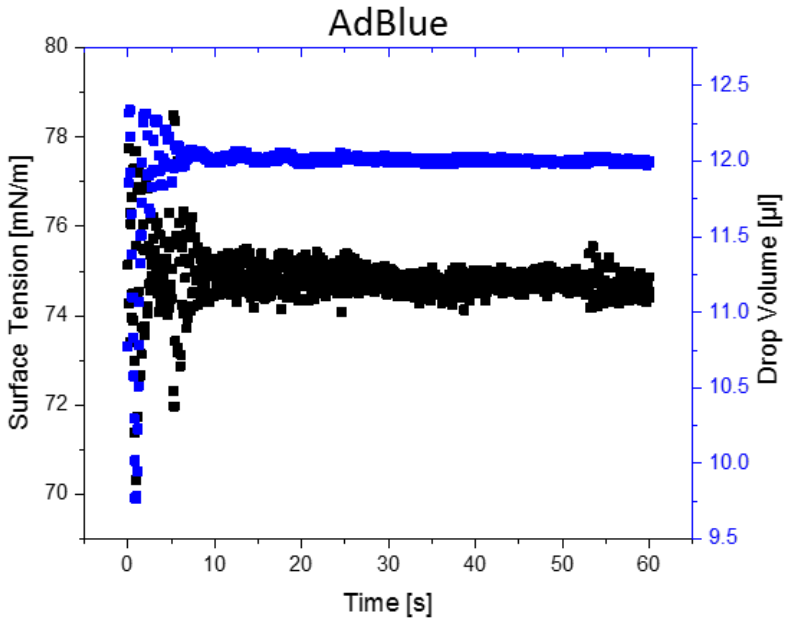


Figure 48: Pendant drop experiment of pure AdBlue performed as described in 5.4.2. On the left axis, the value of surface tension is shown, whereas the axis on the right gives the drop volume during the measurement.

In a next step, the pendant drop measurements of the aqueous solutions of the substances shown in Table 4 at different concentrations in AdBlue were carried out. Most of the concentrations tested were in the range of the corresponding (cmc) value (see Table 4). In case of the Lutensol samples also higher concentrations were tested. Since the cmc describes the concentration of the surfactant at which micelle formation starts [26], micelle dynamics have to be considered in the present case. The results of the pendant drop experiments with decanoic acid, SDS, C9DMPO, Tween 60 and Tween 80 at the highest concentration measured are shown in Figure 49.

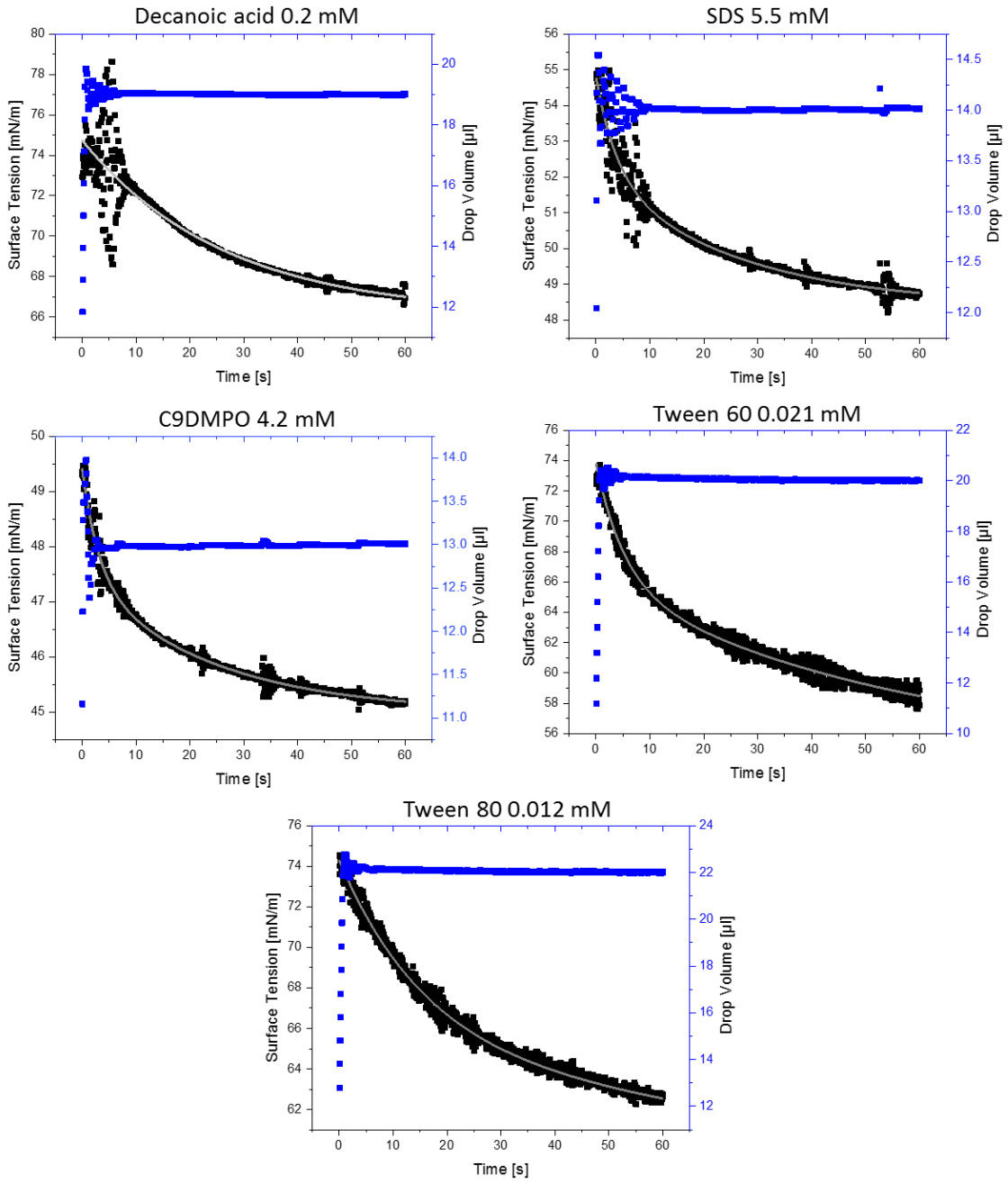


Figure 49: Pendant drop experiments with decanoic acid, SDS, C9DMPO, Tween 60 and Tween 80 in AdBlue in the highest concentration tested performed as described in 5.4.2. On the left axis, the value of surface tension is shown, whereas the axis on the right gives the drop volume during the measurement.

A drop of the surface tension after the formation of the droplet was observed for all samples tested. This is due to the surface-active properties of the additives. The molecules of the investigated substances move from the bulk phase to the interface of the drop. This decreases the surface tension. The intensity of the decrease differed. It depends on the nature of the surface-active

substance. Two different groups can be distinguished. For SDS and C9DMPO, the surface tension decreased down to around 45 mN/m, whereas it stayed around 60 mN/m for decanoic acid, Tween 60 and Tween 80. In all five cases, a constant value of surface tension for the different systems wasn't reached even after 60 s of experiment time. For the present application of AdBlue injection, this timescale is much too long, since the relevant processes for the formation of droplets after injection are occurring on a millisecond scale.

In Figure 50, the results of the pendant drop measurements of the AdBlue samples additivated with Lutensol 100, Lutensol 140 and Dowanol TPM in the highest concentration tested are shown.

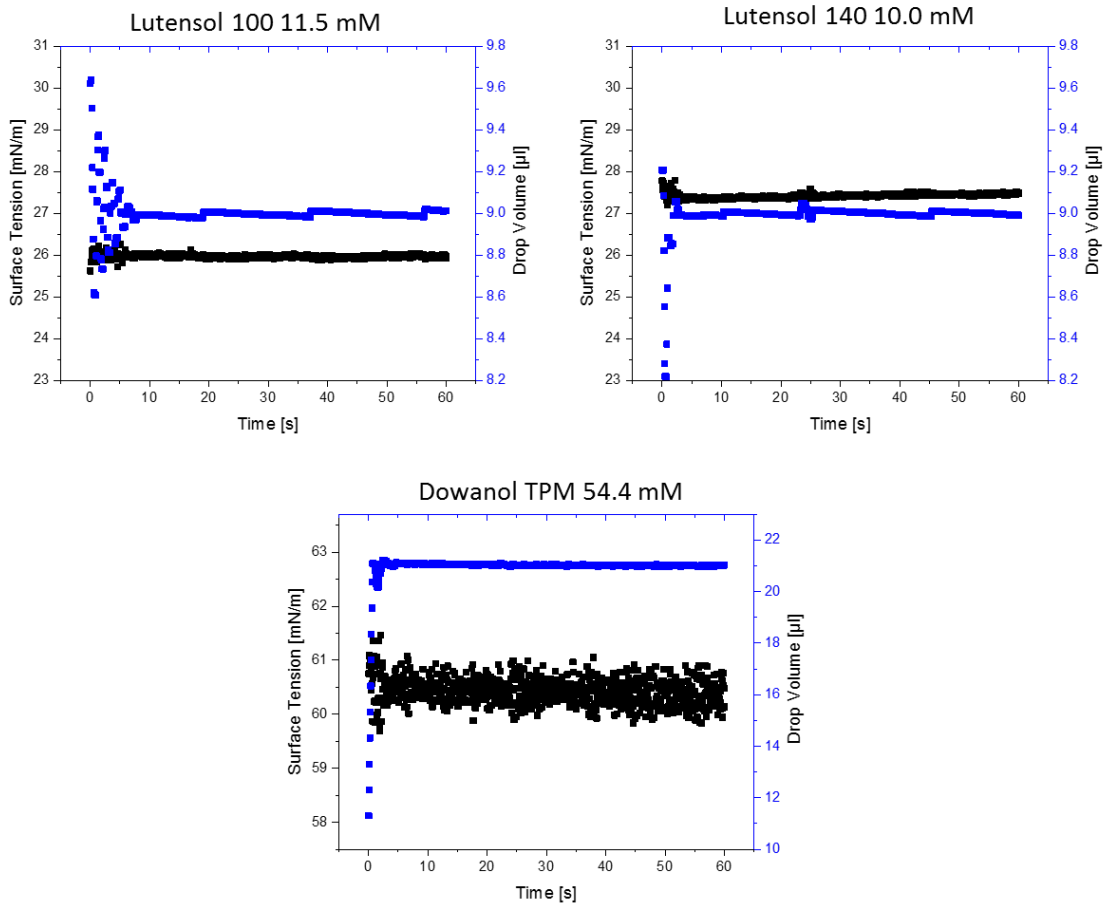


Figure 50: Pendant drop experiments with Lutensol 100, Lutensol 140 and Dowanol TPM in AdBlue in the highest concentration tested performed as described in 5.4.2. On the left axis, the value of surface tension is shown, whereas the axis on the right gives the drop volume during the measurement.

Here, the surface tension curve looked different. No decrease of the surface tension curve during the time of the experiment was observed. The initially detected value kept constant until the end of

the experiment. For Dowanol TPM, the surface tension value was relatively high with 60.5 mN/m. This is not surprising since the tripropylene-glycol-methyl ether cannot be seen as a real surfactant since the amphiphilic character within the structure is not pronounced. For Lutensol 100 and Lutensol 140, the lowest final values of surface tension were detected. With values around 25 mN/m, they showed the typical behavior of highly efficient non-ionic surfactants [38]. The time required to reach the equilibrium value of surface tension was in the millisecond scale and thus not detectable with the applied device. This is the relevant time scale for an AdBlue-injection process. Therefore, it was reasonable to look closer on the sub-second scale. For this, the surfactant with the highest potential, the Lutensol 100, was investigated at different concentrations. In Figure 51 the experimental values during the first second of the pendant drop experiments are shown for Lutensol 100 in different concentrations from 1.4 mM to 11.5 mM.

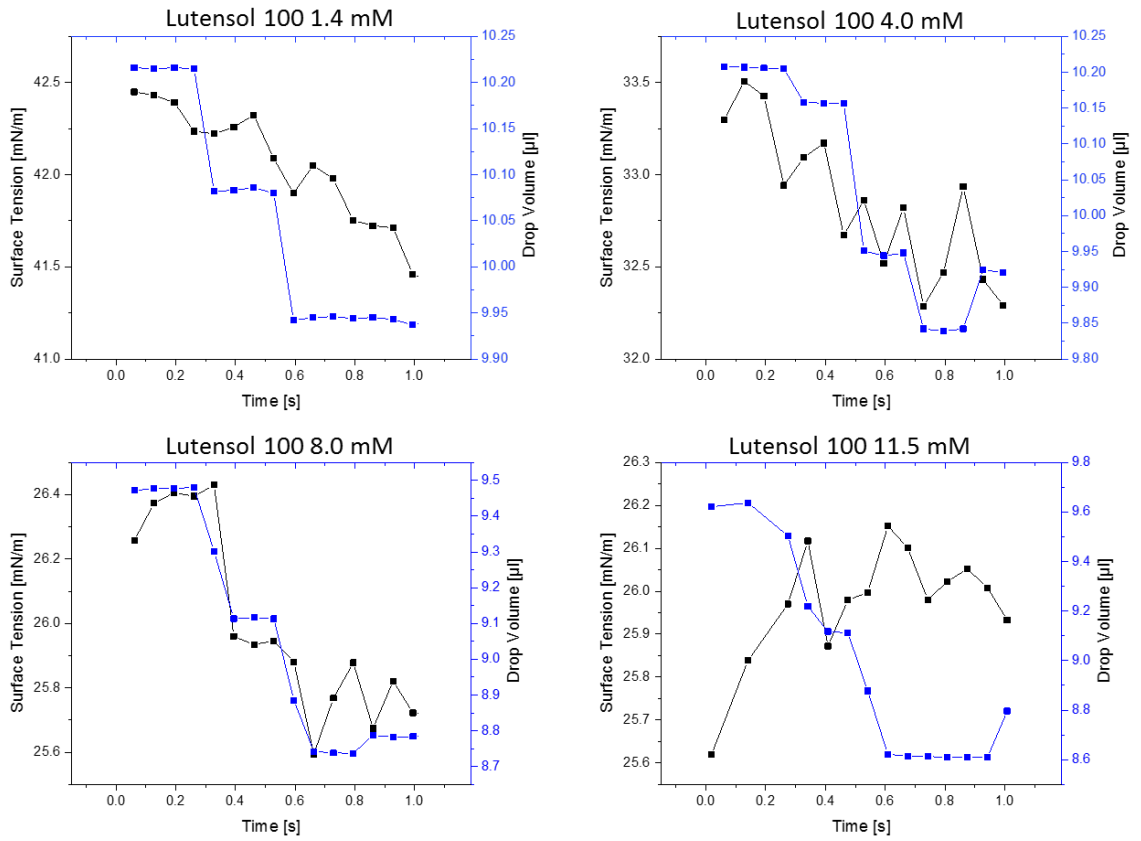


Figure 51: Pendant drop experiments with Lutensol 100 at the concentration of 1.4 mM (top left), 4.0 mM (top right), 8.0 mM (bottom left) and 11.5 mM (bottom right) in AdBlue performed as described in 5.4.2. On the left axis, the value of surface tension is shown, whereas the axis on the right gives the drop volume during the measurement.

In the case of 1.4 mM, 4.0 mM and 8.0 mM Lutensol 100 in AdBlue, an initial drop of surface tension was seen although the value detected at the beginning was already very low. At low concentration of the surfactant, the effect is more pronounced. In the case of the highest concentration, 11.5 mM, the first detected value was already in the range of the final surface tension value of 25 mN/m. This shows that the higher the concentration of the surfactant, the faster is the adjustment of the surface tension by the surfactant. The higher the amount of surfactant molecules in the bulk solution, the higher is the probability and thus the average speed of the surfactant molecules to the drop interface. The newly formed surface is quickly occupied by the surfactant molecules.

Regarding the results of the performed pendant drop measurements, at least two sample solutions showed potential for further investigation. The low surface tension value of < 30 mN/m detected in the case of the Lutensol samples at the highest concentrations together with the high dynamics in the solution might support the formation of small droplets during the injection. To check this hypothesis, the different solutions were investigated using the injection-test bench in the next section.

#### 5.4.3.3.2 Spray imaging and determination of droplet sizes during injection process

In order to evaluate if a rapid decrease of surface tension correlates with improved spray properties for the AdBlue samples, spray pictures were recorded using a software-controlled injection-test bench as described in 5.4.2. The setup is shown in Figure 43. The image evaluation was carried out, besides pure AdBlue, with the following substances: Lutensol 100, Lutensol 140, Dowanol TPM, Tween 60 and Tween 80. The different test solutions were sprayed by a one-hole SCR injector and pictures of the spray cone were made using a CCD camera. The injector is placed to the left of the image border. Different injector opening times and thereby different amounts of liquid in the spray cone were tested. The following injector opening times were used: 1.5 ms, 2.0 ms, 2.5 ms and 3.0 ms. In Figure 52, spray pictures of AdBlue without additive for different injector opening times are shown. As it can be seen, the increase of the injector opening time led to an optically denser spray picture, in which the single droplets partially covered up each other.

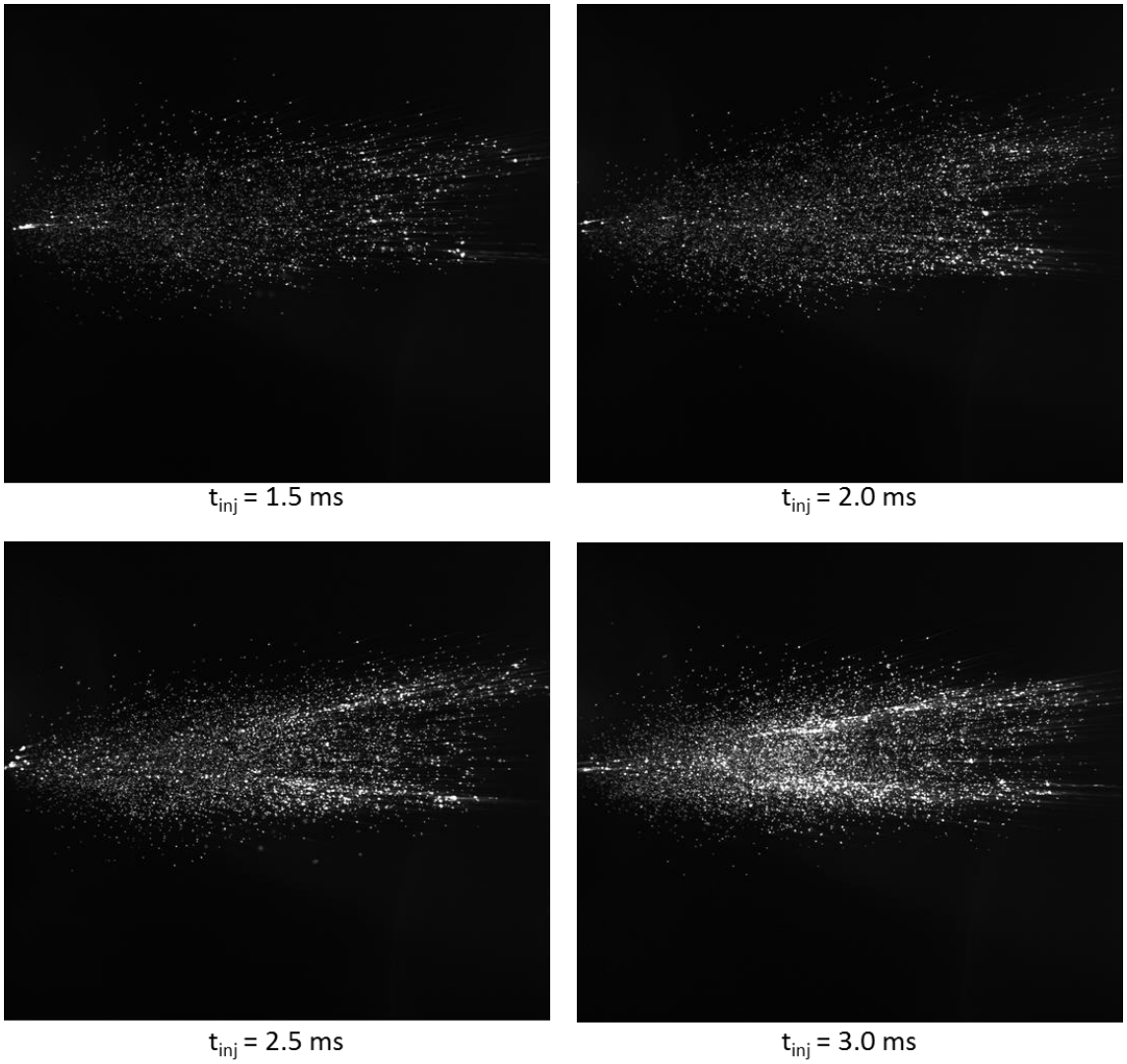


Figure 52: Influence of injector opening time on optical density of spray picture of the pure AdBlue solution measured as described in 5.4.2.

In a next step, the influence of additives on the spray picture was investigated. The following Figure 53 shows a comparison between differently additivated samples and AdBlue for an injection time of 1.5 ms.

As can be seen from the spray pictures, the spraying situation looked relatively similar for AdBlue, Dowanol TPM and the Tween samples. However, in the case of the Lutensol 100 and Lutensol 140 samples, a finer, better-dispersed, spray can be assumed from the spray imaging. Smaller average droplet diameters compared to the AdBlue reference sample seemed to be present for the spray of these samples.

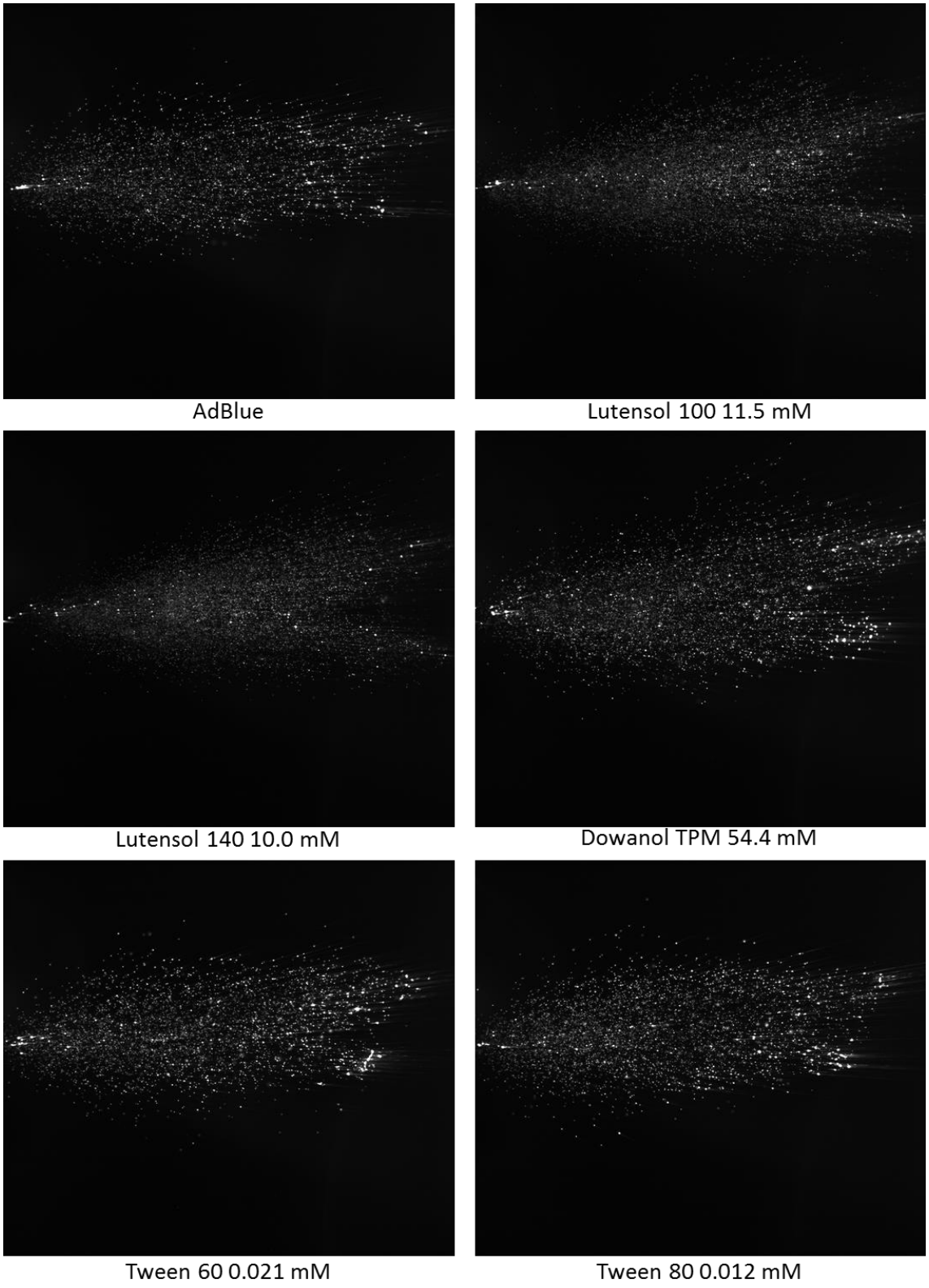


Figure 53: Influence of AdBlue additivation with five different substances (Lutensol 100, Lutensol 140, Dowanol TPM, Tween 60 and Tween 80) on optical density of spray picture measured as described in 5.4.2. Injector opening time: 1.5 ms.

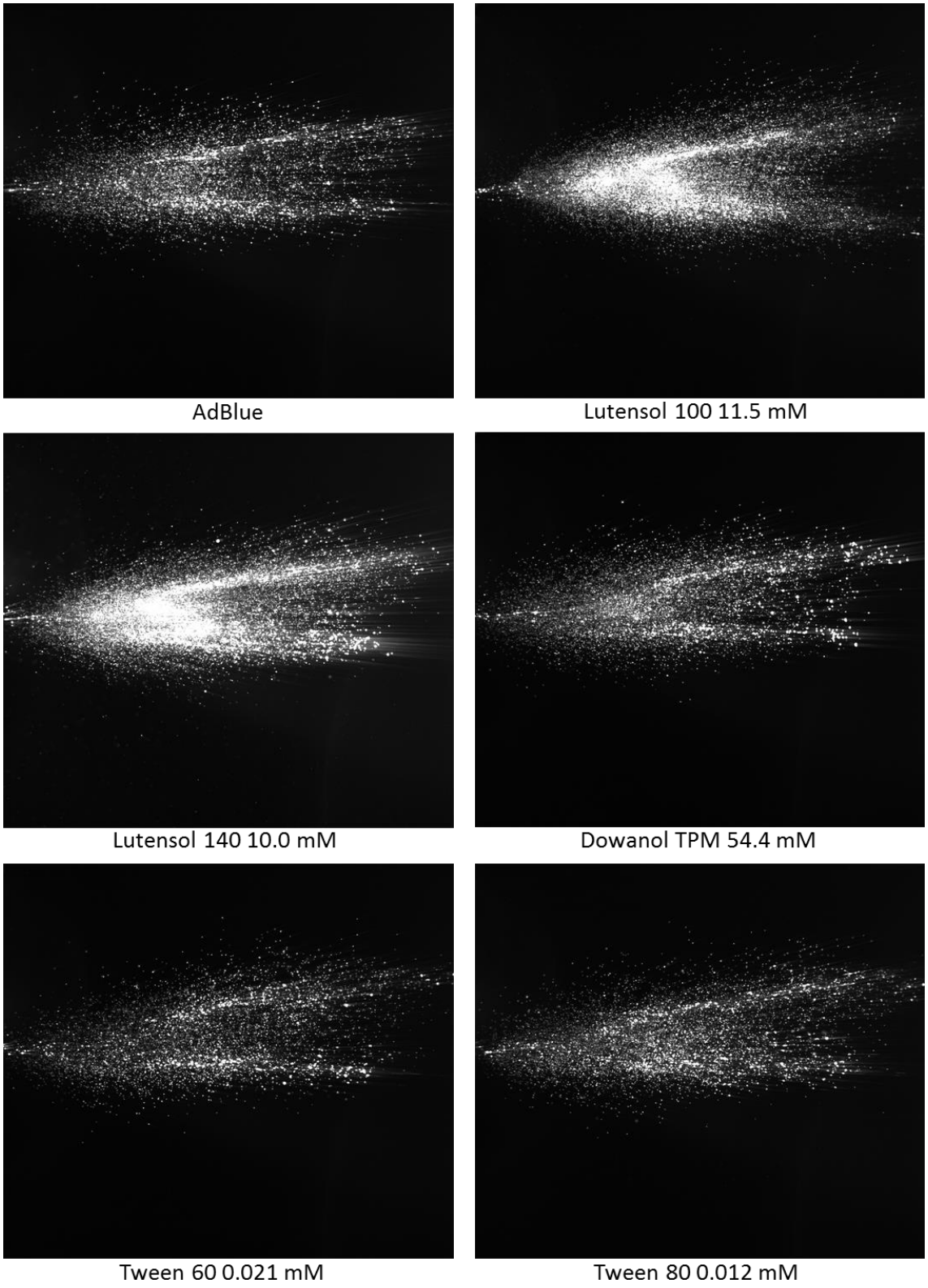


Figure 54: Influence of AdBlue additivation with five different substances (Lutensol 100, Lutensol 140, Dowanol TPM, Tween 60 and Tween 80) on optical density of spray picture measured as described in 5.4.2. Injector opening time: 3.0 ms.

To check the situation for a larger volume of sample inside the spray, the imaging was additionally performed with an injector opening time of 3.0 ms. The results of this experimental series are shown in Figure 54. Also, in this case, the spray pictures for AdBlue, Dowanol, Tween 60 and Tween 80 looked very similar with optically no significant differences to be detected. But, the AdBlue samples additivated with Lutensol 100 and Lutensol 140 again differed from the other spray images. A much higher optical density was found, especially in the middle of the spray cone. This can again be a hint for a better-dispersed spray containing smaller droplets compared to the reference samples.

As already assumed from the dynamic surface tension measurements, the Lutensol 100 additive, and the Lutensol 140 additive, showed the best qualitative results in the optical spraying experiment. Therefore, the influence of the concentration of Lutensol 100 was checked in a further experiment. Besides the sample containing 11.5 mM Lutensol 100, AdBlue additivated with 1.4 mM and 4.0 mM of Lutensol 100 was also tested. The corresponding spray images are shown in Figure 55. The injector opening time was 3.0 ms.

The spray images showed that the optical density was increased by increasing the surfactant amount. Larger and lighter spots were found for higher concentrations of Lutensol 100 in AdBlue.

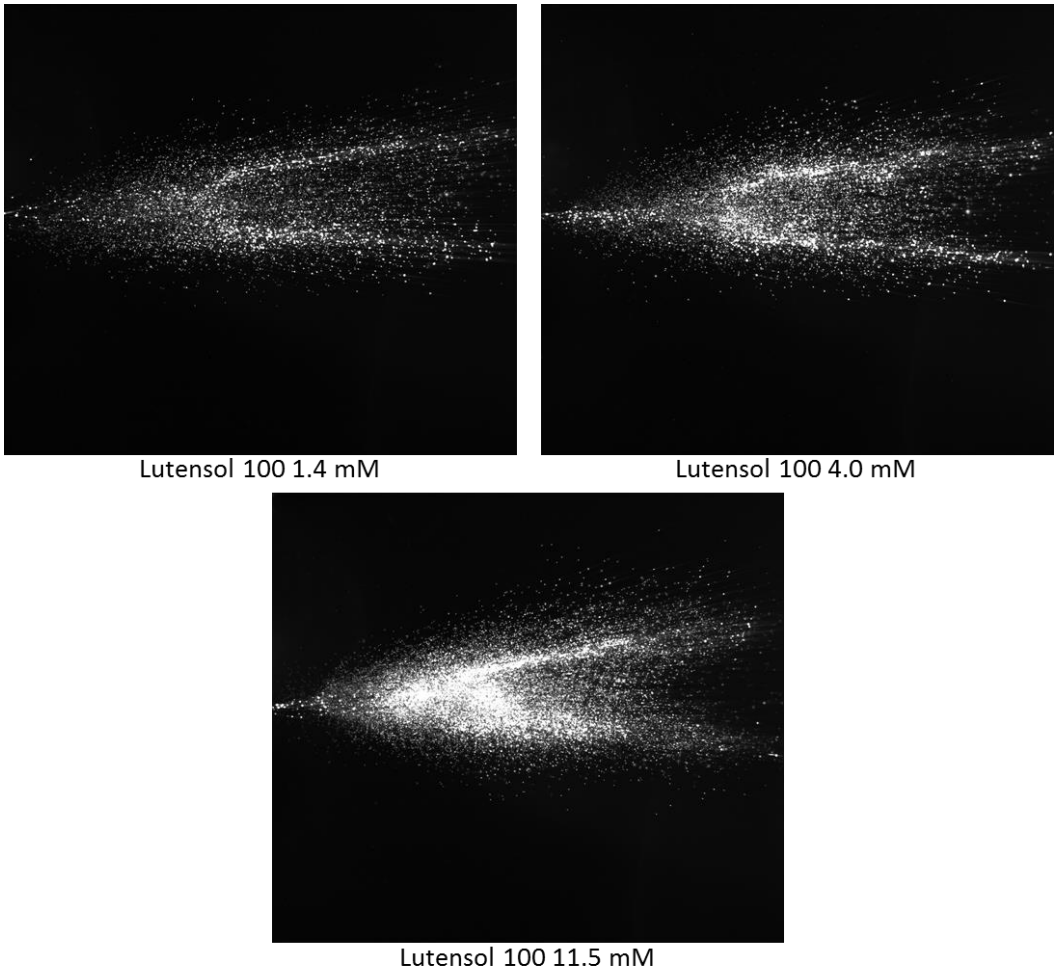


Figure 55: Influence of concentration of Lutensol 100 in AdBlue on optical density of spray picture measured as described in 5.4.2. Injector opening time: 3.0 ms.

In order to enable a numerical evaluation of the recorded spray pictures, the size of the droplets was determined quantitatively. For that, an image evaluation software was applied to the recorded images, as described in 5.4.2. A condition for correct determination of the droplet size is to have a possibly low optical density in order to have as less as possible mutual overlay of the single droplets. Therefore, the size determinations were carried out using the spray images with the lowest injector opening time of 1.5 ms.

Figure 56 shows the values determined for the differently additivated AdBlue samples.

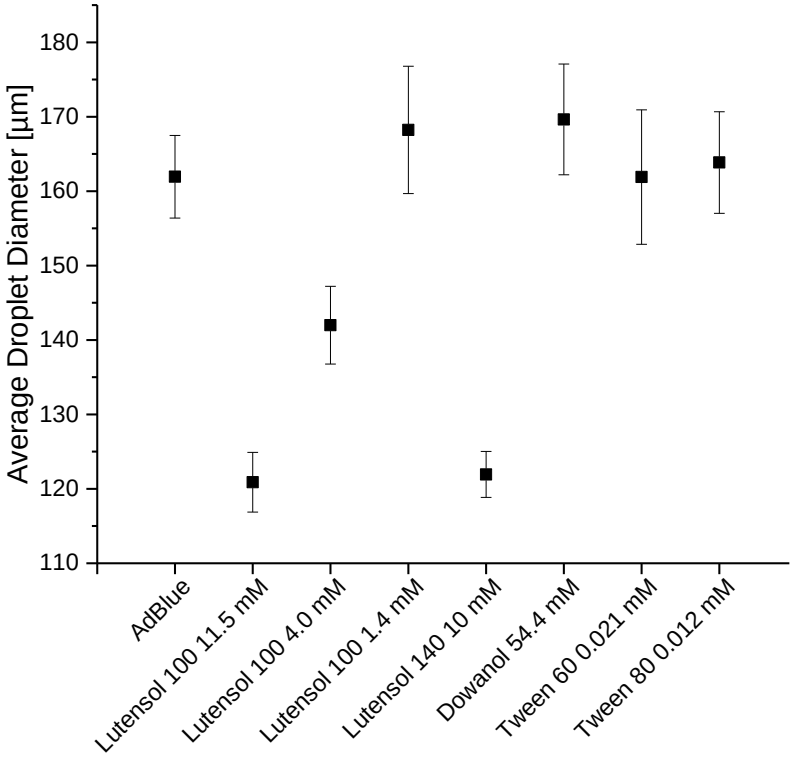


Figure 56: Average droplet diameters determined from the spray images for differently additivated AdBlue samples as described in 5.4.2. Injector opening time: 1.5 ms.

From the numerical results in Figure 56, the correlation of high dynamic surface tension behavior with a small drop size can be proven for the optical results. The determined droplet diameters for all test solutions were in the range of the values described in the literature [3]. The samples Lutensol 100 1.4 mM, Dowanol 54.4 mM, Tween 60 0.021 mM and Tween 80 0.012 mM showed the same average droplet diameter as found for the pure AdBlue sample. In the case of the Lutensol 100 4.0 mM and Lutensol 100 11.5 mM, significantly smaller droplets were formed. In case of the 11.5 mM Lutensol 100, the droplets had an about 30 % smaller diameter compared to AdBlue. For Lutensol 140 10 mM, the droplet size was similar. In addition to the average droplet size of the different samples, Figure 57 shows the maximum droplet diameters calculated for the individual samples. The results showed the same trends and fit to the optical results and the average droplet size determination. Thus, a suitable additivation with surfactants of high interfacial dynamics led to a formation of smaller maximum droplets.

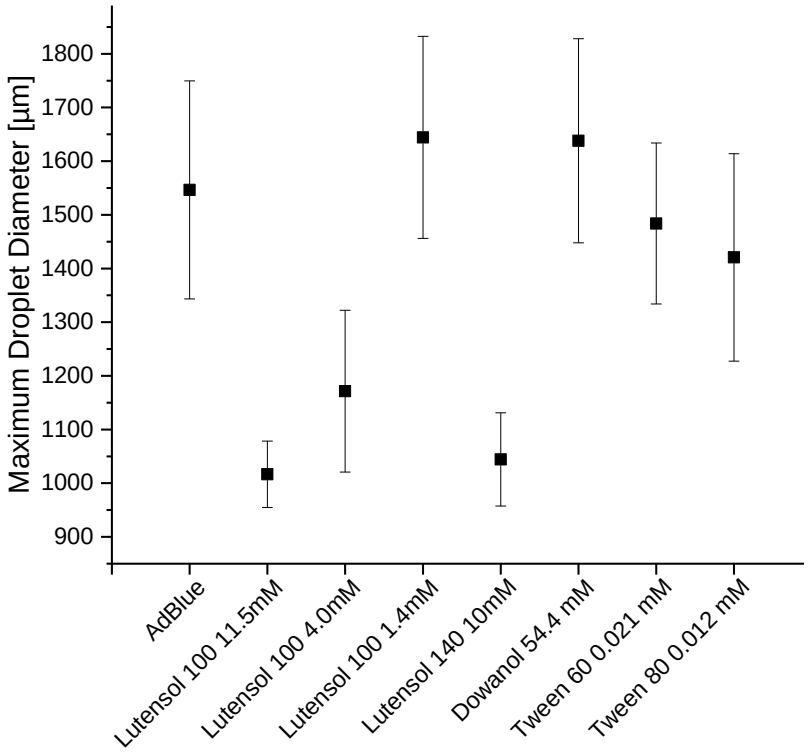


Figure 57: Maximum droplet diameters found in the spray images for differently additivated AdBlue samples as described in 5.4.2. Injector opening time: 1.5 ms.

In Figure 58, the standard deviation of the droplet diameters inside the complete individual spray images is plotted. In addition to smaller droplet diameters, the surfactant addition in case of Lutensol 100 4.0 mM, 11.5 mM and Lutensol 140 10 mM also led to a more uniform distribution of the droplets in the spray, meaning less outliers of larger droplets are formed during the injection process.

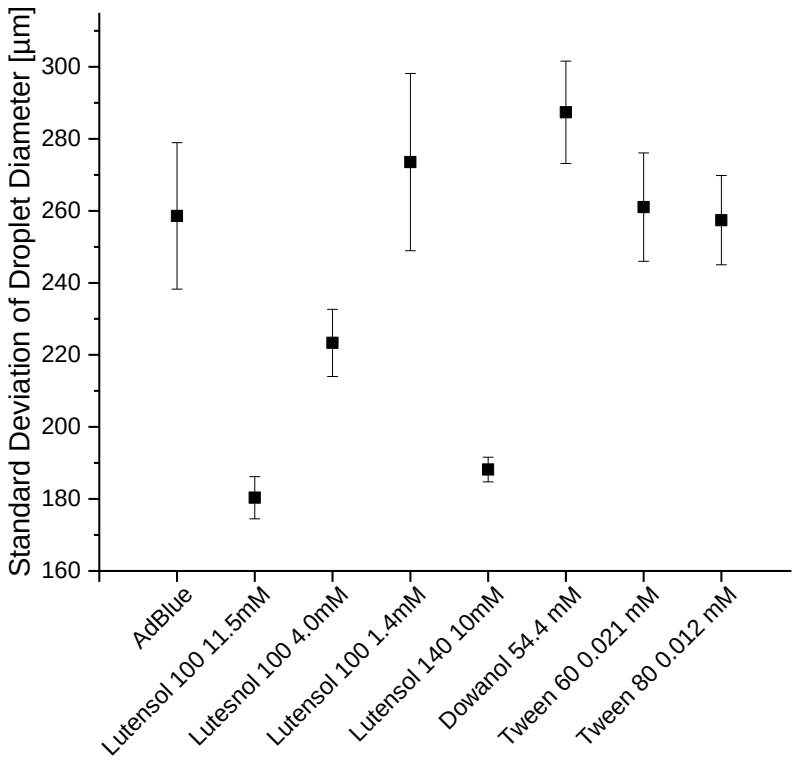


Figure 58: Standard deviation of droplet diameters found in the spray images for differently additivated AdBlue samples calculated as described in 5.4.2. Injector opening time: 1.5 ms.

From the performed experiments, it could be shown that a suitable surface-active additivation of AdBlue can lead to a formation of droplets with smaller average diameters during the injection process. In addition, Figure 58 shows that the additivation reduces the variation in the droplet size of the spray. Both points lead to an improved spray quality and thereby a decrease in deposit formation in the SCR system. Decisive for this process is a high dynamic surface tension behavior of the used surfactant. Lowering the surface tension very rapidly after the formation of a new surface during the injection results in smaller droplets of AdBlue. It could be proven that the value of surface tension in equilibrium is not the decisive point.

#### 5.4.3.3.3 Droplet-wall interaction

As it was shown in the previous section, a suitable additivation of AdBlue led to improved spray properties after injection of the liquid. Thereby, evaporation of the liquid in the hot exhaust gas should be improved. However, as can be found in different studies, even for the best spray, a droplet-wall contact can never be completely excluded [20, 46, 47]. Because of that, in the following study, it was tested if the surfactant additivation of AdBlue also leads to different behavior regarding the byproduct formation after contact of a droplet with a hot surface.

For this purpose, a defined volume of 2 x 50 µl of AdBlue and Lutensol 100 in different concentrations was dropped from a defined height on microscope slides, heated to 215 °C, and the resulting formation of byproduct was gravimetrically analyzed as described in 5.4.2.

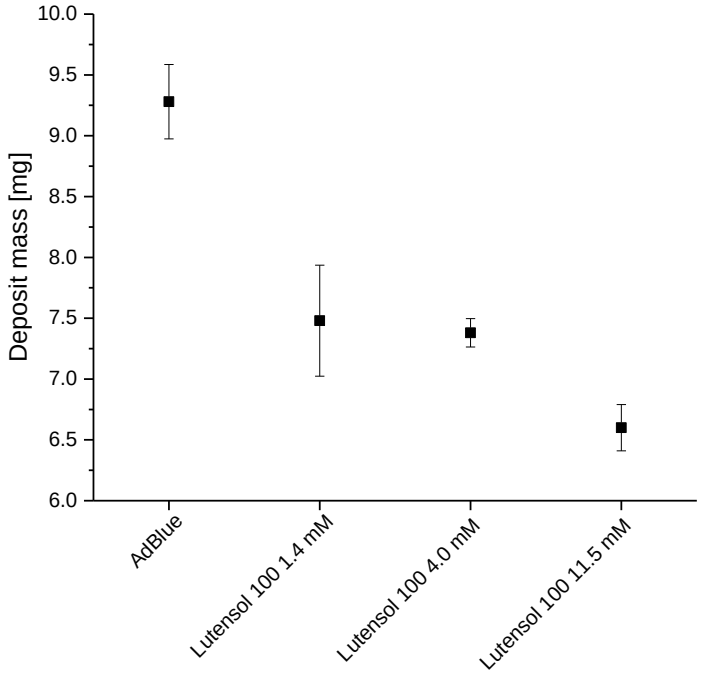


Figure 59: Gravimetrical analysis of the deposit formation after droplet-surface contact of 2 x 50 µl of differently additivated AdBlue samples performed as described in 5.4.2.

As shown in Figure 59, after contact with the hot surface, the Lutensol 100 addition to AdBlue lowered the amount of formed solid deposits significantly. While in the case of pure AdBlue, about 9.3 mg deposits were formed from 100 µl, the addition of 11.5 mM Lutensol 100 led to a reduction of the formation of undesired byproducts to about 6.5 mg, which means a reduction of more than 30 %.

In Figure 60 on the left side, the different slides with 100 µl AdBlue (bottom) and 100 µl Lutensol 11.5 mM in AdBlue (top) are shown.

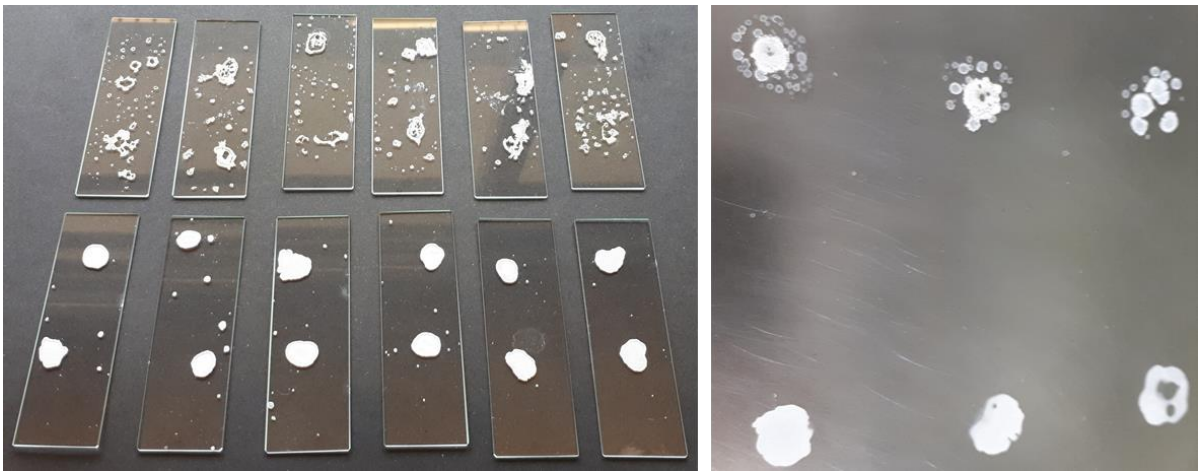

Figure 60: Comparison of deposit formation, left: 2 x 50 µl of AdBlue (bottom) and 2 x 50 µl of Lutensol 11.5 mM in AdBlue (top), right: 50 µl AdBlue (bottom) and 50 µl Lutensol 11.5 mM in AdBlue (top) on a stainless steel plate.

In addition, the test was also performed using a stainless steel plate. The result can be seen in Figure 60 on the right side. The results looked similar. Thus, it could be shown that the surfactant additivation brings, besides formation of smaller droplets inside the spray, also a reduced tendency to form undesired byproducts after contact with building parts of the exhaust pipe. The reason for that can be found in the addition of the surfactant. It reduces the surface tension and leads to a spreading of the liquid sample on the hot surface. By that, a defined volume of liquid gets into contact with a higher area of surface, meaning the heat absorption of the liquid from the surface proceeds faster compared to a liquid having higher surface tension and thereby less spreading effects. Condition for this is a wall temperature lower than a critical (the Leidenfrost) temperature [3].

In summary, the performed experiments showed the positive influence of AdBlue additivation regarding the reduction of deposits during the injection in the SCR process. In 5.4.3.3.1, potential surface-active candidates were selected on the basis of the dynamic surface tension. Sample solutions with high dynamics were tested for their spraying behavior in 5.4.3.3.2. Here, a clear trend was observed. Surfactants with high dynamics decreased the droplet size as well as the droplet size deviation. This was proven in the present section to also decrease the formation of deposits after contact with a hot wall.

### 5.4.4 Conclusion

AdBlue is an essential operating material for commercial SCR systems. However, at low ambient temperatures and at low exhaust gas temperatures, the ammonia-precursor solution brings some problems. On the one hand, AdBlue tends to freeze at temperatures < -11 °C and on the other hand, incomplete decomposition of AdBlue leads to the formation of undesired byproducts at low exhaust temperatures, which can harm the SCR process and even the whole engine itself. In the first part of this study, the lowering effect of the addition of an alternative ammonia precursor on the temperature of inhomogeneity of the precursor solution was investigated. The addition of different solvents did not show potential for the reduction of the temperature of inhomogeneity. In case of the addition of ammonium-based salts, part of the urea from the solution was substituted by ammonium acetate, ammonium carbonate or ammonium bicarbonate. The experimental observations showed that the temperature at which the precursor solution becomes inhomogeneous can be significantly lowered by addition of the described additives. Ammonium carbonate and ammonium bicarbonate, in addition, bring the advantage that applicability of the solution at low engine exhaust temperatures is also enhanced since the species already present partially decomposed urea in aqueous solution.

In the second part of this study, the idea was to add surface-active substances to AdBlue and investigate the connections between the dynamic surface tension of the solution and the resulting reduction of the droplet diameter after injection. Pendant drop measurements of differentially additivated AdBlue solutions were carried out to get information on the behavior of the surface tension as a function of time. The nonionic surfactant Lutensol 100 in the highest concentration tested showed the highest dynamic surface tension behavior. Promising candidate solutions were subsequently tested in a newly arranged injection-test bench on their spraying behavior. Besides an optical evaluation of the spray images, an image evaluation software was used to determine the size of the individual droplets of each spray image. The surfactants with high dynamic surface tension behavior showed high dispersion in the spray, which was proven by the corresponding numerical evaluation. The decisive point for the formation of small droplets was found to be a very fast decrease of the surface tension after forming a new surface. The interaction of a defined volume of test solution with a hot surface was investigated in the last part. Here, a significant decrease of the formation of solid byproducts was found in the case of additivated AdBlue solution.

All in all, two different approaches for the optimization of applicability properties of the AdBlue solution were shown and proven to be an easy and sufficient way to minimize certain disadvantages of the SCR process. The replacement of urea by an alternative ammonia precursor can shift the temperature at which the solution becomes inhomogeneous to lower temperatures, thereby reducing the need for heating processes of the AdBlue tank. Moreover, with the addition of a small amount of the right surfactant, e.g. Lutensol 100, better injection spray can be realized and the formation of solid byproducts can be reduced. These results, therefore, enable an optimization of the SCR process without big efforts.

### 5.4.5 References


[1] H. L. Fang, H. F. M. DaCosta, *Applied Catalysis B: Environmental* **2003,** *46*, 17-34.

[2] F. Birkhold, U. Meingast, P. Wassermann, O. Deutschmann, *Applied Catalysis B: Environmental* **2007,** *70*, 119-127.

[3] T. Lauer, *Chemie Ingenieur Technik* **2018,** *90*, 783-794.

[4] M. Lecompte, J. Obiols, J. Cherel, S. Raux, *SAE International Journals of Fuels and Lubricants* **2017,** *3, 10*.

[5] P. Braun, J. Gebhard, F.-M. Matysik, H.-P. Rabl, *Chemie Ingenieur Technik* **2018,** *90*, 762-773.

[6] P. Braun, H.-P. Rabl, F.-M. Matysik, *Chemie Ingenieur Technik* **2019,** *91*, 961-968.

[7] International ISO-Standard: Diesel engines - NOx reduction agent AUS 32: ISO 22241-1:2006, **2006.**

[8] K. Schmidt et al., *International Journal of Advances in Engineering Sciences and Applied Mathematics* **2015,** *7*, *3,* 78-85.

[9] J. O. de Beeck, K. Slusser, N. Booth, *SAE Technical Paper* **2014**, *2014-01-1530*.

[10] P. Braun, J. Gebhard, H.-P. Rabl, *Low-Temperature DeNOx*, Final Report FVV project 1115, Frankfurt am Main, **2017**.

[11] O. Kröcher, M. Elsener, E. Jacob, *Proc. of the 5. Internationales Forum Abgas und Partikelemission*, Ludwigsburg, **2008**.

[12] D. Peitz, *Ph.D. Thesis*, ETH Zurich **2012**.

[13] D. Peitz, O. Kröcher, *4th IAV Conf. MinNOx*, Berlin, June **2012**.

[14] S. Dumas, M. Lopes, *4th IAV Conf. MinNOx*, Berlin, June **2012**.

[15] P. M. Schaber et al., *Thermochimica Acta* **2004,** *424*, 131-142.

[16] S. Eakle, S. Kroll, C. Henry, *SAE Technical Paper* **2016***, 2016-01-2327*.

[17] F. Birkhold, U. Meingast, P. Wassermann, O. Deutschmann, *SAE Technical Paper* **2006***, 2006-01-0643*.

[18] V. O. Strots et al., *SAE International Journal of Fuels and Lubricants* **2010,** *2*, *2*, 283-289.

[19] B. Geringer et al., *Fortschritt-Berichte VDI* **2010,** *12*, *716*, 374-394.

[20] X. Shi, J. Deng, Z. Wu, L. Li, *SAE International Journal of Engines* **2013,** *6, 2*.

[21] S. Fischer, *Ph.D. Thesis*, TU Wien **2012**.

[22] F. Birkhold, *Ph.D. Thesis,* Universität Karlsruhe **2007**.

[23] H. Smith, T. Lauer, M. Mayer, S. Pierson, *SAE International Journal of Fuels and Lubricants* **2014,** *7, 2*, 525-542.

[24] G. M. H. Shahariar, O. T. Lim, *Journal of Mechanical Science and Technology* **2018,** *32, 7*, 3473-3481.

[25] L. Xu et al., *SAE Technical Paper* **2007,** 116, 4, 202-209.

[26] M. J. Rosen, *Surfactants and Interfacial Phenomena*, Wiley, **2004**.

[27] C. E. Stauffer, *Journal of Physical Chemistry* **1965,** *69*, *6*, 1933-1938.

[28] B. Binks, D. Furlong, *Modern Characterization Methods of Surfactant Systems*, **1999**.

[29] J. D. Berry et al., *Journal of Colloid and Interface Science* **2015,** *454*, 226-237.

[30] D. Georgieva, A. Cagna, D. Langevin, *Soft Matter* **2009,** *5*, 2063-2071.

[31] P. W. Atkins, L. dePaula, *Physikalische Chemie,* Wiley-VCH, **2013**.

[32] K. Takaizumi, T. Wakabayashi, *Journal of Solution Chemistry* **1997,** *26*, *10*, 927-939.

[33] Encyclopedia Britannica.

[34] GESTIS Stoffdatenbank.

[35] M. Olszak-Humienik, *Thermochimica Acta* **2001,** *378*, 107-112.

[36] T. F. Tadros, *An Introduction to Surfactants*, De Gruyter, **2014**.

[37] I. D. Robb, *Specialist Surfactants*, Springer, **1997**.

[38] M. J. Schick, *Nonionic Surfactants*, Marcel Dekker Inc, **1987**.

[39] M. J. Hofmann, R. Weikl, H. Motschmann, G. J. M. Koper, *Langmuir* **2015,** *31*, *6*, 1874-1878.

[40] T. Namani, P. Walde, *Langmuir* **2005**, 21, 6210-6219.

[41] M. Altschuler et al., *Biotechniques* **1994**, 17, 434.

[42] sigmaaldrich.com/catalog/product/sigma/p1629?lang=de&region=DE.

[43] D. K. Chou et al., *Journal of Pharmaceutical Science* **2005**, 94, 1368-1381.

[44] M. Siskova, J. Hejtmankova, L. Bartovska, *Collection of Czechoslovak Chemical Communications* **1985,** *50*, *8*, 1629-1635.

[45] R. Breslow, T. Guo, *Proceedings of the National Academy of Sciences of the USA* **1990,** *87*, 167-169.

[46] F. Birkhold, U. Meingast, P. Wassermann, O. Deutschmann, *Applied Catalysis B: Environmental* **2005,** *79*, 119-127.

[47] W. Brack, *Ph.D. Thesis*, Karlsruher Institut für Technologie **2016**.

# 6 SUMMARY

Due to increasing thermal efficiency of modern and upcoming combustion engines, consequently, a decline of the exhaust-gas temperature level can be observed. This fact is problematic for the pollutant limitation by exhaust aftertreatment, as some strategies require a certain temperature level for correct working. Regarding the abatement of nitrogen-oxide emissions, the low-temperature level presents a problem for the currently used exhaust aftertreatment strategies.

Therefore, in chapter 3 of this work, a broadly arranged literature and patent research was carried out with the aim to identify strategies to improve the exhaust aftertreatment of nitrogen-oxide emissions at low exhaust temperatures. The selective catalytic reduction (SCR) technology with the $NO_x$-reducing agent ammonia presents the technology with the highest potential for $CO_2$-optimized nitrogen-oxide aftertreatment. However, it was found that in the low-temperature range, the overall SCR process for nitrogen-oxide aftertreatment is limited by the decomposition of the ammonia-precursor urea.

Because of that, in chapter 5.1, the decomposition of AdBlue-urea was investigated in the liquid phase. In the first part, a screening of different metal oxides was carried out using an autoclave reactor. Three metal oxides ($WO_3$, ZnO and $MoO_3$) were found to significantly increase the urea decomposition and ammonia formation after dissolution in aqueous phase. As actually catalytically active species, metallates must have formed, their catalytic activity, however, was decreasing over 270 min. Additional stabilization for these catalysts is needed. In the second part, strongly alkaline and acidic conditions were found to enhance the ammonia formation from AdBlue.

An electrochemically-induced approach for urea decomposition to ammonia was the topic of chapter 5.2. The species NiOOH was found in previous works to be catalytically active for urea decomposition in highly alkaline AdBlue. Since these conditions are not practically available, in this study, the influence of a nickel surface in ammonium carbonate solutions on ammonia formation from urea was studied. CV studies indicated potential nickel oxide formation, however, the experiments on ammonia formation showed that the oxidation effect of ammonia in ammonium carbonate solution covered any potential ammonia formation effects at the nickel surface. Further studies at elevated temperatures are necessary.

As external acidification or alkalization of AdBlue is practically difficult to carry out, in chapter 5.3 the effect of in-situ alkalization and acidification of an AdBlue sample on ammonia formation was tested. Various parameters of an electrolysis of the AdBlue sample were checked. In both electrochemical compartments, the anodic and the cathodic half-cell significantly increased ammonia concentrations were measured. For temperatures up to 80 °C and currents between 10 mA and 100 mA, the concentration of ammonia was in the order: anodic compartment > cathodic compartment > reference. In addition, the formation of byproducts was analyzed by an IC/HPLC approach. Oxidation of ammonia was found to produce nitrate and nitrite, which might be optimized by further research.

Chapter 5.4 is addressed to the applicability enhancement of AdBlue at low temperatures. First, the focus was on a lowering of the temperature at which AdBlue cannot be used without external heating, precisely -11 °C. Addition of alternative solvents was problematic, as the solubility of urea was not high enough. Substitution of small amounts of urea by ammonium carbonate, ammonium bicarbonate and ammonium acetate, however, showed the desired effect of a temperature shift at which AdBlue became inhomogeneous. The second part focuses on the tendency of AdBlue to form undesired byproducts in the exhaust tract after injection at low exhaust temperatures. The effect of the addition of a surfactant on the spraying behavior of AdBlue was investigated. A software-controlled in-house made injection-test bench was set up in order to visualize the spray of differently additivated AdBlue samples. Besides an optical image evaluation, numerical evaluation was possible by applying an image evaluation software. It was found that the dynamic surface tension, meaning the highly rapid decrease of the surface tension of the sample solution after forming a new surface, is the decisive factor for achieving smaller droplet diameters and thereby an improved spray. As smaller droplets can evaporate easier and faster in the hot exhaust tract, the tendency to form undesired deposits can be lowered.

All in all, this thesis gives an overview of the problematic nitrogen-oxide emission reduction at low exhaust temperatures and presents some potential approaches and strategies to improve the decomposition of AdBlue-urea to ammonia required for the correct working of a SCR system.

# 7 ZUSAMMENFASSUNG IN DEUTSCHER SPRACHE

Aufgrund eines zunehmenden thermischen Wirkungsgrades moderner und zukünftiger Verbrennungsmotoren kann ein hierdurch bedingtes Absinken des Abgastemperaturniveaus beobachtet werden. Diese Tatsache ist problematisch für die Schadstoffbegrenzung mittels Abgasnachbehandlung, da einige Strategien ein bestimmtes Temperaturniveau für korrektes Arbeiten benötigen. In Bezug auf die Reduzierung von Stickoxidemissionen stellt das niedrige Temperaturniveau ein Problem für die aktuell verwendeten Abgasnachbehandlungsstrategien dar.

In Kapitel 3 dieser Arbeit wurde daher eine breit angelegte Literatur- und Patentrecherche durchgeführt, um Strategien zur Verbesserung der Abgasnachbehandlung von Stickoxidemissionen bei niedrigen Abgastemperaturen zu identifizieren. Die SCR-Technologie (selektive katalytische Reduktion) mit dem $NO_x$-Reduktionsmittel Ammoniak bietet das größte Potenzial für eine $CO_2$-optimierte Stickoxid-Nachbehandlung. Es konnte jedoch festgestellt werden, dass im Niedertemperaturbereich das gesamte SCR-Verfahren zur Stickoxid-Nachbehandlung durch die Zersetzung des Ammoniak-Vorläufer-Harnstoffs begrenzt ist.

Aus diesem Grund wurde in Kapitel 5.1 die Zersetzung von AdBlue-Harnstoff in der Flüssigphase untersucht. Im ersten Teil wurde ein Screening verschiedener Metalloxide unter Verwendung eines Autoklav-Reaktors durchgeführt. Es wurde festgestellt, dass drei Metalloxide ($WO_3$, ZnO und $MoO_3$) die Harnstoffzersetzung und Ammoniakbildung nach Auflösung in der wässrigen Phase signifikant erhöhen. Als tatsächlich katalytisch aktive Spezies müssen sich Metallate gebildet haben, deren katalytische Aktivität jedoch über 270 min abnahm. Für diese Katalysatoren ist eine zusätzliche Stabilisierung erforderlich. Im zweiten Teil wurde festgestellt, dass stark alkalische und saure Bedingungen die Ammoniakbildung aus AdBlue verstärken.

Ein elektrochemisch induzierter Ansatz zur Zersetzung von Harnstoff zu Ammoniak war Thema des Kapitels 5.2. Die Spezies NiOOH erwies sich in früheren Arbeiten als katalytisch aktiv in der Zersetzung von Harnstoff in hochalkalischem AdBlue. Da diese Bedingungen in der Praxis nicht vorliegen, wurde in dieser Studie der Einfluss einer Nickeloberfläche in Ammoniumcarbonat-Lösungen auf die Ammoniakbildung aus Harnstoff untersucht. CV-Studien wiesen auf eine mögliche Nickeloxidbildung hin. Die Versuche zur Ammoniakbildung zeigten jedoch, dass der Oxidationseffekt von Ammoniak in Ammoniumcarbonat-Lösung jegliche mögliche Ammoniakbildungseffekte an der Nickeloberfläche überdeckte. Weitere Untersuchungen bei erhöhten Temperaturen sind nötig.

Da eine externe Ansäuerung oder Alkalisierung von AdBlue in der Praxis schwer durchführbar ist, wurde in Kapitel 5.3 der Einfluss der in situ-Alkalisierung und Ansäuerung einer AdBlue-Probe auf die Ammoniakbildung untersucht. Verschiedene Parameter einer Elektrolyse der AdBlue-Probe wurden untersucht. In beiden elektrochemischen Kompartimenten, der anodischen und der kathodischen Halbzelle, wurden signifikant erhöhte Ammoniakkonzentrationen gemessen. Für Temperaturen bis 80 °C und Ströme zwischen 10 mA und 100 mA lagen die Ammoniakkonzentrationen in der Reihenfolge Anodenraum > Kathodenraum > Referenz. Zusätzlich wurde die Bildung von Nebenprodukten durch einen IC/HPLC-Ansatz analysiert. Es wurde festgestellt, dass die Oxidation von Ammoniak Nitrat und Nitrit erzeugt, was durch weitere Untersuchungen optimiert werden könnte.

Kapitel 5.4 befasst sich mit der Verbesserung der Anwendbarkeit von AdBlue bei niedrigen Temperaturen. Im ersten Teil lag der Fokus auf einer Absenkung der Temperatur, bei der AdBlue ohne externes Beheizen nicht mehr verwendet werden kann, nämlich von -11 °C. Die Zugabe alternativer Lösungsmittel war problematisch, da die Löslichkeit von Harnstoff nicht hoch genug war. Die Substitution kleiner Mengen Harnstoff durch Ammoniumcarbonat, Ammoniumhydrogencarbonat und Ammoniumacetat zeigte jedoch den gewünschten Effekt einer Temperaturverschiebung, bei der AdBlue inhomogen wurde. Der zweite Teil befasst sich mit der Eigenschaft von AdBlue, nach der Einspritzung bei niedrigen Abgastemperaturen unerwünschte Nebenprodukte im Abgastrakt zu bilden. Der Einfluss eines Tensidzusatzes auf das Sprühverhalten von AdBlue wurde untersucht. Ein softwaregesteuerter, im Hause produzierter Injektionsprüfstand wurde eingerichtet, um das Sprühbild von AdBlue-Proben mit unterschiedlichen Additiven zu visualisieren. Neben einer optischen Bildauswertung war auch eine numerische Auswertung mittels einer Bildauswertungssoftware möglich. Es hat sich gezeigt, dass die dynamische Oberflächenspannung, d.h. die sehr schnelle Abnahme der Oberflächenspannung der Probelösung nach Bildung einer neuen Oberfläche, der entscheidende Faktor für das Erreichen kleinerer Tropfendurchmesser und damit eines verbesserten Sprays ist. Da kleinere Tröpfchen im heißen Abgastrakt leichter und schneller verdunsten können, kann die Neigung zur Bildung unerwünschter Ablagerungen verringert werden.

Alles in allem gibt diese Arbeit einen Überblick über die problematische Reduzierung der Stickoxidemissionen bei niedrigen Abgastemperaturen und stellt einige mögliche Ansätze und Strategien zur Verbesserung der Zersetzung von AdBlue-Harnstoff zu Ammoniak vor, die für eine korrekte Funktionsweise eines SCR-Systems erforderlich ist.

# ERKLÄRUNG

Ich erkläre hiermit an Eides statt, dass ich die vorliegende Arbeit ohne unzulässige Hilfe Dritter und ohne Benutzung anderer als der angegebenen Hilfsmittel angefertigt habe; die aus anderen Quellen direkt oder indirekt übernommenen Daten und Konzepte sind unter Angabe des Literaturzitats gekennzeichnet.

Weitere Personen waren an der inhaltlich-materiellen Herstellung der vorliegenden Arbeit nicht beteiligt. Insbesondere habe ich hierfür nicht die entgeltliche Hilfe eines Promotionsberaters oder anderer Personen in Anspruch genommen. Niemand hat von mir weder unmittelbar noch mittelbar geldwerte Leistungen für Arbeiten erhalten, die im Zusammenhang mit dem Inhalt der vorgelegten Dissertation stehen.

Die Arbeit wurde bisher weder im In- noch im Ausland in gleicher oder ähnlicher Form einer anderen Prüfungsbehörde vorgelegt.

Regensburg, den 31.07.2019

_____

Peter Braun